Aus der Klinik für Kinder-Onkologie, Hämatologie und klinische Immunologie

der Heinrich-Heine-Universität Düsseldorf

Direktor: Univ.-Prof. Dr. Arndt Borkhardt

In vitro characterization of organ toxicity of chemotherapy and targeted inhibitors for the therapy of childhood acute lymphoblastic leukemia using high-throughput drug screening

Dissertation

zur Erlangung des Grades eines Doktors der Medizin der Medizinischen Fakultät der Heinrich-Heine-Universität Düsseldorf

vorgelegt von

Titus Julius Maximilian Watrin

im Jahre 2024

Als Inauguraldissertation gedruckt mit Genehmigung der

Medizinischen Fakultät der Heinrich-Heine-Universität Düsseldorf

gez.:

Dekan: Prof. Dr. Nikolaj Klöcker

Erstgutachter: Prof. Dr. Arndt Borkhardt

Zeitgutachter: Prof. Dr. Nikolas Stoecklein

Drittgutachter: Prof. Dr. Martin Stanulla

In liebevollem Gedenken an meine Mutter - und mein Vorbild - die diese Arbeit von Beginn an unterstützt hat.

Ich vermisse Dich sehr!

Publications

Peer-reviewed Papers:

Reusing SB, Vallera DA, Manser AR, **Watrin T**, Bhatia S, Felices M, Miller JS, Uhrberg M, Babor F. CD16xCD33 Bispecific Killer Cell Engager (BiKE) as potential immunotherapeutic in pediatric patients with AML and biphenotypic ALL. Cancer Immunol Immunother. 2021 Dec;70(12):3701-3708. doi: 10.1007/s00262-021-03008-0. Epub 2021 Aug 16. Erratum in: Cancer Immunol Immunother. 2021 Sep 7;: PMID: 34398302; PMCID: PMC8571204.

Schedel A, Friedrich UA, Morcos MNF, Wagener R, Mehtonen J, **Watrin T**, Saitta C, Brozou T, Michler P, Walter C, Försti A, Baksi A, Menzel M, Horak P, Paramasivam N, Fazio G, Autry RJ, Fröhling S, Suttorp M, Gertzen C, Gohlke H, Bhatia S, Wadt K, Schmiegelow K, Dugas M, Richter D, Glimm H, Heinäniemi M, Jessberger R, Cazzaniga G, Borkhardt A, Hauer J, Auer F. Recurrent Germline Variant in RAD21 Predisposes Children to Lymphoblastic Leukemia or Lymphoma. Int J Mol Sci. 2022 May 5;23(9):5174. doi: 10.3390/ijms23095174. PMID: 35563565; PMCID: PMC9106003.

Athanasios Oikonomou*, Luigia Valsecchi*, Manuel Quadri*, **Titus Watrin***, Katerina Scharov, Simona Procopi, Jia-Wey Tu, Melina Vogt, Angela Maria Savino, Daniela Silvestri, Maria Grazia Valsecchi, Andrea Biondi, Arndt Borkhardt, Sanil Bhatia, Giovanni Cazzaniga, Grazia Fazio°, Michela Bardini°, Chiara Palmi°. High-throughput screening as a drug repurposing strategy for poor outcome subgroups of pediatric B-cell precursor Acute Lymphoblastic Leukemia. Biochem Pharmacol. 2023 Sep 15;:115809. doi: 10.1016/j.bcp.2023.115809. [Epub ahead of print] PubMed PMID: 37717691.

Athanasios Oikonomou, **Titus Watrin**, Luigia Valsecchi, Katerina Scharov, Angela Maria Savino, Julian Schliehe-Diecks, Michela Bardini, Grazia Fazio, Silvia Bresolin, Andrea Biondi, Arndt Borkhardt, Sanil Bhatia, Giovanni Cazzaniga, Chiara Palmi. Synergistic drug interactions of the histone deacetylase inhibitor givinostat (ITF2357) in CRLF2-rearranged pediatric B-cell precursor Acute Lymphoblastic Leukemia identified by high-throughput drug screening. Heliyon. 2024 July. doi: 10.1016/j.heliyon.2024.e34033 [Epub ahead of print]

Poster/Oral presentations and other contributions:

Luigia Valsecchi, Simone Naso, Simona Procopio, Mario Mauri, Rocco Piazza, **Titus Watrin**, Sanil Bhatia, Valentina Pasquale, Elena Sacco, Chiara Palmi, Grazia Fazio, Luca Trentin, Silvia Bresolin, Andrea Biondi, Giovanni Cazzaniga, Michela Bardini; The RNA Binding Protein Musashi-2 (MSI2) Sustains the Growth and the Leukemogenic Potential of MLL-Rearranged Acute Lymphoblastic Leukemia, and It Is Involved in Glucocorticoid Resistance. Blood 2022; 140 (Supplement 1): 8827–8828. doi: https://doi.org/10.1182/blood-2022-166313

Grazia Fazio, Grazia Fazio, Manuel Quadri, Silvia Bresolin, Chiara Palmi, Michela Bardini, Athanasios Oikonomou, Alberto Peloso, **Titus Watrin**, Jia-Wey Tu, Katerina Scharov, Sanil Bhatia, Arndt Borkhardt, Andrea Biondi, Giovanni Cazzaniga; 3081 – LCK Drug Targeting in PAX5 Rearranged Cases in Poor Risk Childhood B-Cell Precursors Acute Lymphoblastic Leukemia. Experimental Hematology 2022, Volume 111, Supplement: Page S85. doi: https://doi.org/10.1016/j.exphem.2022.07.137

Franziska Auer , Carolina Vicente-Dueñas , Sanil Bhatia , Triantafyllia Brozou , Carolin Melzig , **Titus Watrin** , Rabea Wagener , Ute Fischer , Isidro Sánchez-García , Arndt Borkhardt , Julia Hauer; CREBBP Variants can Predispose to Childhood Leukemia Indepentdently of a Syndromal Rubinstein-Taybi Pehnotype. EHA Library; Jun 12 2020; https://library.ehaweb.org/eha/2020/eha25th/294262/franziska.auer.crebbp.variants.can.predispose.to.childhood.leukemia.html?f=listing=0*browseby=8*sortby=1*search=crebbp

Results were also published in the final report for the support of the “Gesellschaft für Kinderkrebsforschung”.

Summary (German)

Die akute lymphatische Leukämie (ALL) ist die häufigste Krebserkrankung im Kindesalter. Obwohl sich die Fünf-Jahres-Überlebensraten in den letzten Jahren drastisch verbessert haben und inzwischen bei über 90 % liegen, ist sie immer noch die häufigste Todesursache durch Krebs bei Kindern. Die moderne pädiatrische Onkologie steht bei der Behandlung der ALL vor zwei Herausforderungen: Zum einen erhöhen akute und langfristige unerwünschte Arzneimittelwirkungen die Morbidität und Mortalität von ALL-Patienten. Andererseits sprechen Hochrisiko-Subgruppen bei den derzeitigen Behandlungsprotokollen häufig nicht ausreichend an. Zielgerichtete Therapien versprechen, beiden Herausforderungen zu begegnen, indem sie wirksamere und weniger toxische Behandlungen versprechen.

In dieser Arbeit wird ein Hochdurchsatz-*Drug Screening* (HTDS) eingesetzt, um (I) den Zusammenhang zwischen dem interindividuellen Ansprechen von Fibroblasten auf Arzneimittel und den klinischen Daten zu Therapienebenwirkungen zu untersuchen und (II) anhand von Zelllinien und Patientenproben nach vielversprechenden Wirkstoffen für die Behandlung von Hochrisikosubtypen zu suchen.

(I) Bei dem HTDS von insgesamt 51 Fibroblasten Proben von Patienten konnte ein interindividuelles Ansprechen auf die einzelnen Wirkstoffe festgestellt werden. Allerdings zeigte sich kein Zusammenhand zwischen diesem interindividuellen Ansprechen und den klinischen Daten zu Nebenwirkungen während der Therapie. Daher wurde eine fokussiertes *Drug Screening* verwendet, das dem Therapieprotokoll der ALL angelehnt ist. Auch hier zeigte sich kein Zusammenhang, weder zischen dem Grad, noch der Häufigkeit von Nebenwirkungen und den *in vitro Drug Screening* Daten.

(II) Bei dem HTDS von insgesamt 35 Leukämie Zelllinien und 31 Patientenproben konnten die etablierten, genetischen Subgruppen das Gesamtansprechen nicht akkurat abbilden. Als *proof-of-concept* zeigte jedoch die Subgruppe mit der Translokation BCR-ABL1 ein verstärktes Ansprechen auf Tyrosin Kinase Inhibitoren (TKi). Zudem waren Polo-like Kinase Inhibitoren (BI2536 und Volasertib) besonders effektiv gegen die T-ALL Subgruppe. Währenddessen stellte der FMS-like Tyrosin Kinase 3 Inhibitor (FLT3i) Lestaurtinib die beste Option für die KMT2Ar Subgruppe. Zusätzlich korrelierte die Expression von CD13 in B-ALL mit einer Sensitivität für FLT3i, während B-ALLs mit cytoplasmatischem IgM empfindlicher waren für klassische Chemotherapeutika.

Zusammenfassend konnte kein Zusammenhang zwischen dem interindividuellen Ansprechen und den klinischen Daten von Patienten festgestellt werden. Allerdings konnte hier verschiedene therapeutische Alternativen für Subgruppen mit hohem oder mittlerem Risiko dargestellt werden, die weitere Untersuchungen rechtfertigen.

Summary (English)

Acute lymphoblastic leukemia (ALL) is the most prevalent childhood cancer. While five-year survival rates have significantly improved and now exceed 90%, it remains a leading cause of cancer-related childhood mortality. Modern pediatric oncology confronts two key challenges in ALL treatment: first, adverse drug effects, both short-term and long-term, elevate the burden on ALL patients, and second, existing treatment protocols often fall short in tackling high-risk ALL subtypes, leading to treatment failures. Targeted therapies offer a promising solution, aiming to deliver more effective and less toxic treatments for ALL.

In this study, ex vivo high-throughput drug screening (HTDS) was employed with the dual aims of (I) exploring the relationship between interindividual drug responses in patient-derived fibroblasts and their clinical data related to therapy-induced adverse events and (II) identifying potential therapeutic agents for managing high and medium-risk leukemia subtypes.

(I) Employing HTDS on 51 patient-derived fibroblasts, distinct inter-individual drug responses were observed. However, this individual drug response did not show any apparent connection with the occurrence of adverse events in the patient cohort. Subsequently, a focused screening was carried out using 25 patient-derived fibroblasts, replicating the ALL therapy protocol. However, here as well no correlation was observed between the number or severity of adverse events and the drug sensitivity in *ex vivo*.

(II) In ex vivo HTDS involving 35 leukemia cell lines and 31 patient-derived cells, the established genetic subgroups failed to predict overall drug responses accurately. However, as a proof of concept, within distinct leukemia subgroups, tyrosine kinase inhibitors (TKIs) demonstrated efficacy, particularly in the BCR-ABL1 subgroup. Remarkably, medium-risk T-ALLs demonstrated differential sensitivity to polo-like kinase (PLK) inhibitors (BI2536 and Volasertib), while high-risk KMT2Ar B-ALLs showed sensitivity to the FMS-like tyrosine kinase 3 (FLT3) inhibitor (Lestaurtinib). Notably, CD13 expression correlated with FLT3 inhibitor sensitivity, and cytoplasmic IgM expression was linked to classical chemotherapeutic agent sensitivity.

To conclude, using high-throughput drug screenings no correlation was evidenced between inter-individual drug response and clinical adverse events. Nevertheless, the study highlighted various potential treatment possibilities for high- and medium-risk ALL, warranting deeper investigation.

List of Abbreviations

Abbreviation	Meaning
AE	adverse events
AF4	ALL1-fused gene from chromosome 4
AIEOP BFM	Associazione Italiana Ematologia Oncologia Pediatrica Berlin Frankfurt Münster
Akt	Protein kinase B
ALL	acute lymphoblastic leukemia
AML	acute myeloid leukemia
ATP	adenosine triphosphate
B-ALL	B-cell acute lymphoblastic leukemia
BAK	Bcl-2 homologous antagonist killer
BAX	Bcl-2-associated X protein
BCL-2	B-cell lymphoma 2
BCR-ABL1	breakpoint cluster region - Tyrosine-protein kinase ABL1 rearranged ALL
BET bromodomain	Bromodomain and Extra-Terminal motif
BH3	Bcl-2 homology domain 3
BIR	baculoviral inihibitor of apoptosis repeat
BRCA	Breast cancer type 1 susceptibility protein
BRD4	Bromodomain-containing protein 4
BTK	Bruton´s tyrosine kinase
CD	cluster of differentiation
CDK	cyclin-dependent kinases
CML	chronic myeloid leukemia
CNS	central nervous system
CO2	Carbondioxide
CTCAE	NCI Common Terminology Criteria for Adverse Events
CTG	CellTiter-Glo reagent
cyIgM	cytoplasmatic immunoglobulin M
DMEM	Dulbecco´s Modified Eagle´s Medium
DMSO	Dimethyl sulfoxide
DMSZ	Leibniz Institute DSMZ-German Collection of Microorganisms and Cell Cultures GmbH
DNA	Deoxyribonucleic acid
DPBS	Dulbecco´s Phospate Buffered Saline
DSS	Drug Sensitity Score
EBV	epstein-barr virus
EGFR	epithelial growth factor receptor
EMA	European Medicines Agency

Abbreviation	Meaning
ERK	Extracellular signal-regulated kinase
ETV6-RUNX1	translocation-Ets-leukemia virus 6 - runt-related transcription factor 1 rearranged ALL
EZH2	Enhancer of zeste homolog 2
EZH2i	Enhancer of zeste homolog 2 inhibitor
FACS	Fluorescence Activated Cell Sorting
FasL	Fas ligand
FBS	fetal bovine serum
FDA	Food and Drug Administration
FLT3	FMS-like tyrosine kinase 3
FLT3-L	FMS-like tyrosine kinase 3 ligand
g	g-force
h	hours
HDAC	Histone deacetylases
HDACi	Histone deacetylases inhibitor
HSPC	hematopoietic stem and progenitor cells
HSP90	heat shock protein 90
HSP90i	heat shock protein 90 inhibitor
HTDS	High Throughput Drug Screening
IC50	half maximal inhibitory concentration
IDH	Isocitrate dehydrogenase
IgM	Immunoglobulin M
IL-6	interleukine 6
JAK	Janus kinase
KMT2Ar	Histone-lysine N-methyltransferase 2A rearranged
KS-test	Klomogorov-Smirnov-test
MACS	Magnetic-activated cell sorting
MAPK	mitogen-activated protein kinase
MEK	MAPK/ERK Kinase
mg	miligram
ml	mililiters
mM	millimole
MRD	minimal residual disease
ms	milisecond
MSC	mesenchymal stem cells
mTOR	mammalian target of rapamycin
NCI	National Cancer Institute
NF-κB	Nuclear factor kappa-light-chain-enhancer of activated B cells
NFAT	Nuclear factor of activated T-cells
nl	nanoliter
NUDT15	Nudix hydrolase 15 gene

Abbreviation	Meaning
PARP	Poly ADP ribose polymerase
PBMC	peripheral blood mononuclear cell
PBS	Phosphate buffered saline
PCR	polymerase chain reaction
PDX	patient derieved xenograft modell
Ph	Piladelphia chromosome
PI3K	Phosphoinositide 3-kinase
PLCg	Phospholipase C
PLK	Polo-like Kinase
PTEN	Phosphatase and tensin homolog
RAF	Raf kinase
RAS	RAS kinase
Rb	retinoblastoma protein
RLU	Relative light unit
RNA	Ribonucleic acid
RPMI	Roswell Park Memorial Institute
RT-PCR	real time polymerase chain reaction
SCF	Stem cell factor
STAT	signal transducer and activator of transcription
STR	short tandem repeat
SYK	spleen tyrosine kinase
T-ALL	T-cell acute lymphoblastic leukemia
TCF3-HLF	Transcription factor 3 - Hepatic leukemia factor rearranged ALL
TCF3-PBX1	Transcription factor 3 - Pre-B-cell leukemia transcription factor 1 rearranged ALL
Tki	tyrosine kinase inhibitors
TNF	tumor necrosis factor
TPMT	Thiopurine methyltransferase
WHO	world healthy organisation
µl	microliters

Table of contents

1 Introduction

1.1 Incidence and Prognosis

Acute lymphoblastic leukemia (ALL) is the most common childhood cancer [1]. Today the five-year survival rate exceeds 90%. Nevertheless, ALL remains the leading cause of death in pediatric oncology patients [2]. The highest peak of incidence can be observed between the ages of three and five. Both very young patients under one year and patients older than ten years show a poor prognosis [2]. ALL in young adults and adolescents is significantly rarer [1]. ALL is more often diagnosed in male patients. The male sex has a poorer prognosis than the female [2-4]. This phenomenon could be explained by a more frequent extramedullary or testicular relapse, and more central nervous system (CNS) derived relapses. Analogically to gender, different ethnic and racial groups show a higher vulnerability towards ALLs and - through adverse genetic mutations – a worse outcome [5]. Lastly, comorbidity involving Down Syndrome also dramatically impacts the prognosis. Down Syndrome is associated with ALL, and patients with Trisomy 21 seem to suffer from more treatment-related morbidities and lower therapy response [6]. Additionally, more unfavorable genetic lesions are observed in Down Syndrome ALL. The Children´s Oncology group reported comparable event-free and overall survival of Down Syndrome ALL if patients with unfavorable genetic lesions were excluded [7].

Different disease-related risk factors could be identified. For instance, testicular involvement as its own has been associated with worse outcomes in early studies, but through improved therapy, it is no longer counted as a risk factor in modern protocols [8]. Besides, the involvement of the CNS at diagnosis is discussed as a risk factor [9, 10]. Most importantly, the CNS is a potential site for relapse, as not all drugs can overcome the blood-brain barrier. Cranial radiation reduces the number of CNS relapses. Although effective, cranial radiation led to a high incidence of therapy-related adverse events and was therefore exchanged for the equally effective intrathecal admission of Methotrexate for most patients[11]. In addition, the distinction of an ALL of the B- or T-cell lineage is an accepted risk factor as the overall survival (OS) of the patients with T-ALL is around 5-10% lower [12]. Reasons for the difference in OS are favorable genetic subtypes, better treatment response, and more options of drugs for the B-ALL lineage. Besides, the median age at diagnosis is higher in the T-ALL group. Moreover, an increased white blood cell count over 50.000/µl at diagnosis is associated with inferior outcomes for B-ALLs [13]. The prognosis of T-ALL patients with highly elevated white blood cells can be improved by intensifying the induction phase [14].

As many of the here-described prognostic factors confound with genetic and biological subgroups, these favorable or dismal determinants significantly impact the outcome of modern therapy protocols the most [15].

1.2 Pathogenesis of Acute Lymphoblastic Leukemias

ALL is a malignant disease originating from abnormal B-, T- and rarely NK-cell precursors [15]. In these abnormal progenitor cells, differentiation is blocked. A dysregulated proliferation results in a relentless expansion of these cancerous cells, repressing the normal hematopoiesis in the bone marrow over time. The immature blasts can circulate in the peripheral blood and manifest in different organs to cause various possible symptoms [16]. While the exact mechanisms of leukemogenesis are still to be explored, germline mutations occupy a unique position [17]. In adults, cancers are often lifestyle-associated and defined by somatic mutations obtained throughout the lifetime. Childhood cancer, however, is more often conditioned by germline mutations. But ALL relevant mutations and translocation are regularly found in healthy children [18]. Thus, further crucial mutations acquired during early life are needed for leukemia to initiate. Moreover, association studies of environmental risk factors, such as maternal alcohol consumption during pregnancy, passive smoking, or magnetic fields, failed to elucidate the pathogenesis sufficiently [19-22]. Therefore, ionizing radiation is still the only fully validated risk factor for leukemia.

1.3 Classification System

The WHO currently defines only a small group of subtypes for both B- and T-cell acute leukemias [23]. However, a variety of different B-ALL subgroups with recurrent genetic alterations are established with constantly more emerging [24]:

- ETV6-RUNX1
- KMT2Ar
- BCR-ABL1
- DUX4r
- TCF3-PBX1
- ZNF384r
- MEF2Dr
- BCL-2/MYC
- NUTM1r
- HLF1r (most common TCF3-HLF1)

- iAMP21
- Ph-like
- PAX5 P80R
- IKZF1 N159Y
- ETV6-RUNX1-like
- KMT2A-like
- ZNF384-like
- CRFL2r
- High hyperdiploid
- Low hypodiploid
- Near haploid
- Low hyperdiploid
- Others

For T-ALL fewer recurrent alterations and subgroups have been described [25]:

- Early T-cell Progenitor (ETP)
- TLXr
- TLX1/NKX2.1
- TAL/LMO

Many of these genetic lesions could show prognostic and therapeutic relevance. Recently, these genetic subtypes became the focus of targeted therapy by searching for new targets implementing next-generation sequencing methods [26].

Besides recurrent genetic alterations, both B- and T-ALL can be divided by their expression of different clusters of differentiation (CD). However, until now the prognostic and therapeutic relevance is limited.

1.4 Clinical Presentation and Symptoms

With an incidence of around 4 per 100.000, ALL remains a rare disease in children [1]. The symptoms of an ALL are often unspecific, which makes the diagnosis tricky. It requires a detailed medical history and physical examination. If an ALL seems plausible, the illness can only be confirmed by a bone marrow puncture – an invasive and elaborate procedure. This diagnostic step is the gold standard. In a retrospective study analyzing data from the university hospital Duesseldorf, the medical history most often included exhaustion, skin or mucosal bleedings, and

a history of repeated infections as main clinical symptoms. Moreover, the examination often revealed hepatosplenomegaly alone or combined with lymphadenopathy respectively [27]. Other studies also elaborated on the importance of musculoskeletal symptoms at diagnosis [28]. The laboratory findings include anemia, thrombocytopenia, and an increase or decrease in white blood cell counts, while mostly more than one lineage is affected [16, 27]. Nevertheless, various organ infiltration, such as CNS infiltration, is possible. Thus, many different symptoms and laboratory findings are conceivable.

1.5 Diagnostic Steps and Methods

For the diagnosis of an ALL, several steps are needed. These steps should be performed in ascending order of invasiveness. Therefore, one of the first stages is peripheral blood sampling and investigating it with microscopy and flow cytometry. Although the microscopy of a blood smear is cheap and widely available, it requires experience. Its validity varies between investigators. Automated systems could objectify this method [29]. Flow cytometry is a reliable tool for detecting and predicting leukemia and its phenotype [30]. However, high costs and elaborate execution limit the wide usage, and flow cytometry is often only available at large centers. While peripheral blood sampling is essential for establishing a tentative diagnosis, the bone marrow puncture and investigation of the gained sample remains the gold standard. Moreover, lymphomas and leukemias may exhibit overlapping symptoms, leading to the need to distinguish them by evaluating the quantity of blasts present in the bone marrow. The threshold for an ALL is more than 25% blasts in the bone marrow [31]. Besides, the bone marrow aspirate is also used for several other methods, including chromosomal analysis, FACS, RT-PCR, and in recent years increasingly genomic- and proteomic methods [32]. After diagnosis, several other tests are required to evaluate organ infiltration. For preventing relapse, extramedullary infiltration sites have been proven to be of high importance [33]. Moreover, the blood-brain barrier represents an obstacle to sufficient therapy of leukemic blasts in the central nervous system. Therefore, a lumbar puncture is performed to determine blasts in the liquor, which significantly influences the treatment protocol [34]. Three different grades of CNS involvement are defined: “1” as no blasts detectable, “2” as <10 blasts detectable, and “3” as >10 blasts detectable. Furthermore, testing, for example, cardiovascular health is performed to determine a baseline for possible adverse events and patients’ fitness.

1.6 Therapy

1.6.1 Current Therapy

State-of-the-art therapy of ALL is a multidrug chemotherapy regime. International protocols vary slightly, but all show the same structure as the AIEOP BFM ALL protocol currently used in Germany: First, an induction is started, followed by a consolidation, reinduction, and finally, a maintenance phase. Moreover, different therapy branches are available depending on the lineage and prognosis of the disease. The here described protocol is the AIEOP BFM 2017 [34].

1.6.1.1 Induction Phase

This phase is equal for most patients. As soon as the diagnosis is made, the induction phase is initiated. The current AIEOP BFM ALL 2017 and the older 2009 protocol include a glucocorticoid prophase of one week with Prednisolone and one intrathecal dose of Methotrexate. After the first week, the Prednisolone response is measured as the blast percentage in the peripheral blood using flow cytometry. If the blast count is lower than 1000/µl, the patient is considered a Prednisolone good responder. In contrast, in less than 10% of the cases, the blast count remains elevated - a Prednisolone bad responder - and predicts a worse outcome for T-ALL[35, 36]. Therefore, these patients are enrolled in an intensified treatment branch, including one dose of Cyclophosphamide in the induction phase and a modified consolidation phase. Besides beginning the chemotherapy, this phase is also used for further biological testing to finalize the exact subtype and adapt the treatment protocol.

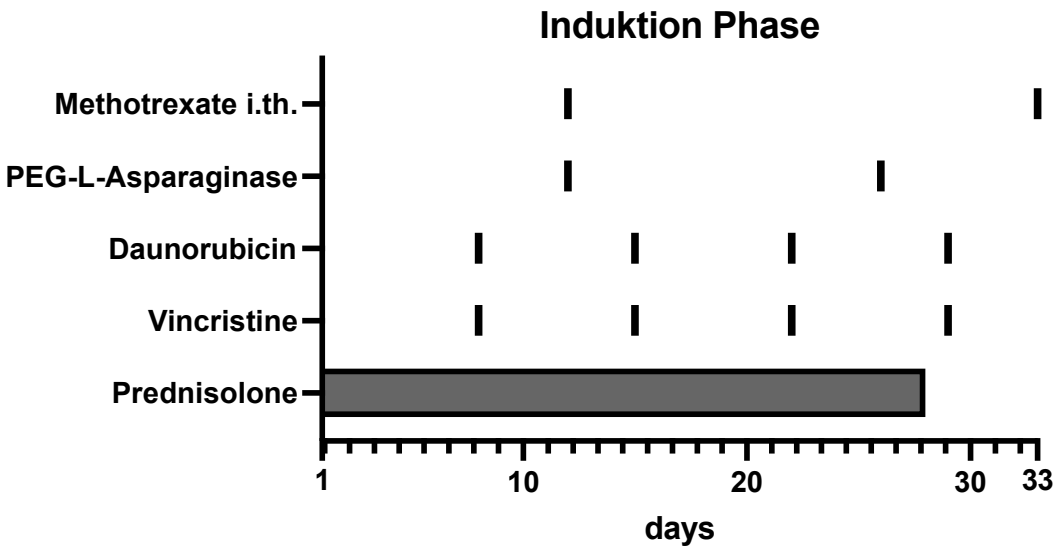

Figure 1 Outline of the treatment of ALL according to the AEIOP-BFM2017 protocol. Here displayed is the induction phase. Methotrexate is applied intrathecal (i.th.). Tapering of Prednisolone is not shown. Here shown outline is an example of a therapy for a standard-risk patient..

After the initial prophase, the multidrug phase is started, as shown in Figure 1. Hereby, the drugs Vincristine, Daunorubicin, and PEG-Asparaginase are administrated. Depending on the CNS status at diagnosis, two to four intrathecal doses of Methotrexate are additionally given. After the first induction phase, minimal residual disease (MRD) testing with PCR is performed in the BFM protocol. The measurement of minimal residual disease is completed with flow cytometry on day 15. Flow cytometry is a widely available and established technique to measure MRD. The measurement at day 15 is only used if the MRD-PCR data is unavailable. Next to clinical and biological factors, MRD is an essential tool for therapy stratification. Several studies could prove MRD as a prognostic factor for the outcome and risk of relapse [37-39].

1.6.1.2 Consolidation Phase

Depending on the results of the MRD testing after the induction – or if not available the results of the flow cytometry measurement on day 15 - further treatment is stratified. High variability between the different therapy arms can be observed. Especially in the high-risk subgroups, randomizations between different arms are performed. They are aiming to investigate new and improved strategies for these subsets. However, for all patients – even if they responded well in the induction phase – the therapy is intensified in the consolidation.

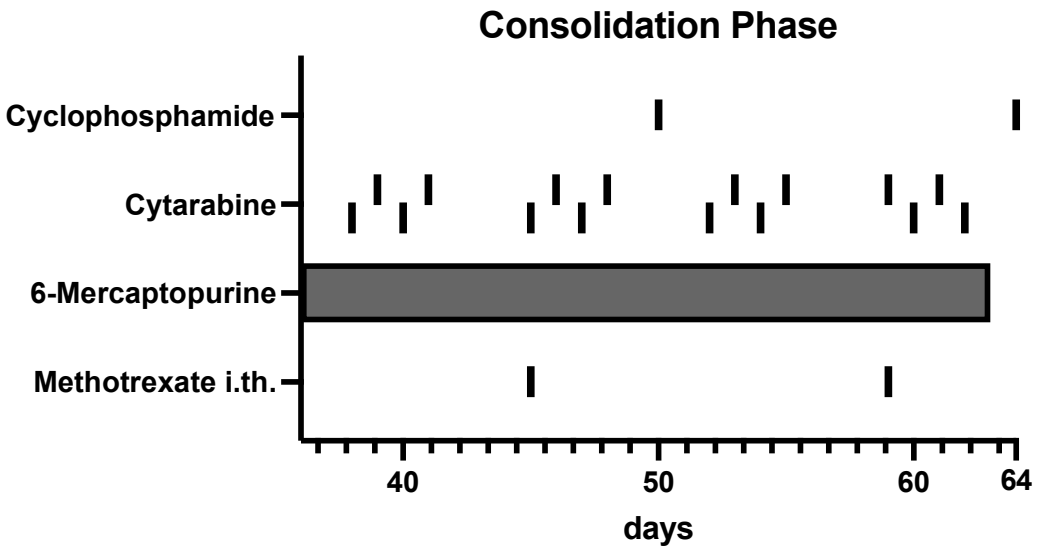

Figure 2 Outline of the treatment of ALL according to the AEIOP-BFM2017 protocol. Here displayed is the consolidation phase. Methotrexate is applied intrathecal (i.th.). Here shown outline is an example of a therapy for a standard-risk patient.

The basic consolidation phase includes Mercaptopurine with pulses of Cytarabine, Cyclophosphamide, and intrathecal Methotrexate, as seen in Figure 2. However, depending on the therapy response during the induction phase, the consolidation can be prolonged and enlarged with the following substances: Vincristine, Dexamethasone, PEG-Asparaginase, and Bortezomib. At the end of the consolidation phase, another MRD testing is performed. The results are essential for the last treatment stratification. Finally, for high-risk patients, the MRD decides on the indication of a hematopoietic stem cell transplantation.

1.6.1.3 Extracompartment Phase and High-Risk Blocks

The extracompartment phase is only administered to non-high-risk patients to clear out extramedullary blasts. To reach extramedullary blasts, drugs need to penetrate tissue well. Thus, the backbone of the extracompartment phase consists of high-dose Methotrexate and Mercaptopurine, as seen in Figure 3. Leucovorin rescue is additionally administered to prevent excessive adverse events. High-risk subgroups, however, will get high doses of different drugs in a complex sequence administered with several MRD tests, resulting in an allogeneic hematopoietic stem cell transplantation for most patients.

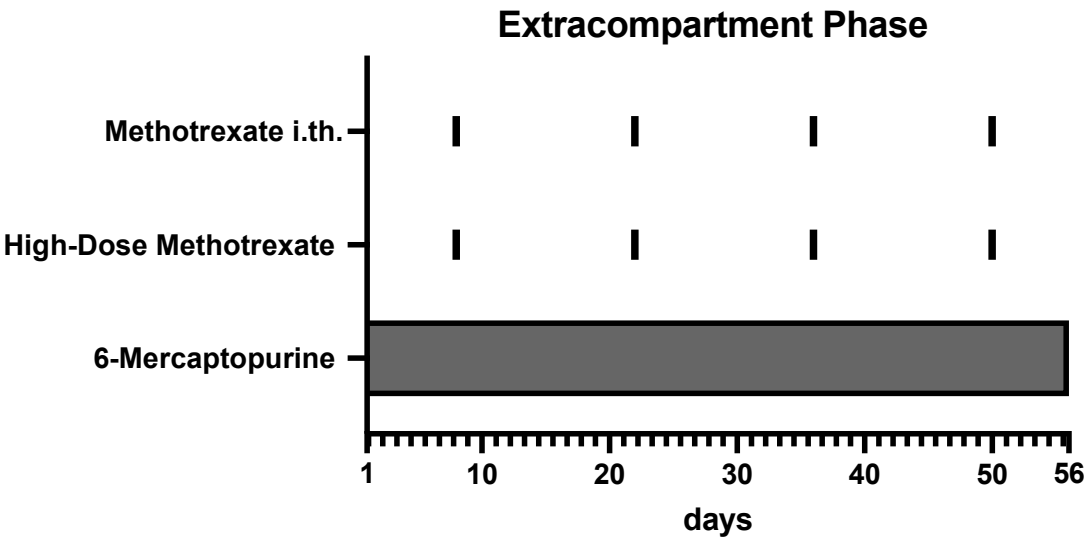

Figure 3 Outline of the treatment of ALL according to the AEIOP-BFM2017 protocol. Here displayed is the extracompartment phase. Methotrexate is applied intrathecal (i.th.). Here shown outline is an example of a therapy for a standard-risk patient.

1.6.1.4 Reinduction Phase

The reinduction phase is the last phase before starting the maintenance for all non-high-risk subgroups. It includes the kind of drugs of the induction with Dexamethasone exchanged for Prednisolone, Doxorubicin for Daunorubicin, and Cyclophosphamide, Cytarabine, and Thioguanine added, as seen in Figure 4.

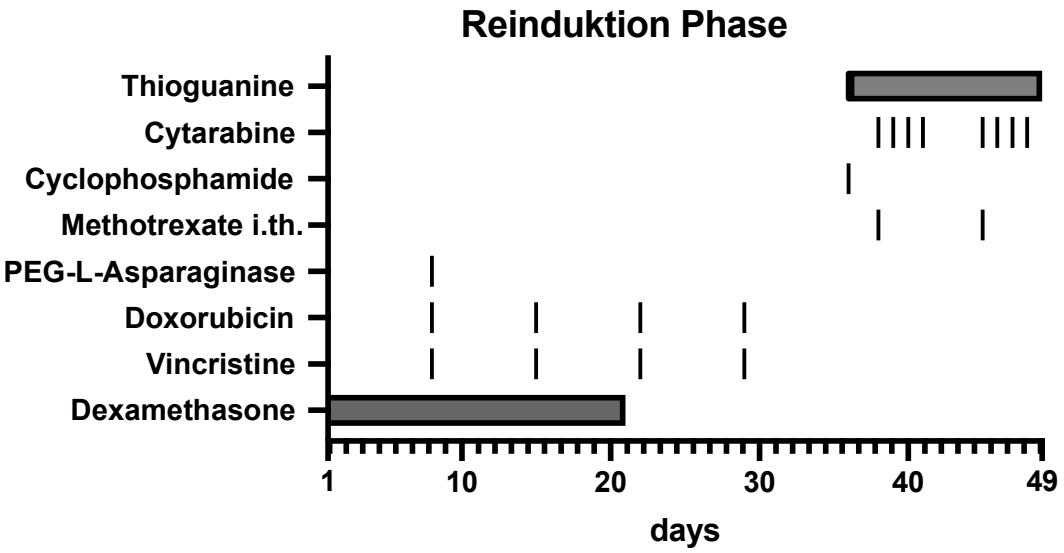

Figure 4 Outline of the treatment of ALL according to the AEIOP-BFM2017 protocol. Here displayed is the induction phase. Methotrexate is applied intrathecal (i.th.). Tapering of Dexamethasone is not shown. Here shown outline is an example of a therapy for a standard-risk patient.

1.6.1.5 Maintenance Phase

The total therapy for all patients takes two years, and after the last reinduction phase, the maintenance is begun. During this time, low doses of Mercaptopurine and Methotrexate plus six doses in six-week intervals of intrathecal Methotrexate are administered. In addition, a small subset of patients with CNS involvement above the age of four will receive cranial radiation.

1.7 Emerging Therapies

New therapies to treat acute leukemias and other malignancies emerge rapidly. Therefore, only targeted therapies of relevant proteins and pathways in acute leukemias were used in this work.

1.7.1 Classical Chemotherapeutics

Classical chemotherapeutics include antimetabolites, antimitotics, alkylating agents, topoisomerase inhibitors, and glucocorticoids. Antimetabolites are substances that mimic pyrimidine or purine bases, causing functional alterations, or acting as inhibitors to impede their synthesis. Thus, DNA replication is inhibited, and cell growth stops [40]. These antimetabolites are commonly used in chemotherapy protocols. The current therapy protocol for ALL includes at least four antimitotics: Cytarabine, 6-Mercaptopurine, 6-Thioguanine, and Methotrexate.

Antimitotics are taxanes or vinca-alkaloids, which inhibit cell proliferation by interfering with the spindle apparatus. As a result, cells cannot advance from the metaphasis [41]. One of these antimitotics, Vincristine, is currently also used in the induction and reinduction phase of the ALL treatment protocol.

Alkylating agents interact with the DNA directly. Cross-links and double-strand breaks inhibit DNA synthesis and replication [42]. Cyclophosphamide is a potent alkylating agent, that is currently used in the ALL treatment.

Topoisomerase inhibitors block the said protein and, therefore, also inhibit replication and cause double-strand breaks [43]. Topoisomerase inhibitors are often used in the therapy of leukemias and lymphomas. Moreover, Daunorubicin and Doxorubicin are currently used in the therapy of childhood ALL.

Lastly, glucocorticoids have several mechanisms of action which still need to be fully understood. They are reported to bind to intracellular receptors, which then alternate gene expression via NF-κB. As a result, the gene expression is changed to an anti-inflammatory state

in healthy cells. In malignant cells, the pathway to cell death is not understood yet [44]. Glucocorticoids are often the backbone of the therapy of lymphoid malignancies. Therefore, Prednisolone and Dexamethasone play a crucial role in the treatment protocol of ALL.

While these drug classes are not new, effective combinations and new application forms are current research matters.

1.7.2 Epigenetic Modifiers

The group of epigenetic modifiers consists of HDAC inhibitors (HDACi), EZH2 inhibitors (EZH2i), and BET bromodomain inhibitors. HDAC inhibitors block the enzymatic activity of histone deacetylases, preventing the removal of acetyl groups from histone proteins. Histone acetylation plays a crucial role in regulating gene expression by modulating chromatin structure. By increasing histone acetylation, HDAC inhibitors promote a more open chromatin conformation, allowing for enhanced gene transcription. The approved HDAC inhibitors currently in use are primarily pan-HDAC inhibitors, capable of targeting all isoforms of HDAC. However, ongoing research initiatives focus on the design of HDAC isoform-specific inhibitors, aiming to alleviate the toxicity concerns often associated with pan-HDAC inhibitors [45]. EZH2 inhibitors exert their effect by preventing the methylation of histone H3, which subsequently leads to the restoration of transcriptional activity [46]. BET bromodomain inhibitors target key regulators in gene transcription. Especially, BRD4 has been the focus of preclinical drug development for its role in transcription initiation, elongation, and enhancement [47].

1.7.3 Proteome Affecting Drugs

This group consists of two classes: Proteasome and HSP90 inhibitors (HSP90i). Proteasomes are proteins that degrade others and contribute 80% of protein turnover. Through its connection to many relevant signaling pathways, cell cycle regulators, and tumor suppressors, proteasomes became an attractive target for drug development [48]. HSP90 is part of a protein complex relevant to the correct folding of proteins. It interacts with over 400 client proteins involved in crucial pathways for cancer cell survival. In addition, oncoproteins such as BCR-ABL1 have been described to be stabilized by HSP90, making inhibitors of HSP90 an attractive target [49].

1.7.4 Signaling Pathway Inhibitors

Signaling pathway inhibitors target essential kinases relevant for cell survival and proliferation, such as Aurora kinase A, Polo-like kinase (PLK), cyclin-dependent kinases (CDK), epithelial growth factor receptor (EGFR), FMS-like tyrosine kinase 3 (FLT3), PI3K, AKT, mTOR,

Janus kinase (JAK), RAS, RAF, MAPK, Bruton´s tyrosine kinase (BTK), and BCR-ABL1. Aurora kinase A is an oncogene that plays a role in tumorigenesis and mitosis. Moreover, it interacts with other signaling pathways relevant to leukemia, such as PI3K and WNT signaling. Thus, inhibiting Aurora kinase A could target leukemic cells through different mechanisms of action. The most popular Aurora kinase A inhibitor, Alisertib, is currently in a phase III trial [50]. Similarly, PLKs are also serine/threonine kinases with key regulatory roles in mitosis on different levels. PLK1 is the best studied isoenzyme. Besides its role in mitotic initiation and execution, it interacts with signaling pathways, such as PI3K/AKT/mTOR. While Volasertib also inhibits other kinases accounting for adverse drug effects, BI2536 seems to inhibit PLK1 more specifically [51].

CDKs are well-regulated kinases that initiate the transition from G1 to S phase in the cell cycle, interacting with transcriptional factors like E2F and tumor suppressors like Rb. CDKs are activated by pathways often dysregulated in cancer, such as RAS/RAF/MAPK, PI3K/AKT/mTOR, WNT/beta-catenin, and JAK/STAT. In healthy cells, CDKs are well-regulated endogenously. In cancer cells, CDKs are often down- or upregulated. Inhibition of CDKs has shown senescence induction as expected, as well as immune-modulatory effects and metabolism changes. Immune modulation is attributed to CDKi-mediated MHC upregulation and interferon induction. Altered gene expression of CDK inhibition most likely changes the metabolisms [52].

EGFR is a membrane-based signaling receptor that binds epithelial growth factor (EGF). Upon binding EGF, the receptor activates the RAS/RAF/MAPK pathway, which mediates cell survival and proliferation. EGFR overexpression and mutations are common in solid tumors. Immunotherapies and small molecule inhibitors have been established to treat solid tumors. Small molecule inhibitors targeting EGFR or other polypeptide growth factor receptors have also been described to be effective against leukemic cell lines [53].

FLT3 is a class III receptor tyrosine kinase first detected in 1991 [54-56]. In early B-cell development, FLT3 is expressed and promotes proliferation and inhibition of differentiation [57, 58]. A variety of downstream kinases are associated with this receptor. These include the RAS-, PI3K-, and JAK/STAT-pathway [58-60].

The PI3K/AKT/mTOR pathway is often misregulated in B- and T-ALLs. In B-ALL, fusion proteins like the BCR-ABL1 and ETV6-RUNX1 directly activate the pathway. In T-ALL, negative regulators – mainly PTEN – are frequently mutated. Thus, consecutive activation of this pathway leads to proliferation and chemotherapy resistance [61]. Numerous small molecule inhibitors have been developed to target PI3K, AKT, or mTOR and are currently tested in treating ALL [62].

JAK and its target STAT are one of the most important pathways in early hematopoiesis. Various stimuli from growth hormones, cytokines, and other hormones activate it. The pathway activation mediates cell survival, stem cell maintenance, self-renewal, and immune cell development through hematopoiesis. Thus, activating mutations exist in ALL and acute myeloid leukemia (AML) [63].

The RAS/RAF/MAPK pathway is central to human malignancies. With 20% of all cancers having mutations in RAS, this pathway is often dysregulated, leading to cell survival, proliferation, and differentiation [64]. In addition, the pathway plays an important role in tumorigenesis in solid and hematological cancers. Mutations in this pathway have been reported to mediate an adverse survival of patients, making it an interesting target for small molecule inhibitors [65].

BTK is a kinase with a central function in B-cell receptor and Toll-like receptor signaling. Upon activation by PI3K or SYK, BTK phosphorylates PLCγ. MYC, NF-κB, and NFAT are consecutively activated through different pathways. Altered gene expression then causes proliferation, survival, differentiation, migration, antibody class switch, and cytokine production. The FDA approved the first BTK inhibitor Ibrutinib in 2014, paving the way for targeting BTK in B-cell malignancies [66].

BCR-ABL1 is a consecutive active tyrosine kinase that phosphorylates several signaling pathways in leukemic blasts [67]. The aberrant protein BCR-ABL1 can be targeted with tyrosine kinase inhibitors (TKi). The first drug of this group – Imatinib – was first described to show specific effects against the oncoprotein BCR-ABL1 in 1996 [68]. However, newer generations of TKis display higher affinity and can overcome some of the most prominent mutations that cause resistance to earlier generations [69].

1.7.5 Others

Besides the earlier explained targets, inhibitors against PARP, BCL-2, NF-κB, and IDH have emerged. PARP is an enzyme that is primarily active in DNA damage response. Moreover, both double- and single-strand breaks are repaired by PARP. Therefore, it has overlapping functions with BRCA in the homologous recombination repair in double-strand breaks. Thus, the loss of function of both proteins leads to multiple double-strand breaks, resulting in cell death. As BRCA is frequently mutated in acute leukemias, PARP could be a promising target for inhibition for these patients [70].

BCL-2 is an antiapoptotic protein. While proapoptotic proteins of the BH3, BAX, and BAK families disrupt the mitochondrial outer membrane integrity, BCL-2 and other anti-apoptotic proteins bind the pro-apoptotic proteins. In healthy cells, the balance between pro- and anti-apoptotic proteins is essential, preventing the development of mutated cells. While malignant cells often upregulate BCL-2 proteins to evade apoptosis. Moreover, this leads to chemotherapy resistance which could be overturned by BCL-2 inhibitors like Venetoclax [71].

NF-κB is a transcription factor that induces proliferation, differentiation, and survival upon activation. It is activated either by the canonical or non-canonical pathway. The canonical pathway is enabled by various stimuli such as pro-inflammatory cytokines, antigens, or cellular stress. The non-canonical pathway, on the other hand, is enabled through a restricted number of stimuli belonging to the tumor necrosis factor (TNF) family [72]. In ALL, most cases show a consecutive activation of the canonical pathway [73]. Thus, inhibition of NF-κB is a logical approach to treating ALL.

IDH is an enzyme of the citric acid cycle that catalyzes the conversion of isocitrate to α-ketoglutarate. IDH mutations often occur in AML – and less frequently in ALL. These mutations can lead to a new function of the enzyme, catalyzing α-ketoglutarate to R-2-hydroxyglutarate (R-2-HG). R-2-HG competes with α-ketoglutarate as a coenzyme for many proteins, causing epigenetics and cell signaling changes [74].

1.8 Challenges in the Treatment of ALL

The present treatment approach for ALL encounters two key hurdles: Firstly, childhood cancer survivors are burdened with adverse drug events and long-term impairments that persist throughout their lives. Secondly, high-risk subtypes of ALL are struggling to achieve satisfactory treatment outcomes. Targeted therapies emerge as a potential solution to these challenges, as they hold the potential to enhance treatment effectiveness while minimizing side effects.

1.8.1 Adverse Events and Long-Term Deficits

Polychemotherapy to treat ALL causes acute and long-term adverse events. Around 3% of patients die due to acute adverse events during treatment [75, 76]. The most common acute adverse events are infections, which are also the primary cause of death [75, 76]. The myelosuppression through chemotherapeutic agents and dysplastic leukemic lymphocytes consolidates these infections. Other non-lethal infections - such as oral mucositis - are also often observed during treatment with Methotrexate and are a significant burden [77]. Further,

polychemotherapy causes anemia and thrombocytopenia, which usually requires transfusion on a regular base. Moreover, neurological adverse events, especially headaches, are experienced. Rarer but severe neurological adverse events include seizure, encephalopathy, cerebrovascular diseases, movement disorders, cranial and peripheral neuropathy, spinal cord syndromes, plexopathy, and myopathy [78]. L-Asparaginase is associated with pancreatitis during treatment [79]. Hepatic and renal damage or failure occur as acute and long-term adverse events [80]. Long-term adverse events are experienced by almost every survivor of childhood cancer above the age of 50 [81]. ALL-survivors suffer from cardiovascular, pulmonary, neurological, and metabolic disorders, as well as growth deficits and secondary neoplasms, [81, 82]. Thus, treatment-related toxicity not only influences the quality of life of cancer survivors but challenges the health economy [83].

Several gene polymorphisms are known to influence the toxicities of chemotherapy. However, only variants of TPMT and NUDT15 are clinically accepted and available for testing [84]. These variants are associated with increased toxicities towards thiopurine-based drugs. Patients carrying either of these polymorphisms need dose reductions up to only eight percent of the original dose [78, 79]. Many other variants relevant to the treatment of ALL have been reviewed by Maamari et al. [85].

Clinical implementation of newfound pharmacogenetic variants is challenging. Firstly, most studies only investigate gene variants in the context of single drug use, while drugs are combined during treatment [85]. Secondly, most studies focus on the effect of variants in exons, while only a few explore the role of other variants, such as miRNAs [86]. Finally, searching routinely for various gene variants before treatment would be time-consuming and very expensive. Therefore, faster and cheaper methods that study pharmacogenetic toxicities in cell-based models would be appreciated.

1.8.2 High-risk Subgroups

This thesis features four different high-risk B-ALL subgroups. These high-risk subgroups are KMT2Ar, BCR-ABL1, Ph-like, and TCF3-HLF:

1.8.2.1 KMT2Ar

Rearrangements of the gene KMT2A define this subgroup. KMT2A, formally known as the mixed-lineage leukemia (MLL) gene, encodes for a protein involved in epigenetic regulation [87]. Over 100 different translocation partners have been described, but most often, AF4 is

translocated with KMT2A in B-ALL [88]. KMT2Ar B-ALL often co-express myeloid markers, such as CD13, CD33, and CD65 [89, 90].

KMT2Ar B-ALL is most often in infants and indicates a very poor prognosis [91, 92]. The 6-year overall survival is estimated at 58 to 62% [93]. Moreover, the poor prognosis is due to resistance to chemotherapy, especially glucocorticoids and L-Asparaginase [94, 95].

1.8.2.2 BCR-ABL1

Blasts of the BCR-ABL1 subgroup are defined by the presence of the Philadelphia chromosome t(9;22). The resulting protein is a consecutive active tyrosine kinase that activates downstream pathways promoting proliferation [67]. Additionally, BCR-ABL1 B-ALL often shows alterations in the IKAROS gene [96]. IKAROS alterations are associated with a worse outcome and convey a resistance even to TKis [97, 98].

The BCR-ABL1 subgroup presents itself slightly differently than other ALLs. The relative incidence of BCR-ABL1 ALL increases with age up to almost 50 % in patients older than 44 years [99]. Further characteristics include a high leucocyte count and an increased incidence of CNS involvement at diagnosis [100].

1.8.2.3 Ph-like

The Ph-like subgroup shows similar gene expression as BCR-ABL1 ALLs but lacks the Philadelphia chromosome. In 2009, den Boer et al. and Mullighan et al. first described this subgroup [101, 102]. Several kinase alternations have been reviewed, resulting in different activated pathways [103]. Similarly to the BCR-ABL1 subgroup, it is associated with a poorer outcome [92].

1.8.2.4 TCF3-HLF

The TCF3-HLF1 is a rare subtype with a bad prognosis. The subtype accounts for around 1% of childhood ALLs and was first described by Raimondi et al. in 1991 [104]. Moreover, patients relapse very early during treatment, and this disease almost always ends fatally in the first two years after diagnosis [105]. A poor prognosis was ascribed to RAS mutations conveying a resistance towards drugs used in induction therapy [106, 107].

1.8.3 Medium-risk Subgroups

Aside from the high-risk subgroups, two medium-risk subgroups are featured in this work. The first group is the T-ALLs. The second group is the TCF3-PBX1 B-ALL.

1.8.3.1 T-ALL

T-ALL are leukemias that arise from T-cell precursors as opposed to the other here-described subgroups that belong to the B-cell lineage. Around 15% of all ALL cases derive from the T-cell lineage [2]. Like B-ALLs, T-ALLs can be subdivided into early T-cell precursor ALL (ETP-ALL), pro-T-ALL, pre-T-ALL, cortical-T-ALL, and mature-T-ALL based on the expression of the CDs. However, these different differentiation stages have proven unable to predict the outcome of pediatric patients effectively [108]. However, T-ALL also displays recurrent alterations, enabling further division into subgroups [109]. Unlike their B-ALL counterparts, studies showed conflicting prognostic relevance of these recurrent alterations. Therefore, T-ALL biomarkers only play a subordinate role in the diagnostic workflow of many therapy protocols [110]. Only MRD has proven effective in predicting the outcome and relapse risk [111].

Since T-ALL patients tend to be older, have higher white blood cell counts at diagnosis, and show more CNS involvement, their outcomes are always lacking behind those of B-ALLs [112]. In addition, unfavorable biological features are more common in T-ALL [113]. Finally, whenever T-ALLs relapse, the therapeutic options are very limited as immunotherapies and targeted inhibitors are often explicitly designed for B-ALLs [114]. Moreover, T-ALL is considered an independent prognostic factor for an unfavorable outcome in relapsed ALL [115]. Thus, finding new targets or agents that can be repurposed is immensely important for these patients.

1.8.3.2 TCF3-PBX1

The translocation t(1;19) results in the TCF3-PBX1 fusion protein, which displays an individual gene expression profile. This translocation occurs in around 5% of childhood B-ALLs [15]. While the fusion protein cannot initiate leukemia alone, mutations of different signaling pathways and cell cycle regulators were explored [116]. Moreover, Diakos et al. uncovered a direct interaction of the fusion protein with signaling pathways and other regulators [117]. Recent clinical studies with intensified chemotherapy have shown an improvement in the outcome of this subtype [118].

1.9 Drug Screening

Phenotypical drug testing is an established method first used almost half a century ago. However, integrating modern techniques allowed upscaling and more reliable usage, resulting in high throughput drug screenings (HTDS) [119]. Compared to techniques used to search for new targets, the advantage is the direct identification of potential agents. In opposition, genetic approaches could identify a magnitude of mutations, which are to some extent druggable, but

failed in predicting cancer-specific drug response alone [120, 121]. Drug Screening of patient-derived samples together with commercially available cell lines or independently could already identify new targets in several studies [106, 120, 122-126]. These studies could also verify their targets using different methods, underlining the potential of phenotypical screenings in target detection. For example, BCL-2 inhibitor Venetoclax was described to target AML blasts efficiently *in vitro* and in xenograft models [127]. Several clinical trials followed, proving Venetoclax as safe and active, especially in combination with hypomethylating agents [128-130]. As a result, this drug was approved for a specific subset of AML patients [131]. This is one successful example to demonstrate the potential of HTDS.

1.10 Study Aim

This thesis aims to explore two distinct applications of high-throughput drug screening:

1. Investigating Inter-individual Drug Response and Its Relationship to Clinical Adverse Events:
    - Utilizing a pipeline for drug screening patient-derived fibroblasts to analyze and distinguish inter-individual drug responses.
    - Exploring potential connections between the inter-individual drug responses observed in fibroblasts during high-throughput drug screening and the clinical adverse events experienced by each individual.
2. Identifying Novel Treatment Agents for High- and Medium-Risk Leukemia Subgroups Using Leukemia Cell Lines and Patient-Derived Samples:
    - Assessing the predictive capability of selected ALL subgroups for their overall drug responses.
    - Employing a three-way approach to analyze high-throughput drug screening results for the finding new agents for high- and medium-risk leukemia subgroups:

      a. Comparing each subgroup to healthy controls.

      b. Comparing each subgroup to all other leukemia subgroups.

      c. Combining the results from both approaches.

2 Material and Method

2.1 General Material

Table 1 Common devices and consumables used.

Devices and Consumables	***Supplier***
Axiovert 40C Microscope	Carl Zeiss
Fresco 21 centrifuge	Thermo Fisher Scientific
Incubator	Binder
Mechanical single- and multichannel pipettes	Eppendorf
Milli-Q Water Purification Systems	Merck Milipore
Mr. Frosty Freezing Container	Thermo Fisher Scientific
Multifuqe 4KR	Thermo Fisher Scientific
Pipetboy acu pippet aid	Integra
Vi-CELL BLU	Beckman Coulter
Vi-CELL XR	Beckman Coulter
Cell culture flasks T25/T75 and culture plates 6-, 12-, 24-, and 96-well	Greiner Bio-One
Centrifuge tubes 15 ml/ 50 ml	Greiner Bio-One
Cryogenic Vials	Corning
Serological pipette 25 ml/ 10 ml/ 5ml (Cellstar)	Greiner Bio-One
-80°C Ultra freezer	Thermo Fisher Scientific
Laminar flow hood	Thermo Fisher Scientific

2.2 Cell Culture

All cells were cultured at 37°C and under 5% CO2. A media consisting of DMEM GlutaMAX supplemented with 20% FBS and 1% Penicillin/Streptomycin was used to culture primary patient fibroblasts. Whereas RPMI1640 GlutaMAX media supplemented with 15% FBS, 60 µl of 55 mM 2-Mercaptoethanol in DPBS, 3 ml of 100 mM Sodium Pyruvate, and 500 µl of 50 mg/ml Gentamicin was used for culturing all leukemia cell lines, primary patient samples and patient samples grown in a xenograft mouse model (PDX). T-cells and T-ALLs PDXs, however, were

cultured in T-cell Expansion Media supplemented with 50 ng/ml SCF, 10 ng/ml IL-2, 10 ng/ml IL-7, 10 ng/ml IGF-1, and 10 ng/ml EGF [132]. Peripheral blood-derived mononuclear cells (PBMCs) were cultured in Mononuclear Cell Medium. Finally, CD34-positive hematopoietic stem and progenitor cells (HSPCs) were cultivated with a media consisting of IMDM supplemented with 10% FBS, 25 ng/ml IL-6, 25 ng/ml SCF, and 25 ng/ml FLT3-L. All cell lines were obtained either as frozen stocks (DSMZ) or from cooperation partners. Short tandem repeat (STR) profiles were performed to ensure the cell lines' authenticity. All sample collections were approved by the ethics vote No. “4886R” and “2019-566-andere Forschung erstvotierend”.

Table 2 Components of media and other reagents used for cell culture

Component	***Supplier***	***Catalog Number***
DMEM GlutaMAX	Gibco	31966-021
Fetal Bovine Serum	Sigma-Aldrich	121031
Penicilin/Streptomycin	Gibco	15140-122
RPMI Medium 1640 GlutaMAX	Gibco	61870-070
2-Mercaptoethanol	Gibco	21985023
Sodium Pyruvate	Gibco	11360070
Gentamicin Regent Solution 50mg/ml	Invitrogen	15710064
LymphoONE T-cell Expansion Xeno-free Medium	Takarabio	WK552S
Recombinant Human SCF	PeproTech	300-18
Recombinant Human IL-2	PeproTech	200-02
Recombinant Human IGF-1	PeproTech	100-11
Recombinant Human EGF	PeproTech	AF-100-15
Recombinant Human IL-7	BioLegend	581904
Recombinant Human IL-6	BioLegend	570804
Recombinant Human FLT3-L	PeproTech	AF-300-19
IMDM Iscove´s Medium	Gibco	12440-053
Mononuclear Cell Medium	PromoCell	C-28030
TrypLE Express Enzyme	Gibco	12605010
Cryo-SFM	PromoCell	C-29910
DMSO	Sigma-Aldrich	D2438
DPBS	Sigma-Aldrich	D8537

2.2.1 Cell Thawing

Frozen vials were thawed in a water bath for approximately 30 seconds and then transferred to a centrifugal tube. Next, 10 ml of media was added before centrifuging at 400xg at room temperature for 5 minutes to reduce the toxic effect of the DMSO in the freezing media. Subsequently, the supernatant was discarded, and the cell pellet was diluted in media to diminish the concentration further. Afterward, the cell suspension is added in a T25 culture flask, laid on the side for adherent cells such as fibroblasts, positioned vertically for suspension cells such as cell lines, or added on feeder layers of mesenchymal stem cells (MSCs). Finally, they were conveyed into the incubator. After the first day of thawing, the media was replaced to discard the remaining DMSO.

2.2.2 Cell Culture of Fibroblasts

Once the adherent fibroblasts covered the whole bottom of the flask, the cells were split either into one T75 culture flask or two T75 culture flasks, depending on the confluency percentage. Concretely, the supernatant was filled into a centrifugal tube, and 2 ml of TrypLE Express was filled in the T25 and 4 ml in the T75, respectively. After incubating the culture flask for approximately 5 minutes at 37°C, the cells were detached by gently tapping the flask. Next, the mixture of TrypLE and cells was added to the centrifugal tube with the media and spun down at 400xg at room temperature for 5 min. Finally, the supernatant was discarded, the cell pellet diluted in 15 ml or 30 ml of media, respectively, and added in one or two T75 cell culture flasks. Once two T75 cell culture flasks are fully grown, one is used for cryopreservation, while the other is used for HTDS and a cell pellet.

2.2.3 Cell Culture Leukemia Cell Lines

Cell lines were cultured vertically in small T25 culture flasks, with one exception (CCRFCREM) placed horizontally. New media was supplied every 3-4 days or when the media turned yellow while keeping the total volume in the T25 flasks as low as possible and not over 15 ml to supply the cells with sufficient nutrients while maintaining oxygen diffusion. Thus, cells required splitting once per week. Concretely, the suspension was aspirated, discarded, and new media was added.

2.2.4 Cell Culture B-ALL PDX and Primary Samples

MSCs were cultured for at least two weeks on 6-well plates before adding the leukemia blasts to ensure a confluent feeder layer. Primary and PDX samples were either thawed from reserves stored in liquid nitrogen or directly cultured after extraction. After the last step of the isolation or washing, the cell pellet is dispersed in media and added to the feeder layer. At least twice a week, new media was added, and once a week, the whole media was changed. This was accomplished by centrifuging the supernatant at 90xg for 10 min at room temperature to minimize the cells' stress and remove apoptotic cells. During this time, a low volume of media was added to the wells to keep them from drying out.

2.2.5 Cell Culture of T-ALL Samples

The cell culture of T-ALL samples was accomplished similarly to the B-ALL cocultures. However, MS5-HDLL1 cells were seeded out in DMEM with 20% FBS and grown until around 90% confluent. Subsequently, the feeder layer was treated with 10 µg/ml of Mitomycin C for 3 hours, inhibiting further growth. After washing three times with DPBS and letting the cells recover for 24 hours, the T-ALL samples were thawed and added to the T-ALL media. During culture, the media was changed every 3-4 days.

2.2.6 Cryopreservation and Cell Harvesting

To make cryopreservation of cells (cryos) or pellets for further experiments, at least five million cells for leukemia cell line or primary leukemia or PDX grown sample and around two million cells for fibroblasts were withdrawn from the culture. Adherent fibroblasts or MSCs were detached using TrypLE Express precisely as described above. Leukemia cells cultured with a feeder layer were gathered using the supernatant with the blasts while preserving the adherent feeder layer. After obtaining, cells were spun down at 400xg, 20°C, and resuspended in freezing media consisting of 45% culture media, 45% FBS, and 10% DMSO. Subsequently, the suspension is fit into each freezing vial and finally kept in an isopropanol bath for at least 24h at -80 °C before transferring them to liquid nitrogen for long-term storage. On the other hand, the cell pellet is washed two times with 1ml of 4°C cold PBS after centrifugation at 400xg, 4°C for 5 minutes each time, the supernatant is discarded, and the dry cell pellet is flash frozen using liquid nitrogen.

2.3 Isolation of Cells from Peripheral Blood or Bone Marrow

2.3.1 Material

Table 3 Material needed for isolating cells from peripheral blood or bone marrow.

Material	***Supplier***	***Catalog Number***
Ficoll-Paque	GE-Healthcare	17-1440-03
Ammonium chloride lysis buffer	UKD pharmacy	-
EasySep Human Cd34 Positive Selection Kit II	StemCell Technologies	17856
EasySep Magnet	StemCell Technologies	18000

2.3.2 Isolation of Blasts and PBMCs

Fresh primary samples had to be segmented into their components to retrieve the leukemia blasts before being cultured or used on the HTDS pipeline. This was performed by Ficoll-Paque separation. In detail, the blood or bone marrow aspirate is diluted 1:1 with PBS and slowly added to 15 ml of Ficoll-Paque. As a result, two layers can be seen, on the bottom, the Ficoll-Paque, and on top, the diluted blood or bone marrow. This is carefully transferred to a centrifuge and spun at 400xg for 20 minutes at room temperature, with the breaks turned to the lowest possible setting. After centrifuging, the following layers are visible from top to bottom: plasma mixed with other components, a small layer of PBMCs, followed by Ficoll-Paque, and a pellet of erythrocytes and granulocytes. The PBMC layer is then taken while the rest can be discarded. Next, the PBMC layer was diluted with 25 ml PBS and spun at 400xg for 5 minutes at room temperature with the brakes on. Subsequently, the cell pellet is dissolved in ammonium chloride for erythrocyte lysis if the pellet is visibly red. To avoid any toxic effect of ammonium chloride, another centrifugation washing step with PBS was performed with the same settings mentioned above. The resulting blasts or PBMCs could be used for culturing or further experiments.

2.3.3 Isolation of Healthy T-cells

A Ficoll-Paque separation of peripheral blood was carried out as described above. T-cells were cultured under the same conditions as the T-ALL patient samples, except feeder cells were not used. T-cells were cultured in the same media as T-ALL, using T-cell Expansion Media supplemented with 50 ng/ml SCF, 10 ng/ml IL-2, 10 ng/ml IL-7, 10 ng/ml IGF-1, and 10 ng/ml

EGF [132]. In a first trial experiment, a lymphocyte percentage measured by flow cytometry after one week of culture was over 99%, with 90% of the total being CD3-positive T-cells. However, further experiments have shown exhaustion of the proliferation capacity and a decrease in cell viability after approximately one week. Therefore, a time point for HTDS was opted for, in which the cells are still proliferating with the sacrifice of the relative number of T-cells measured by FACS. Thus, T-cells were implemented on the HTDS pipeline after three days of culturing. At this point, between 51% to 64% of all cells expressed CD3. In theory, after three more days of culturing during the HTDS, CD3 expression could be expected to be as high as in the trial experiment.

2.3.4 B-cells

Lymphoblastoid Cell Lines (LCLs) were derived from B lymphocytes of healthy donors and immortalized using Epstein Barr virus (EBV) at the BioBank Service, Gaslini Hospital, Genova, Italy, as detailed in a previous publication [133]. These B-LCLs were provided by Dr. Cazzaniga (Centro Ricerca M. Tettamanti, Pediatrics, University of Milano Bicocca, Monza, Italy).

2.3.5 Isolation and Culturing of CD34+ Cells

CD34 cells were isolated from cord blood after Ficoll-Paque separation (mentioned above) by incubation with a cocktail of Fc-Blockers and magnetically labeled CD34 antibodies, following the manufacturer's protocol (StemCell). Hereafter, magnetically labeled cells were added to the separation columns. Then, in sequential washing steps, the cells not expressing CD34 are poured off, while the CD34-positive cells stay in the separation columns fixed to a strong magnet. After several washing steps, the cells were picked up in the CD34 culturing media and transferred to a 24-Well culture plate, where the media was changed every three days.

A trial experiment was performed using MACS isolation, and hematopoietic stem cells could be expanded up to 37.8-fold. However, reproducibility was low, and cells differentiated fast, decreasing the amount of CD34-positive cells after one week to around 40%. Therefore, different kinds of media were tested, and the isolation method was changed. IMDM with 10%FBS, 25ng/ml IL-6, 25ng/ml SCF, and 25ng/ml FLT3-L showed the highest proliferation rate. At the same time, another media could prevent the cells from differentiating better but did not expand the cells to numbers that could be utilized for HTDS. Lastly, the Stemcell EasySep kit was used, reducing the cell´s stress during isolation.

2.4 Viability and Cell Count Determination

The Beckmann Vi-CELL XR or Vi-CELL BLU accomplished viability and cell count determinations. More precisely, 500 µl or 200 µl were removed from the cell suspension, respectively, and added to a counting tube. This was placed into the automated counting machine, which identifies the viability and cell count using the trypan blue staining method. For further experiments, the number of viable cells was the basis for preparations for defined concentrations of cell suspension. If the automated cell counting was unavailable, cells were diluted 1:1 in Trypan Blue and counted with a Neubauer counting chamber. The cell number was then calculated after counting four major squares in the following manner:

$$cell\ count[10^6/ml] = \frac{n*10000}{2\ ml}$$; n=counted cells

2.5 High-Throughput-Drug-Screening

2.5.1 Materials

Table 4 Materials used for the high-throughput-drug-screening.

Material	***Supplier***
D300e Digital Dispenser	Life Sciences Tecan
Multidrop Combi Reagenzien-Dispenser	Thermo Fisher Scientific
Spark 10m	Life Sciences Tecan
384-well Low Flange White Flat Bottom Polystryrene TC-treated Microplate	Corning
1536-well White Polystyrene TC-treated Microplate	Corning
D300e dispensehead cassettes D4 Plus and T8 plus	Life Sciences Tecan HP
384-well white/clear flat bottom, square wells microplate	Corning
Parafilm M	Sigma-Aldrich
CellTiter-Glo 2.0 Cell Viability Assay	Promega
Ethanol 80%	Otto Fischer GmbH & Co. KG
Multidrop small tube metal tip dispensing cassette	Thermo Fisher Scientific

Material	*Supplier*
Multidrop standard tube dispensing cassette	Thermo Fisher Scientific

2.5.2 Aliquoting the Library

To increase the reproducibility and to eliminate freezing-thawing cycles of compounds used to print several versions of the high-throughput library, all compounds were ordered freshly and were aliquoted in one day. Ordered in 10mM stocks in DMSO with a volume of 100 µl, 15 aliquots of 5 µl each were produced. Moreover, the library was aliquoted on white 384-optic well plates using the Eppendorf research pro or Multipette combined with the combi-tips advanced. Additionally, the compounds were sorted from top to bottom, but every second row was left empty, enabling the usage of a multichannel pipette for printing the compounds on the plates later. Four spots were left blank, making small changes between versions possible. Finally, to reduce the activity loss of certain compounds through light exposure, the light of the sterile working bench was turned off. The whole process took approximately twelve hours, at which the compounds were kept at room temperature. Afterward, the plates were wrapped in parafilm and vacuumized, reducing evaporations before being stored at -80°C.

2.5.3 Library Printing

At first, either one of the stock plates with the compounds was thawed at room temperature in the dark or kept on ice, and the remaining compounds were added. Afterward, the computer connected to the Tecan D300e digital dispenser with the printing program was started. While for version 6.1, the stock plate stayed on the ice and was diluted right before the compounds were used, for the following versions, the stock plates were diluted utilizing the Multidrop combi dispenser and remained at room temperature for the whole printing process. The stock plate was diluted for all versions from 5µl of 10 mM to 2.5 mM for each compound. Each compound is printed in six logarithmic concentrations: 8 nM, 50 nM, 223 nM, 1 µM, 5 µM, and 25 µM. Additionally, 24 to 32 wells were filled with DMSO as a control. Moreover, each well is normalized to a volume of 40 nl with DMSO. The outer two to three wells were left empty to avoid the effects of evaporation. The transfer of the compounds from the stock plate to the printing cassettes was performed with a Multichannel pipette. However, the volume pipette onto the cassette was higher than required to prevent running out of the compound for the last plates. Also, the printing was executed throughout the night, reducing the time the compounds were at room temperature and avoiding potentially additional freezing-thawing cycles. As a result, around 60 high-throughput-drug-screening plates could be produced in each version,

taking about 24 hours. Ultimately, all plates are wrapped in parafilm and vacuum sealed before storing at -80°C. To secure the quality of each version, a HTDS with one cell line was conducted, and the previous version was compared with the newly printed version.

2.5.4 Linear Range Experiments

At the end of the HTDS, a CellTiter-Glo (CTG) Viability assay (Promega) is carried out. Since this assay results in a luminescent signal that takes advantage of the ATP produced by the cells in each well, it correlates with the viability. More precisely, the CTG reagent consists of firefly luciferase and luciferin- the substrate. But the reaction needs ATP, which is provided by the cells in this assay. Moreover, the amount of ATP correlates with the number of viable cells. Thus, this assay can be used to determine the viability of cells. However, cells proliferate slower at higher densities or the viability can even be reduced at very high or very low concentrations. Therefore, a linear range experiment was conducted to determine the range of densities at which the proliferation rate of the cell suspension can be assumed consistent without compromising the viability without any compounds added.

2.5.4.1 Linear Range Experiment for Leukemia Cells

An experiment for the cell lines was conducted with six commercially available cell lines and one PDX sample. Each sample was pipette onto a white 1536-well plate with 4 µl per well in 10 different densities in triplicates. The following densities were aimed for in a dilution series pipetted with the Eppendorf Research Pro: 8000, 5000, 4000, 3000, 2000, 1000, 800, 600, 500, and 300 cells per well, respectively. Increasing reproducibility, cells were filtered before being utilized for the dilution series. Furthermore, for this experiment, only cell lines with a viability of over 85% were used while attempting to increase the experiment's validity by including cell lines from different subgroups of acute leukemias. In addition, media was filled in the outer wells with the Multidrop combi dispenser, preventing evaporation effects on the plate. After incubation of the plate at 37°C under 5% CO2 for 72h – similar to the actual HTDS conditions – the plate was removed from the incubator, and a CTG assay was performed. In detail, the Multidrop combi dispenser was washed with ethanol and water before 1:1 diluted CTG reagent with PBS was primed into the tubes. Next, the plate was filled with 4 µl of CTG reagent per well and shaken for 30 seconds, ensuring cell lysis. Subsequently, the plate is incubated at room temperature for 10 minutes in the dark to stabilize the signal before using the Tecan 10M Spark to measure the luminescent signal. Moreover, an integration time of 100 ms per well was applied. Afterward, the data was plotted in a linear regression model. Step by step, the extreme densities were excluded from the calculation, aiming for the highest possible R^2.

2.5.4.2 Linear Range Experiment for Fibroblasts on 1536-well Plates

A linear range experiment was conducted for the fibroblasts similar to the one for leukemic cell lines with some modifications. Firstly, only two fibroblast lines were used, one healthy and one primary patient. Moreover, twelve different densities – 3000, 2000, 1500, 1000, 800, 600, 400, 300, 200, 150, 100, and 50 cells/well - were applied. All cell suspensions were prepared in 2 ml Eppendorf tubes before seeding them onto the plate because the Multidrop combi dispenser was used instead of a pipette. By selecting the desired rows and placing each hose in a different Eppendorf tube, 30 replicates for each concentration were printed on the plates. Finally, the incubation and readout with the CTG assay were executed as described previously.

2.5.4.3 Linear Range Experiment for Fibroblasts on 384-well Plates

As the linear range experiments from the 1356-well plates could not be translated to a smaller format in a previous experiment by other members of the working group, a separate experiment was implemented, again very similar to the linear range experiment of the leukemic cell lines with slight modifications: Firstly, the following concentrations (cells/well) were seeded in six replicates with 30 µl per well: 10000, 7500, 5000, 4000, 3000, 2500, 2000, 1500, 1000, 750, 500, and 100. Furthermore, only three fibroblast cell lines were included, of which two were already used in the linear range determination for 1536-well plates. Moreover, the readout was performed by adding 30 µl of CTG assay reagent diluted 1:4 with DPBS onto the plate and setting the Tecan 5M Spark to an integration time of 500 ms. The data analysis, however, was done similarly.

2.5.5 High-Throughput-Drug-Screening of Fibroblasts

At first, the cells were detached and counted as described before. Afterward, 1.25 to 1.8 million cells were removed from the original cell suspension and centrifuged at 400xg at 20°C for 5 minutes. Subsequently, the cell pellet is dissolved in 10 ml of fresh culture media and filtered through a 40 µm cell strainer. Moreover, the Multidrop combi dispenser is started and washed using ethanol, followed by distilled water and DPBS. Next, the prepared cell suspension was primed into the tubing, and 4µl per well was seeded onto a beforehand thawed HTDS plate. If more than one cell line is screened at the same time, in between different cell lines, the tubing is cleaned using DPBS. The plate is then incubated at 37°C under 5% CO2 for 72 hours. Once this time was over, the Multidrop was again washed with ethanol and water before 4 µl per well of the CTG reagent, diluted 1:1 with PBS, was added. After shaking the plate for approximately 30 seconds and letting the luminescent signal stabilize for 10 minutes at room temperature in the

dark, the Tecan 10M Spark was harnessed for measuring. Moreover, an integration time of 100ms per well was applied.

2.5.6 High-Throughput-Drug-Screening of Leukemia Cells

Fundamentally speaking, the HTDS of leukemic samples was executed similarly to the one described for the fibroblasts. However, three modifications were implemented: Firstly, suspension cell lines did not have to be detached and could be harvested as described previously. Secondly, the cell count of the prepared suspension was raised to 0.5 million cells per ml for growing cell lines in culture and increased even higher to at least 1 to 1.5 million cells per ml for fresh samples, respectively. At last, the cells were strained using a 20 µm cell strainer. This had two advantages: on the one hand, the leukemic cells are smaller, and therefore low mesh size filters prevent cell clumps, while on the other hand, unwanted co-culture cells such as MSCs could be filtered out to a certain extent.

Table 5 Display of the ALL samples screened based on their subgroups and cell origin.

	T-ALL	KMT2Ar	Ph-like	BCR-ABL1	TCF3-PBX1	TCF3-HLF1
commercial cell lines	DND41	ALLPO	MUTZ5	KCL22	697	HAL01
	HBPALL	KOPN8	MHHCALL4	K562	RCH-ACV	
	KOPTK1	SEM		SUPB15	Kasumi-2	
	CCRFCEM	RS4;11				
	HSB2					
	P12					
	PEER					
	Jurkat					
	Loucy					
	PF382					
	RPMI8402					
	SUPT1					
	Molt4					
PDX and primary samples	PS30	PS01	PS07		PS15	PS18
		PS02	PS08		PS16	PS19
		PS03	PS09		PS17	PS20
		PS04	PS10			
		PS05				
		PS06				

2.5.7 Protocol Plates for Fibroblasts

These plates were designed to recapitulate the protocol IA of the AIEOP ALL BFM 2017 regime. Therefore, the following single drugs and combinations were tested for in technical triplicates:

Table 6: Drugs and concentrations on the protocol plates for fibroblasts.

Drug/Combination	***Number of wells***	***Highest concentration [µM]***	***Lowest concentration [µM]***
Prednisone	9	100	0.005
Vincristine	9	10	0.0005
Daunorubicin	9	100	0.005
MetHothrexate	9	100	0.005
L-Asparaginase	9	10	0.0005
All combined	10	8.8 (Prednisone) 0.028 (Vincristine) 4.4 (Daunorubicin) 2.0 (Methotrexate) 4.0 (L-Asparaginase)	0.022 (Prednisone) 0.0007 (Vincristine) 0.011 (Daunorubicin) 0.005 (Methotrexate) 0.01 (L-Asparaginase)
Prednisone + Vincristine + Daunorubicin	10	30.0 (Prednisone) 1.0 (Vincristine) 15.0 (Daunorubicin)	0.15 (Prednisone) 0.005 (Vincristine) 0.075 (Daunorubicin)
Prednisone + Methothrexate + L-Asparaginase	9	15.4 (Prednisone) 3.5 (Methotrexate) 7.0 (L-Asparaginase)	0.022 (Prednisone) 0.005 (Methotrexate) 0.01 (L-Asparaginase)

The plates were normalized to 1% DMSO and randomized individually. In the combination wells, the concentrations of the drugs to each other were steady. According to the IA protocol, the concentration of Prednisolone was twofold higher than Daunorubicin, while MTX was 2.2-fold lower, Vincristine 157.14-fold lower, and L-Asparaginase 1.1-fold lower concentrated in comparison to Daunorubicin. The concentration for L-Asparaginase was calculated by dividing the indicated IU by the specific activity of the L-Asparaginase ordered from Medchem Express. After printing the plates, they were stored at -20°C. The HTDS was performed as described above

for fibroblasts. The only modification was a cell concentration of 200 cells/well -as determined in the linear range experiment - in a volume of 30µl. Upon the readout, the CTG was diluted 1:4 in DPBS and dispensed 1:1 on the plate.

2.5.8 Data Analysis

The raw data was sorted for each compound and normalized to the DMSO wells. A non-linear regression model (log(inhibitor) vs. normalized response) with variable slope was applied in GraphPad Prism to determine the IC50 values. Furthermore, the multivariant DSS3 was calculated in R for a more exact comparison of different drug responses [134]. Heatmap visualization was also performed in R, plotting DSS values with unsupervised clustering of the compounds and the samples. “Euclidean” was utilized as a distance clustering computation, while “ward.D2” was computed for the unsupervised clustering method. [135]

2.6 FACS Analysis

2.6.1 Materials

Table 7 Materials used for FACS analysis of samples.

Materials	***Supplier***	***Catalog Number (Clone)***
CytoFLEX	Beckman Coulter	-
CytoFLEX Sheath Fluid	Beckman Coulter	B51503
APC anti-human CD79a	BioLegend	333506 (HM47)
APC/Fire 750 anti-human CD10	BioLegend	312230 (HI10a)
FITC anti-human IgM	BioLegend	314506 (MHM-88)
Pacific Blue anti-human CD19	BioLegend	302224 (HIB19)
PE anti-human CD179a	BioLegend	347404 (HSL96)
Alexa Flour 700 anti-Human CD22	BioLegend	302520 (HIB22)
PE/Cyanine7 anti-human CD20	BioLegend	302311 (2H7)
PE/Dazzle 594 anti-human CD34	BioLegend	348209 (581)

Materials	***Supplier***	***Catalog Number (Clone)***
PerCP/Cyanine 5.5 antihuman CD38	BioLegend	356613 (HB-7)
PE anti-human CD13	Beckman Coulter	A07762 (SJ1D1)
APC anti-human CD45	BioLegend	368512 (2D1)
APC anti-human CD3	BioLegend	300312 (HIT3a)
FITC anti-human CD4	BioLegend	317408 (OKT4)
Pacific Blue anti-human CD8	BioLegend	344717 (SK1)
Permeabilization buffer	Thermo Fisher Scientific	00833356
IC Fixation Buffer	Thermo Fisher Scientific	00822249

2.6.2 Surface Marker Staining

10^5-10^6 Living cells were washed two times with DPBS and stun down at 400xg for 5 min at room temperature. After the last washing step, the supernatant was again discarded, and the pellet was dissolved in 100µl of DPBS. The FACS Antibody was added to this solution, and the mixture was incubated for at least 20min at 4°C in the dark. Afterward, the cells were again washed with DPBS once and immediately read out with the Cytoflex.

2.6.3 Intracellular Staining

After the last washing step, as described above, the pellet was dissociated in IC Fixation Buffer and incubated for 30 min at room temperature in the dark. After centrifuging and discarding the supernatant, the pellet was washed with 200µl of 1X Permeabilization Buffer. Afterward, the pellet was assimilated in 100µl of 1x Permeabilization Buffer and the respected FACS antibody. This was incubated for 30min at room temperature, protected from light. In the end, the sample was rewashed and diluted in the 1X Permeabilization Buffer before being read out with the Cytoflex immediately.

2.7 Clinical Data Extraction

General patient information such as age at diagnosis, diagnosis, the subtype of leukemia, treatment protocol, and treatment response were analyzed. However, a suitable period for data gathering had to be defined to determine adverse events suffered by a patient and compare it to the HTDS. As the first 33 days of the AIEOP BFM 2009 and 2017 protocol match each other and only minimal modifications are implemented for high-risk leukemias, the highest number of

comparable subjects could be expected for this period. However, since the following chemotherapy admission starts on day 36, the period was extended to that date. All guide values were extracted from the CTCAE v.5 as grade 3 or higher adverse events [136]. In detail, the following adverse events were analyzed:

Table 8 Overview of the adverse events analyzed for each patient. All guide values were taken from the CTCAE V.5. Only grade 3 or higher adverse events were measured.

Hepatotoxicity			
ALT/GPT	**AST/GOT**	**gammaGT**	**Bilirubin (total)**
>120U/l?	>145U/l?	>225U/l?	>3mg/dl?
if yes, how many?	if yes, how many?	if yes, how many?	if yes, how many?
if yes, highest value?	if yes, highest value?	if yes, highest value?	if yes, highest value?

Myelosuppression		
Hb	**Leukocytes**	**Thrombocytes**
Hb <8g/dl	Leukocytes <2.000/µl	Thrombocytes <50.000/µl
if yes, how many?	if yes, how many?	if yes, how many?
if yes, lowest value?	if yes, lowest value?	if yes, lowest value?

Neurotoxicity				
seizure?	enzephalopathy?	cerbrovascular disease?	ataxia/ movement disorders?	cranial neuropathy?
spinal syndrome?	plexopathy?	peripheral neuropahty?	Gullian-Barre-Syndrome?	myasthenia?

others		
Serious infection with proof of germs	**Pancreatitis**	**Mucositis**
yes/no?	Clear diagnosis?	Hospitali-zation necessary?
if yes, how many?		if yes, how many?

2.8 Statistical Analysis

All analyses were conducted with GraphPad Prism Version 9 or R studio. A likelihood of a type one error below 5% was interpreted as significant if not otherwise mentioned.

2.8.1 Analysis of Fibroblast HTDS

Firstly, drugs that were inconsistent in the different library versions were excluded from further analysis. Next, drugs that showed no effect in any sample were deleted before outliers were detected. DSS values of over one and a half times the interquartile range added or subtracted to the third or first quartile were defined as outliers, respectively. Moreover, groups were characterized by searching for DSS values exceeding the 0.2 or 0.8 quintiles. To determine the significance of the groups, a non-parametric Kolmogorov-Smirnov-Test of distribution was conducted. Correction for the accumulation of the type one error when testing multiple hypotheses was done with the Bonferroni-Dunn method. At last, drugs for which outliers or significant groups could be calculated but showed a range between the highest and lowest value below 10 DSS points were eliminated.

2.8.2 Analysis of HTDS Data from Leukemia Samples

The mean values of the subgroups were subtracted with the highest value of the healthy controls finding potential drugs for future treatment. Moreover, a non-parametric Mann-Whitney U-test was performed between the subgroups. A score for every drug was calculated by awarding one point for each significant test against another subgroup, suggesting a more specific targeting with a higher score. Afterward, these results were combined with the comparison with the healthy controls. The violin plots were computed using R and the “ggplot2” package [137]. The Kruskal- and Wilcox-Test were performed with the “rstatix” package. The Bonferroni method was used to correct for multiple testing. For detecting possible drug combinations, spearman correlation was computed and displayed using the “corrplot” package in R [138]. Lastly, a Mann-Whitney-U-test – without correction for multiple testing – was assessed for the samples with CD13 or IgM against the non-expressing samples.

2.8.3 Correlation of HTDS Data and Clinical Data

DSS values were computed using the mean viability for each concentration. Furthermore, spearman correlation was performed and plotted using the “corrplot” package in R [138]. With this, the “number of AE categories” was defined as the total amount of different – above described- adverse events detected. On the other hand, the “total number of AE” displays the sum of all incidents of adverse events (AE); for example, anemia was often experienced more than once. In the other categories, the highest or lowest values, respectively, were used.

2.8.4 Heatmaps and Principal Component Analysis

Heatmaps were calculated with R studio using the packages “ComplexHeatmap”, “RColorBrewer”, “dendextend”, “dendsort”, and “colorspace” [135]. The number of rows and columns split was manually assigned. The methods “Euclidean” and “Ward.D2” were used for the unsupervised clustering. The principal component analysis was also performed with R studio using the “ggplot2” and “factoextra” packages [139]. Scaling was not applied when calculating the principal component analysis.

3 Results

3.1 Establishment

3.1.1 Enhanced Methodology Improves Reproducibility in High-Throughput Drug Screening (HTDS)

When first testing the library for its reproducibility between two different printing cycles, it appeared that significant improvement would be needed as the correlation was at only R^2=0.16 (Figure 5A).

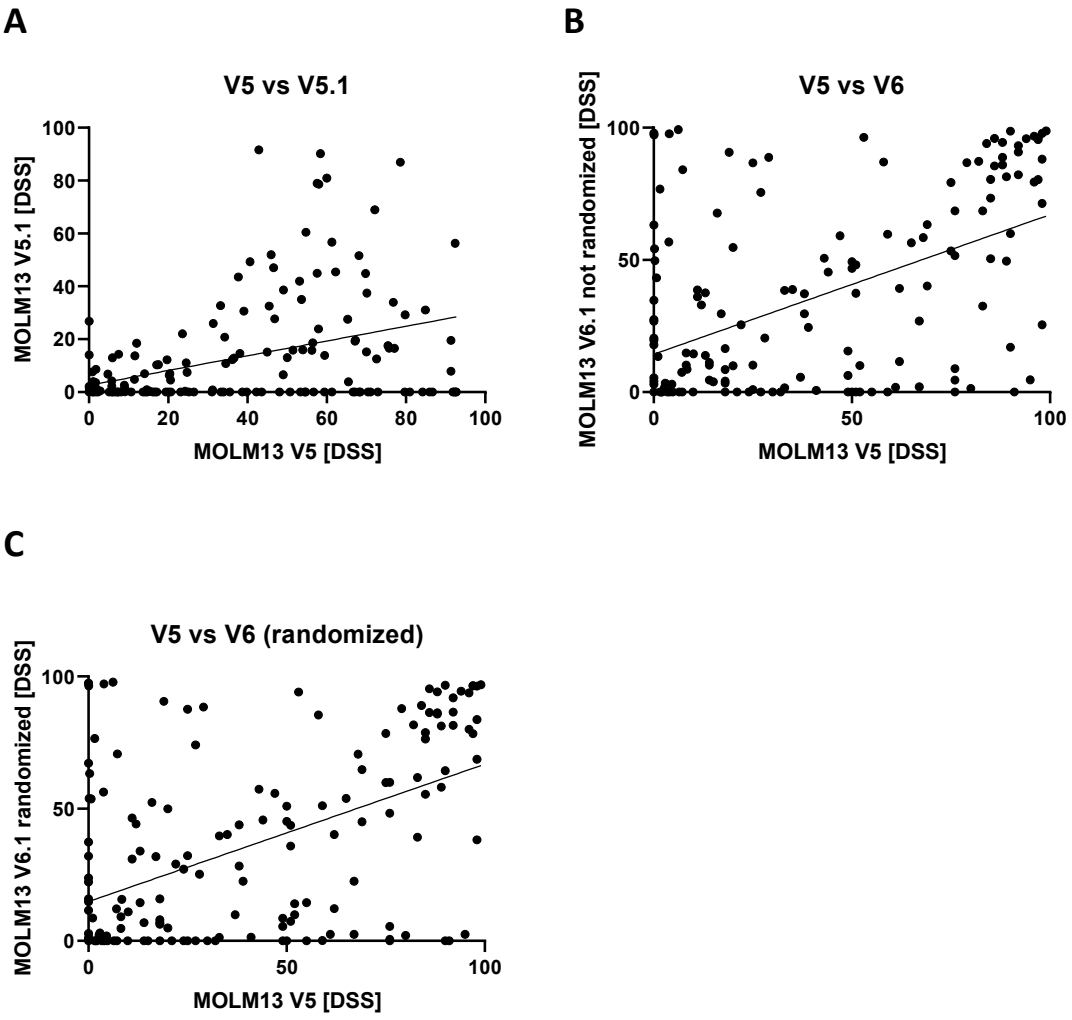

Figure 5 Visualization of the linear regression for comparing different versions of the libraries using the DSS values. (A) Comparing versions 5 and V5.1 with the old compounds (Equation: Y=0.2789*X + 2.580, R^2=0.16). (B), (C) Comparison of the old library V5 with the newly ordered library V6.1. While (B) uses the unrandomized plates

(Equation: Y=0.5279*X + 14.31, R^2=0.27), (C) implements the data from the randomized plates (Equation: Y=0.5200*X + 14.84, R^2=0.27).

Two main reasons seemed to cause the low reproducibility: First, the compounds used at the time were thawed and frozen several times, reducing the activity each time. Secondly, to avoid working throughout the night, the plates were frozen in the middle of the printing round and thawed the next day. This decreased the activity of up to half a plate and enlarged the plate effect. Thus, the whole library was ordered newly and aliquoted in one day. Each aliquot was only used once, reducing thawing and freezing cycles. Moreover, printing was performed in one session. Subsequent comparison of the old and new libraries resulted in a very low correlation (R^2=0.27), as seen in Figure 5B-C. Interestingly, some new drugs showed lower activity than in the old library. Possible explanations could be another company chosen and differences between the specific batches. Next, the plates' reproducibility and whether randomization could increase it were tested. While the correlation of two technical replicates showed a high correlation with R^2=0.99, astonishingly, randomization decreased it marginally ($R^2_{randomized}$=0.97; difference=0.02) (see Figure 6A-C).

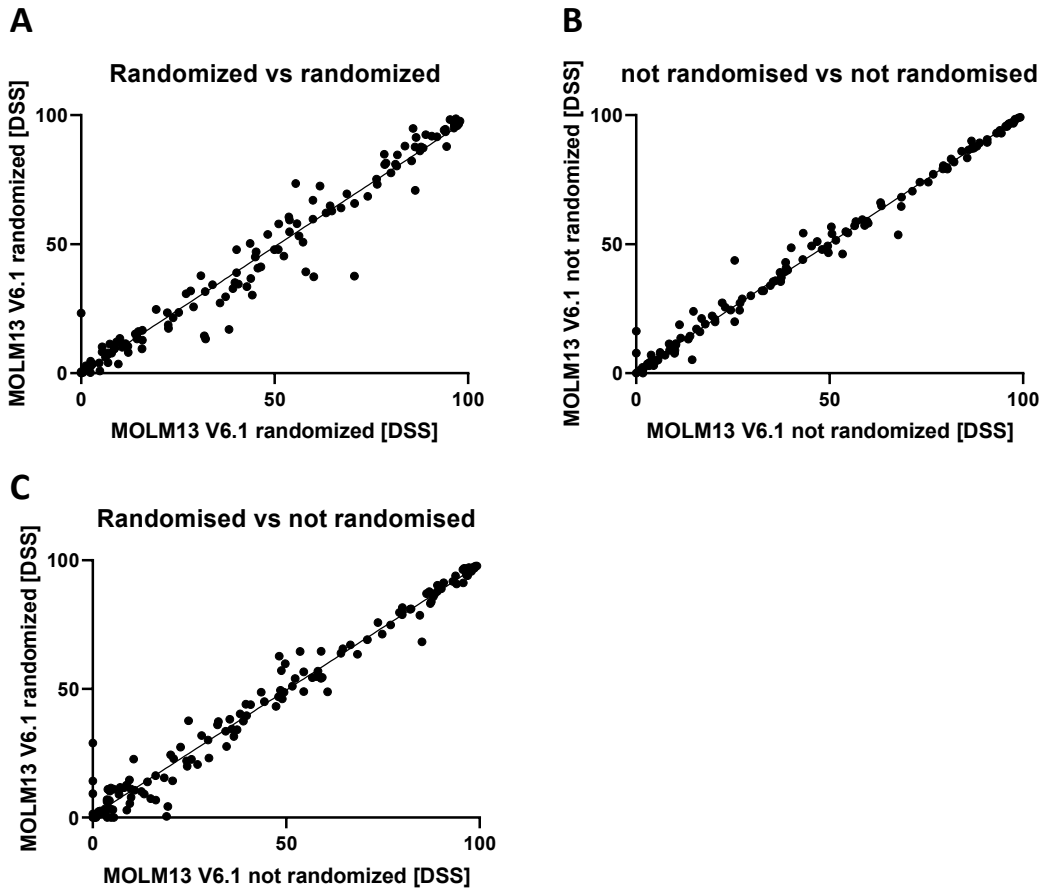

Figure 6 Visualization of the linear regression for comparing technical replicates using the DSS values. (A), (B), and (C) display the reproducibility in one version on randomized and not randomized plates, as well as the comparison of unrandomized and randomized plates (Equation (A): Y=0.9849*X - 0.2239, R^2=0.97; Equation (B): Y=0.9927*X + 0.7314, R^2=0.99; Equation (C): Y = 0.9762*X + 0.6886, R^2=0.98).

Since the randomization was time-consuming, technically challenging, and prone to human mistakes, it was decided to forgo it. After human errors caused the second printing round to be unusable, the protocol was further developed. Thus, the aliquot would be initially diluted and kept at room temperature for the printing session. The following comparison of the first and third versions showed a high correlation (R^2=0.95), suggesting good reproducibility between different printing rounds (see Figure 7A). The correlation of subsequent versions using the same improved protocol showed values near those of technical replicates in one version ($R^2_{V6.3\text{-}V6.4}$=0.98; $R^2_{V6.4\text{-}V6.5}$=0.91; $R^2_{V6.5\text{-}V6.6}$=0.91) (see Figure 7A-D). Therefore, the reproducibility of the HTDS in one or more versions can be presumed.

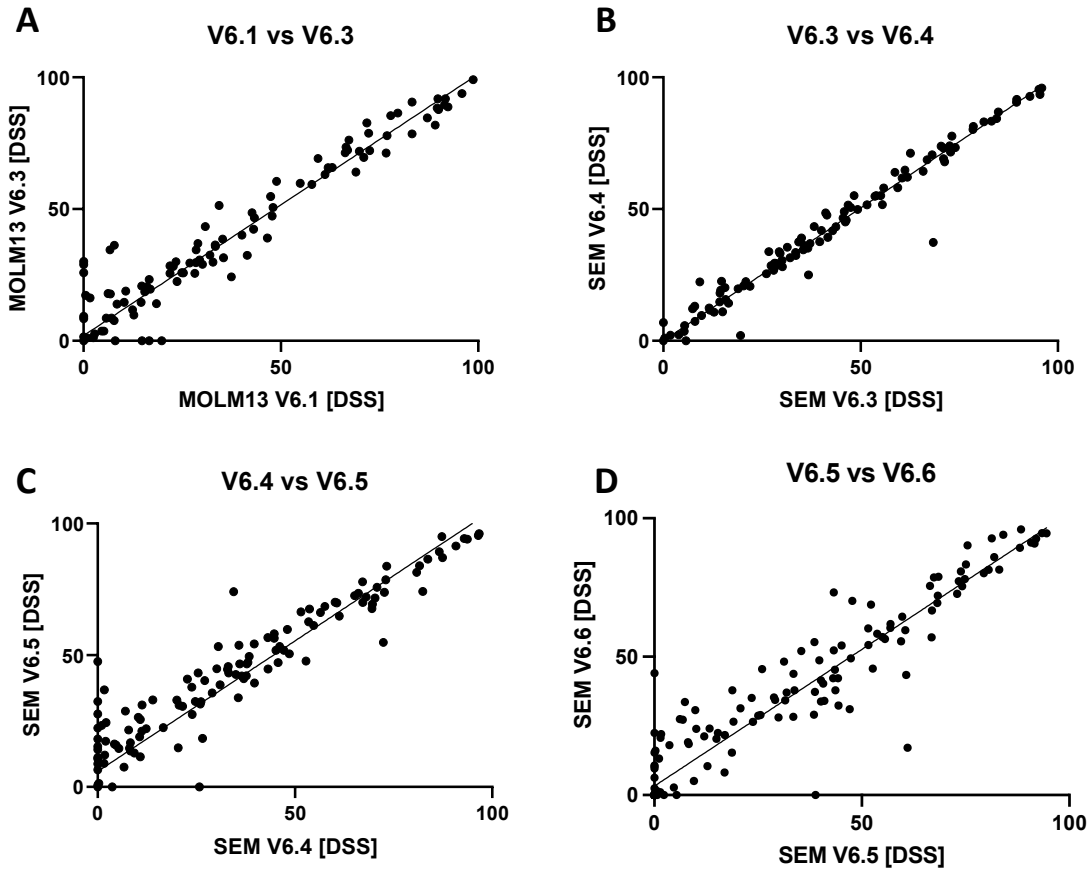

Figure 7 Visualization of the linear regression for comparing different versions of the library and technical replicates using the DSS values. (A), (B), (C), and (D) show the correlation of subsequent versions of the library (Equation (A): Y = 0.9924*X + 1.973, R^2=0.95; Equation (B): Y = 1.003*X + 0.3132, R^2=0.98; Equation (C): Y = 0.9907*X + 5.902, R^2=0.91; Equation (D): Y = 0.9865*X + 3.282, R^2=0.91).

3.1.2 Linear Range Experiment for Fibroblasts on 1536-well Plates

Technical issues were faced during the linear range experiment as evaporation was not considered beforehand. Thus, the outer three wells had to be excluded from further analysis resulting in an uneven number of replicates per condition. However, a good data basis can be assumed because the number of replicates still ranged from 14 to 38. One cell line showed an unusual signal decrease for two conditions. The most reasonable explanation is a technical issue during sample preparation. Nevertheless, the collected data suggest a linear range of fibroblasts up to 800 cells/well (Figure 8C). A higher cell count per well would reduce background noise and inaccuracies caused by small disparities during cell seeding. Therefore, a concentration of the high end of the linear range was chosen for the experiments.

3.1.3 Linear Range Experiments for Protocol-based Plates to Screen Fibroblasts

For the 384-well plates, however, the linear range only could be assumed until 2000 cells/well (Figure 8B). Moreover, an acceptable signal was observed for all conditions, although 100 cells/well were barely over the set threshold of 100,000 RLU. In the first experiment, two different time points (72h vs. 144h) were compared with one sample. While the overall IC50 values were lower for the longer time point, only two of the five drugs showed activity. Therefore, one more plate with the same sample was seeded at a lower cell count of 200 cells/well. With these conditions, an activity of L-Asparaginase could also be noticed. Both Prednisone and Methotrexate were inactive, even at very high concentrations. Prednisone was not expected to have a cytotoxic effect on fibroblasts, while high concentrations of folic acid in the media presumably antagonized Methotrexate.

3.1.4 3.1.3 Linear Range Experiments for Leukemia Blasts

By testing leukemia cell lines and a PDX sample of different subgroups, linearity until 800 cells/well ($0.2*10^6$ cells/ml) could be noticed (Figure 8A). Unfortunately, this experiment was conducted after many HTDS were already done at a higher cell count. Besides, the DMSZ advises not to split most cell lines below concentrations of $0.5*10^6$ cells/ml. Thus, cells could be unspecific sensitive at lower concentrations. Moreover, higher numbers of cells per well reduced background noise - as stated above – and reduced the effect of small technical inaccuracies during cell seeding, which could be even more significant for fast-proliferating cells. To summarize, due to the increase of the concentration to $0.5*10^6$ cells/ml, the cells are not in the linear range of the CTG assay but could show a more specific response with higher reproducibility. While *in vitro* grown samples were screened at this concentration, freshly available samples had to be seeded at a higher cell count of 1.0 to $1.5*10^6$ cells/well to archive signals over the threshold of 10,000 RLU.

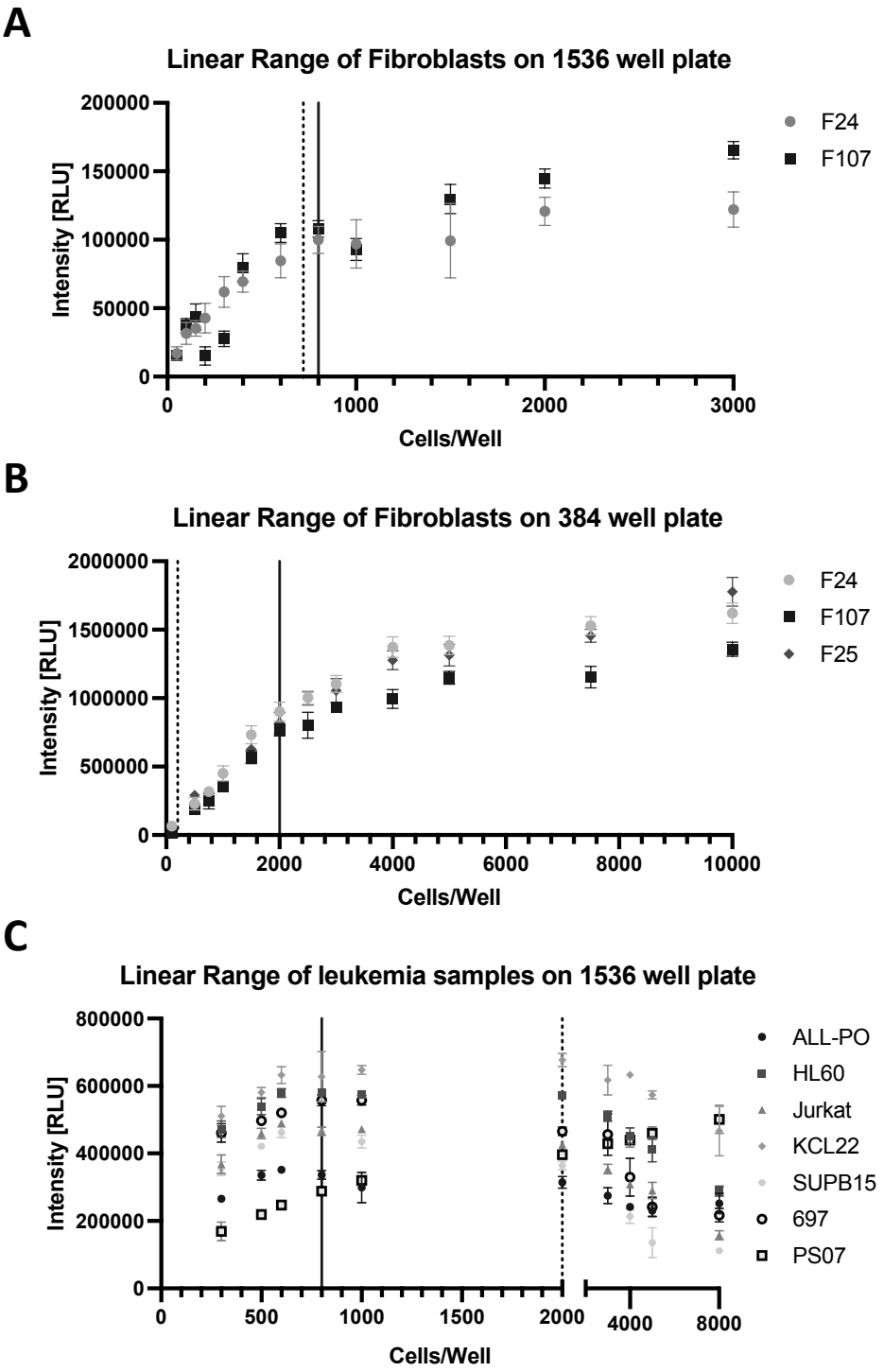

Figure 8 Figures (A-C) display the intensity of luminescent measured by RLU in relationship to the cell count seeded 72h before. The black line marks the cell count until a linear range is estimated by calculating the highest R^2 with at least four conditions. The dotted line marks the cell seeding concentration utilized in subsequent drug screenings.

3.2 Fibroblast HTDS

3.2.1 HTDS of Fibroblasts Reveals an Interindividual Distinctive Drug Response

The HTDS and subsequent analysis were performed for 41 samples from ALL patients and ten from patients with other malignant diseases. Non-ALL samples originated from patients with the following diseases: AML (one patient), Lymphoma (one Hodgkin-Lymphoma, two Burkitt-Lymphoma), four with malignant CNS tumors (three Medulloblastoma, one Ependymoma), Nephroblastoma (one patient), and Neuroblastoma (one patient). Replicates for the HTDS were available for five samples, and mean values for each drug were calculated. Three HTDS replicates had to be excluded as they did not correlate with the other replicates, most likely due to technical issues. Thus, 51 samples were included in the analysis in total. A flowchart of the analysis is displayed in Figure 9. Data were available for up to 191 drugs. However, not all drugs were consistent for every version on which samples were screened. Therefore, drugs missing in at least one version were excluded from further analysis. Of the 171 drugs remaining, 37 drugs showed a DSS score of zero for all samples, suggesting no measurable response. For the remaining 134 drugs, outliers were calculated, and “sensitive”, “resistant”, and “normal response” groups were created. The “sensitive” group was defined as samples showing a DSS value higher than the 0.8 quintiles of each drug. Analogous, the “resistant group” displayed samples with a decreased DSS below the 0.2 quintiles. All samples between the 0.2 and 0.8 quintiles were labeled as “normal response” for that drug. Likewise, samples outside the 1.5-fold interquartile range added or subtracted from the third or first quartile, respectively, were titled outliers for this concrete drug. While for 83 drugs, “sensitive” groups could be detected, which were large enough to compute statistics, for only 51 drugs, “resistant” groups met the criteria. Next, a statistical test should be conducted to determine the independence from the “normal response” group. The Mann-Whitney-U-test compares the median of the ranks but not the actual values. However, the groups were created by ranking the values and using the quintiles, creating a bias for this test. Thus, the Kolmogorov-Smirnov test was chosen, comparing the distribution of the groups. While all resistant groups were significant ($p<0.05$), ten sensitive groups did not meet this level and were excluded. Similarly to the groups detected, for only six drugs, resistant outliers were observed, while 112 drugs had sensitive outliers. This could be due to the scale of the DSS score being limited to zero, and fibroblasts are overall quite resistant tissue. Although outliers or groups could be recognized for some samples, some drugs displayed such low DSS values that they were more susceptible to impreciseness. Thus, drugs that did not meet a range between the highest and lowest value of over ten DSS points were eliminated from

the analysis. As a result, 82 drugs contained either one of the above-described categories. Moreover, all samples responded to at least one drug, resulting in no samples being classified as “normal response” for all drugs. In total, 162 data points were considered sensitive outliers, 440 as the significant “sensitive” group, and 151 as both sensitive outliers and the significant “sensitive” group. At the same time, no samples proved to be resistant outliers alone, but 423 occurred as the significant “resistant” group and 17 as both resistant outlier and the significant “resistant” group. The detailed analysis results with all 82 drugs and 51 samples can be seen in Figure 10, with a color code for each data point.

Using this analysis, it was shown that fibroblasts have different drug responses in the interindividual comparison. Next, it was necessary to demonstrate whether there is a relationship between this interindividual drug response and specific germline mutations or the clinical data.

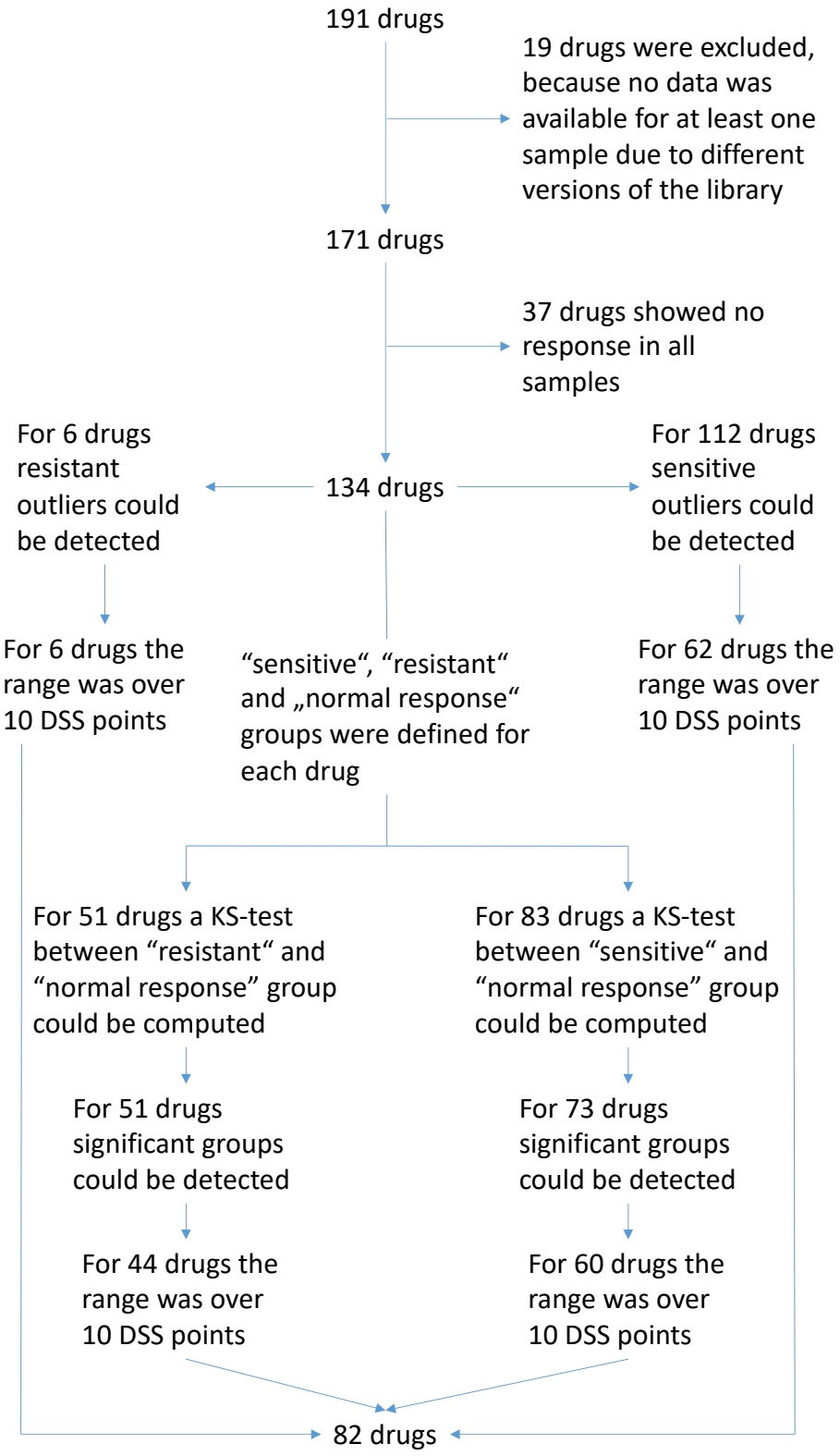

Figure 9 Flowchart of the analysis. A total of 51 samples were analyzed as described. The "resistant" and "sensitive" groups were defined by a drug sensitivity score (DSS) value below the 0.2 quintiles or over the 0.8 quintiles. All other values were categorized as "normal response". Significance was tested for with a Klomogorov-Smirnov-test (KS-test). Outliers were searched for with the 1.5-fold interquartile range added or subtracted from the first or third quartile, respectively.

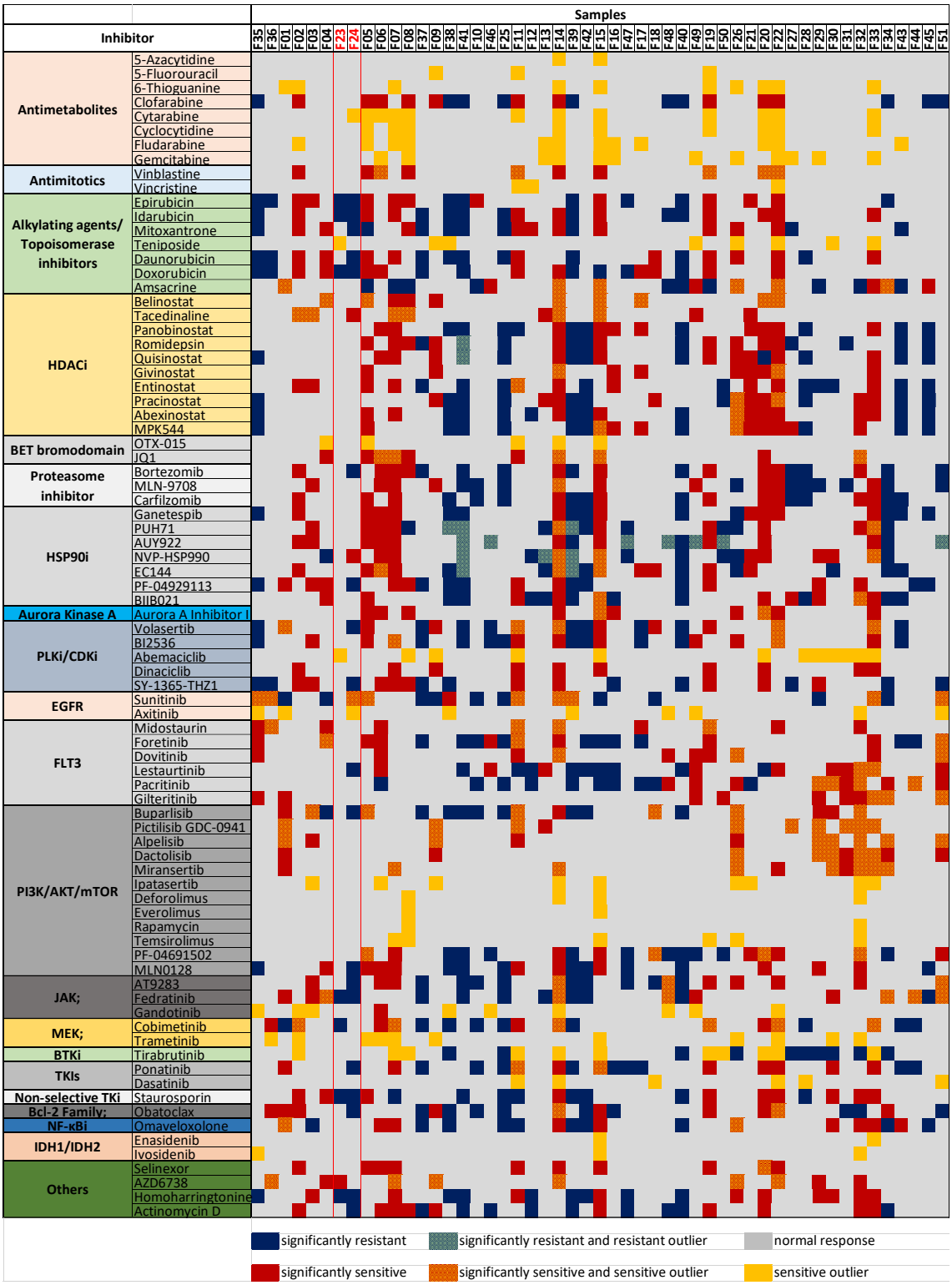

Figure 10 Analysis results of the fibroblast drug screening displayed in a heatmap. For each of the 82 drugs which showed a differential response in the analysis, the samples are classified as “significantly resistant” (blue), “significantly sensitive” (red), “significantly resistant and resistant outlier” (blue and green striped), “sensitive outlier” (yellow), “significant sensitive and sensitive outlier” (yellow and red striped), and “normal response” (grey). Samples that were grouped in either the “sensitive” or “resistant” group and passed the Kolmogorov-Smirnov test were then

classified as “significantly sensitive” and “significantly resistant”. In contrast, groups that did not pass it were changed to “normal response”. Two samples are marked red, which harbor a RAD21 mutation.

3.2.2 RAD21-Mutated Fibroblasts are Resistant to Anthracyclines

To test the analysis and its relation to germline variants, two cohort patients with known germline variants in the RAD21 gene were drug screened and analyzed. Both samples are marked red in Figure 10. Here, the sample F24 showed resistance to Mitoxantrone, Daunorubicin, Bortezomib, BIIB021 – an HSP90 inhibitor –, Dactinomycin, and Obatoclax, as well as some kinase inhibitors, such as Volasertib, SY-1365-THZ1 (CDKi), Lestaurtinib, Buparlisib, MLN0128 (mTORi), AT9283 (JAKi), and Ponatinib. In contrast, the sample was more sensitive to Cytarabine, Tacedinaline, NVP-HSP990 (HSP90i), Sunitinib, and Axitinib. The other sample carrying a mutation in the same gene exhibited a less resistant profile overall with sensitivity towards Abemaciclib, AZD6738 (ATM/ATRi), and Teniposide while expressing decreased activity towards Cobimetinib. However, although both samples did not inherit the same mutation, the drugs for which both samples expressed similar reactions are more interesting in understanding the role of germline variants in the gene of interest. Both samples were resistant to Epirubicin, Idarubicin, Doxorubicin, Fedratinib, Staurosporin, and Homoharringtonine. These results indicate that these mutations impact fibroblast signaling cascades, while no exact pathway seemed particularly affected. Nevertheless, both samples were resistant to at least three anthracyclines, and F24 was resistant to all anthracyclines and Mitoxantrone. Only the sensitivity of F23 to Teniposide does not fit the overall resistance toward topoisomerase inhibitors.

To test these hypotheses in another model, HEK293T cells that overexpressed RAD21 and carried either of the mutations were drug screened again and compared to the overexpression alone and the wild-type cells. Interestingly, the overexpression of RAD21 had the greatest impact on the response to anthracyclines and other drugs, as the difference between the wild-type cells and the overexpression of RAD21 was the highest (see Figure 11). Moreover, only Staurosporine presented a higher sensitivity in the mutations while achieving DSS values more closely to the wild-type cell line. All the other drugs responded roughly the same in the mutation and overexpression alone cell lines.

In conclusion, both RAD21-mutated fibroblasts exhibited inherent resistance to anthracyclines. However, the outcomes observed in RAD21-mutated fibroblasts could not be reproduced in HEK293T models with (wt or mut) RAD21 overexpression. It appears that the enforced RAD21 expression in HEK293T cells has a high impact on the drug screening profiles, underscoring the need for improved (inducible) models to replicate the germline variants.

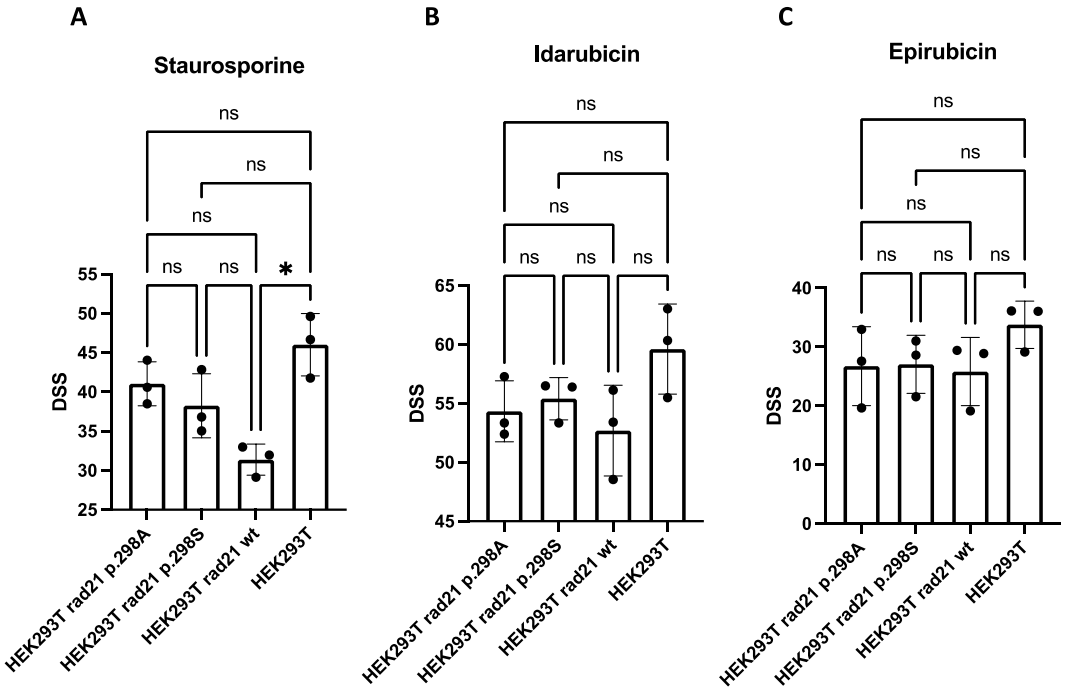

Figure 11 Bar graphs of the drug screenings of HEK293T wild type cells (HEK293T), RAD21 overexpression (HEK293T rad21 wt), or RAD21 overexpression and either one of two mutations (HEK293T rad21 p.298S and HEK293T rad21 p.298A). Representative Drugs were chosen for the anthracyclines. A Kruskal-Wallis test was performed for each graph individually (A: p=0.01; B: p=0.33; C: p=0.32), followed by a Dunn´s-multiple comparison test. (p>0.05=ns; p<0.05=*)

3.3 Fibroblast Drug Screening and Clinical Data

3.3.1 Patient Characteristics

Table 9 shows the patient characteristics of the cohort used to search for connections between the drug screening of fibroblasts and the clinical data. Clinical data were available for 43 patients. For four of these patients, no HTDS data were available, but they were included on the protocol-based plates. Patient samples of this cohort were randomly selected to be screened on the protocol-based plates.

Table 9 Characteristics of patients investigated for the combination of drug screening and clinical data.

Characteristics	***N (%) [high-throughput format]***	***N (%) [protocol-based plates]***
Total patients	39	25
Males	22 (56.4%)	14 (56%)
Females	17 (43.6%)	11 (44%)
Age (in years)		
Mean	5.90	5.32
Standarddeviation	4.45	4.25
Range	1.7-17	0.3 – 15.4
ALL Subtype		
B-ALL	35 (89.7%)	21 (84%)
High hyperdiploid	9 (23.1%)	5 (20%)
ETV6-RUNX1	8 (20.5%)	3 (12%)
KMT2Ar	1 (2.6%)	2 (8%)
TCF3-PBX1	1 (2.6%)	1 (4%)
BCR-ABL1	1 (2.6%)	1 (4%)
Others/unknown	15 (38.5%)	9 (36%)
T-ALL	4 (10.3%)	4 (16%)
CNS Status		
1	33 (84.6%)	19 (76%)

Characteristics	***N (%) [high-throughput format]***	***N (%) [protocol-based plates]***
2 (a and b)	4 (10.3%)	2 (8%)
3	0 (0.0%)	1 (4%)
Not assessable	2 (5.1%)	3 (12%)
Treatment Protocol		
AIEOP BFM 2009	24 (61.5%)	15 (60%)
AIEOP BFM 2017	14 (35.9%)	9 (36%)
EsPhALL-2017	1 (2.6%)	1 (4%)
Prednisone response		
Good (<1000 blasts/µl)	35 (89.7%)	23 (92%)
Poor (>1000 blasts/µl)	4 (10.3%)	2 (8%)

3.3.2 Occurrence and Severity of Adverse Events Differ Between Patients

There are notable differences in the frequency of adverse events in the first 36 days of the AIEOP BFM protocols. The most common effects of the treatment included myelosuppression with an incidence of 83-93% depending on the cell lineage, followed by increased liver markers (13-62%, depending on marker), serious infections, and mucositis with 9.3% each. While no patient was diagnosed with a pancreatitis, only three had neurotoxicity. Only two patients underwent the therapy up to day 36 without any depression of cell lineages in the peripheral blood above grade three or higher, defined by the CTCAE v.5. Interestingly, these two patients also did not suffer any other side effects that were investigated. Furthermore, one more patient only experienced leukocytopenia, while the hemoglobin and thrombocyte levels never decreased below the threshold. Six patients only had reductions in two of the three cell lineages. In contrast, 34 patients went through adverse events grade three or higher for all three cell lineages at least once. Therefore, patients with lower myelotoxicity seemed to have lower toxicity overall. Supporting this hypothesis, no serious infections or neurotoxicity occurred in patients with lower myelotoxicity. Moreover, only three of these patients suffered from hepatotoxicity - defined as two markers elevated above grade three. In contrast, in the group of patients with all lineages decreased, 18 patients experienced hepatotoxicity, four had serious infections, three suffered from neurotoxicity, and four suffered mucositis. Thus, the

myelosuppression's magnitude could indicate severe adverse events such as serious infections or hepatotoxicity. A detailed graph of all 43 patients and each adverse event analyzed can be found in Figure 12. As differences in both the frequency of adverse events and the HTDS could be observed, a connection between both was searched for.

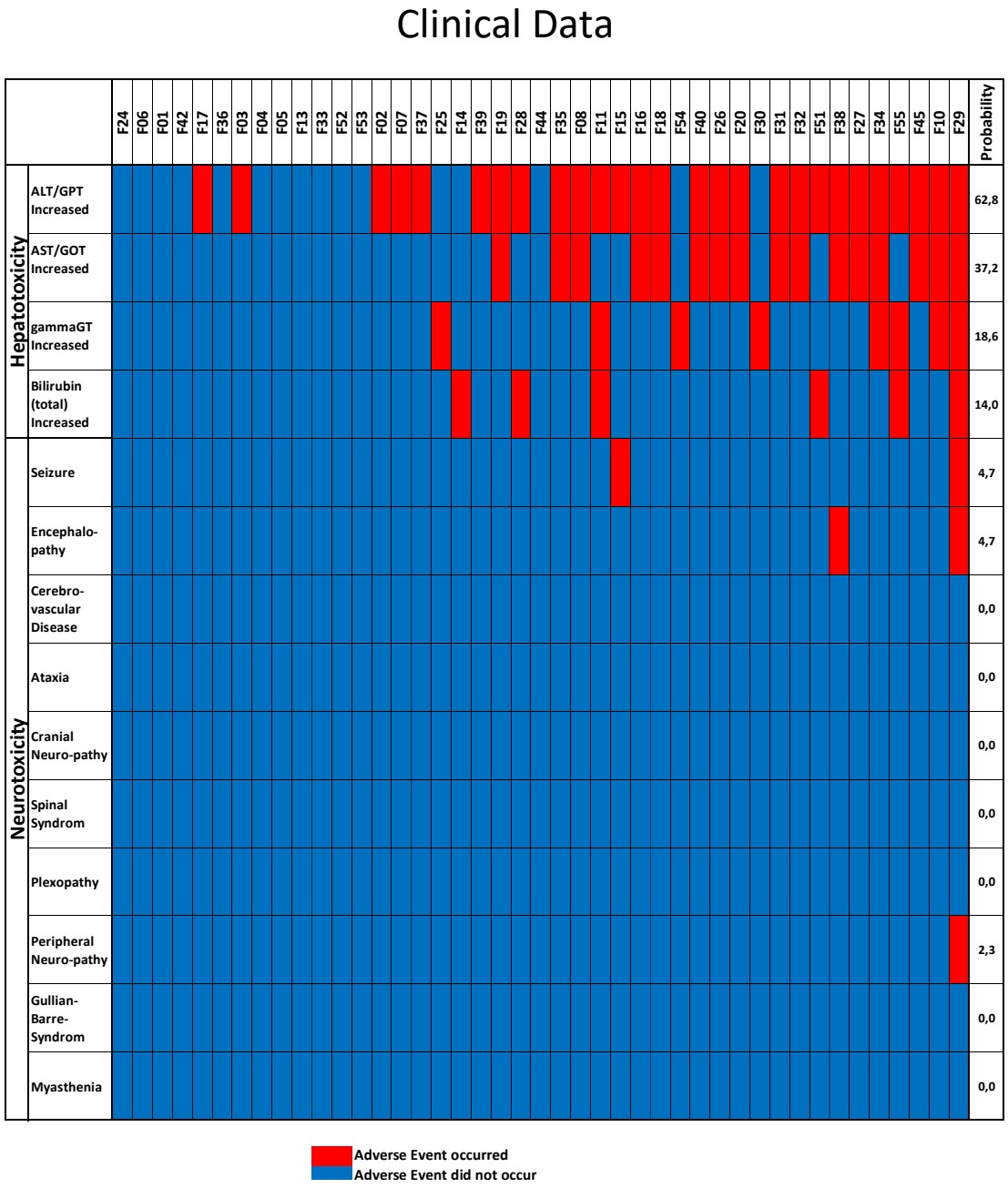

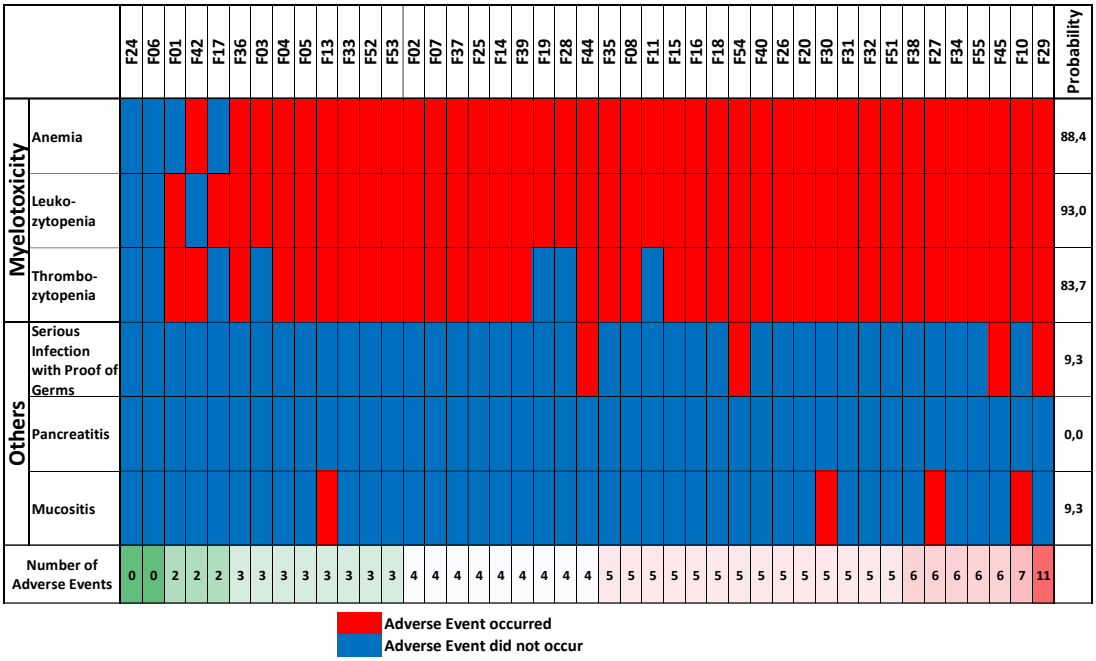

Figure 12 A heatmap giving an overview of the adverse events from day 1 to 36. For each patient, "red" marks the occurrence of the adverse event, while blue is awarded otherwise. The probability of each adverse event was calculated by dividing the number of patients that suffered from this by the total number of patients and multiplying by 100. In contrast, the number of adverse events is calculated using the number of different categories of adverse events that occurred.

3.3.3 Drug Screening and Adverse Events

3.3.3.1 Interindividual Drug Response in HTDS and Adverse Events do not Correlate

Firstly, a connection between the adverse events until day 36 and the HTDS was searched for. Only two of the five drugs administered in the protocol demonstrated a response in the HTDS of fibroblasts, so a rather unsatisfactory fit for this model was already expected. In the analysis, the sensitive group for Vincristine was not upheld as significant; therefore, only three outliers could be detected. As a result, only Daunorubicin was eligible for the analysis in connection with adverse events. Thus, the three groups - "resistant", "normal response", and "sensitive" – which resulted from the analysis were compared in their incidence of adverse events. For 43 patients, data for adverse events were available. For four of these, no high-throughput data were analyzed, and they were excluded. Therefore, 20 patients showed a normal response, ten were classified as resistant, and nine as sensitive. No apparent trend was noted when comparing these groups for the incidence of each adverse event analyzed (see Figure 13). Although serious infections were only seen in the normal response and sensitive group, the overall incidence was low and thus susceptible to inaccurateness. Moreover, the

incidence of elevated markers for hepatic injury and hepatotoxicity overall did not follow a trend for the three HTDS groups. Similarly, the myelosuppression and the three cell lineages were not more often abnormal in the sensitive group than in the resistant. Neurotoxicity and mucositis even occurred only in the resistant and normal response groups.

Concluding, no connection was evident between the HTDS and the adverse events of patients during the first 36 days. However, as only one of five drugs could be investigated, the validity of this model was greatly compromised. Thus, a plate was designed based on the BFM 2017 treatment regime protocol IA.

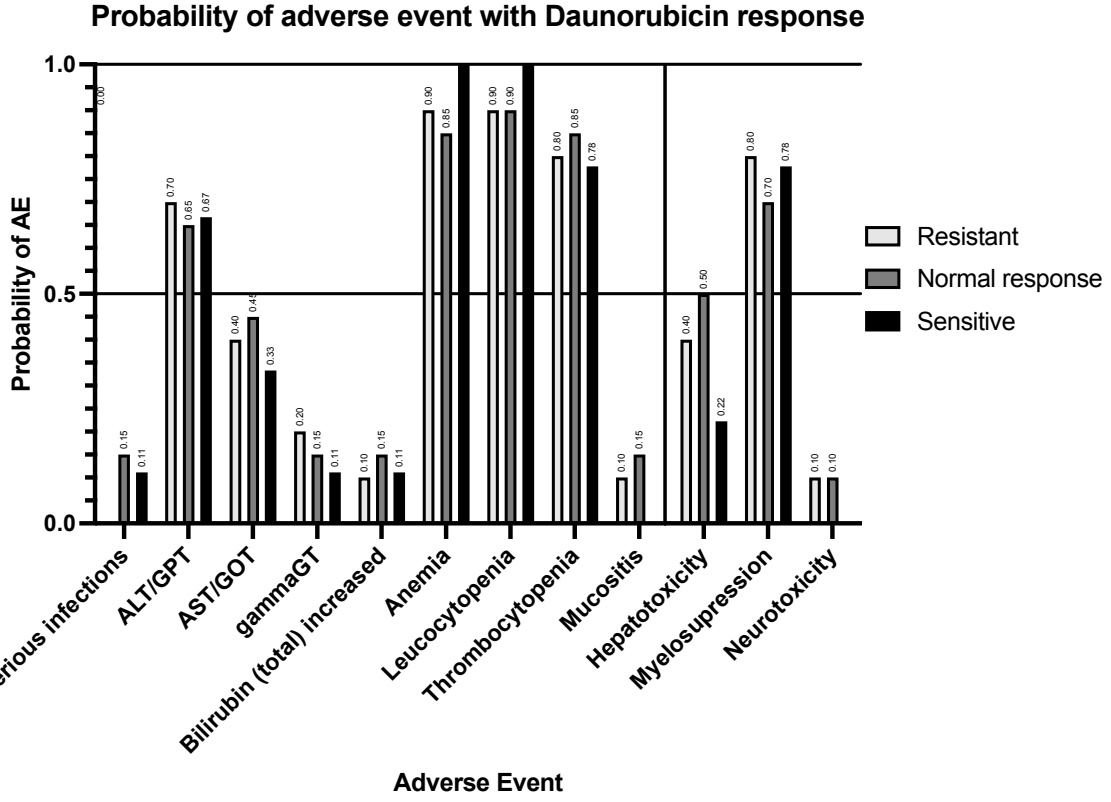

Figure 13 Bar graph of the probability of each adverse event compared to the response to Daunorubicin in the high throughput drug screening. Response to Daunorubicin was analyzed as described above. The probability is also noted on top of each bar. Hepatotoxicity was defined as at least two markers being elevated above the threshold, while for myelosuppression, all three lineages had to be reduced. Neurotoxicity was seen as at least one neurological adverse event in the period.

3.3.3.2 Drug Screening Based on Therapy Protocol Falls Short in Predicting Adverse Events

Based on the treatment protocol, the newly designed plates included ten wells with all five drugs in the same fold concentration to each other. This was seen as the most logical

combination to evaluate the overall adverse events throughout the first 36 days. A total of 25 samples could be screened on these plates. A score was calculated for the adverse events, which awards one point for each category of adverse events that occurred. For example, a patient with anemia, mucositis, and increased ALT would be assigned a score of three points. Subsequently, a linear regression model was calculated for the DSS values of the all-drugs-combined combination and the score for adverse events. The graph of the linear regression is displayed in Figure 14A. The equation was calculated as $Y = 0.8733 * X + 33.76$. However, the R^2 was only 0.0563, and the 95% confidence interval for the slope ranged from -0.6689 to 2.416. Thus, the slope did not significantly differ from zero, and a correlation between the adverse events and the DSS value of the drug screening could not be assumed. Moreover, a correlation matrix was calculated with the DSS and IC50 values from the drug screening, the number of categories of adverse events (see above), and the overall number of adverse events – which was calculated by adding up the occurrences of each adverse event –, as well as the most extreme value for each adverse event if it was evaluated. Again, this matrix displayed a low correlation between the experimental and clinical data (see Figure 14B). As described above, the degree of myelotoxicity was observed to interrelate with the overall extent of severe adverse events. Thus, the DSS scores for patients with all three cell lineages decreased were compared to those for which only up to two were abnormal (see Figure 15A). In line with the other test, the mean DSS values were not significantly different (Mann-Whitney-U test p=0.98). Furthermore, the mean DSS values of patients with hepatotoxicity, neurotoxicity, or serious infections were equal to those with low or no myelotoxicity (Kruskal-Wallis test p=0.98, see Figure 15B).

To summarize these results, no apparent correlation between the drug screening of fibroblasts and the patient's clinical data was evident.

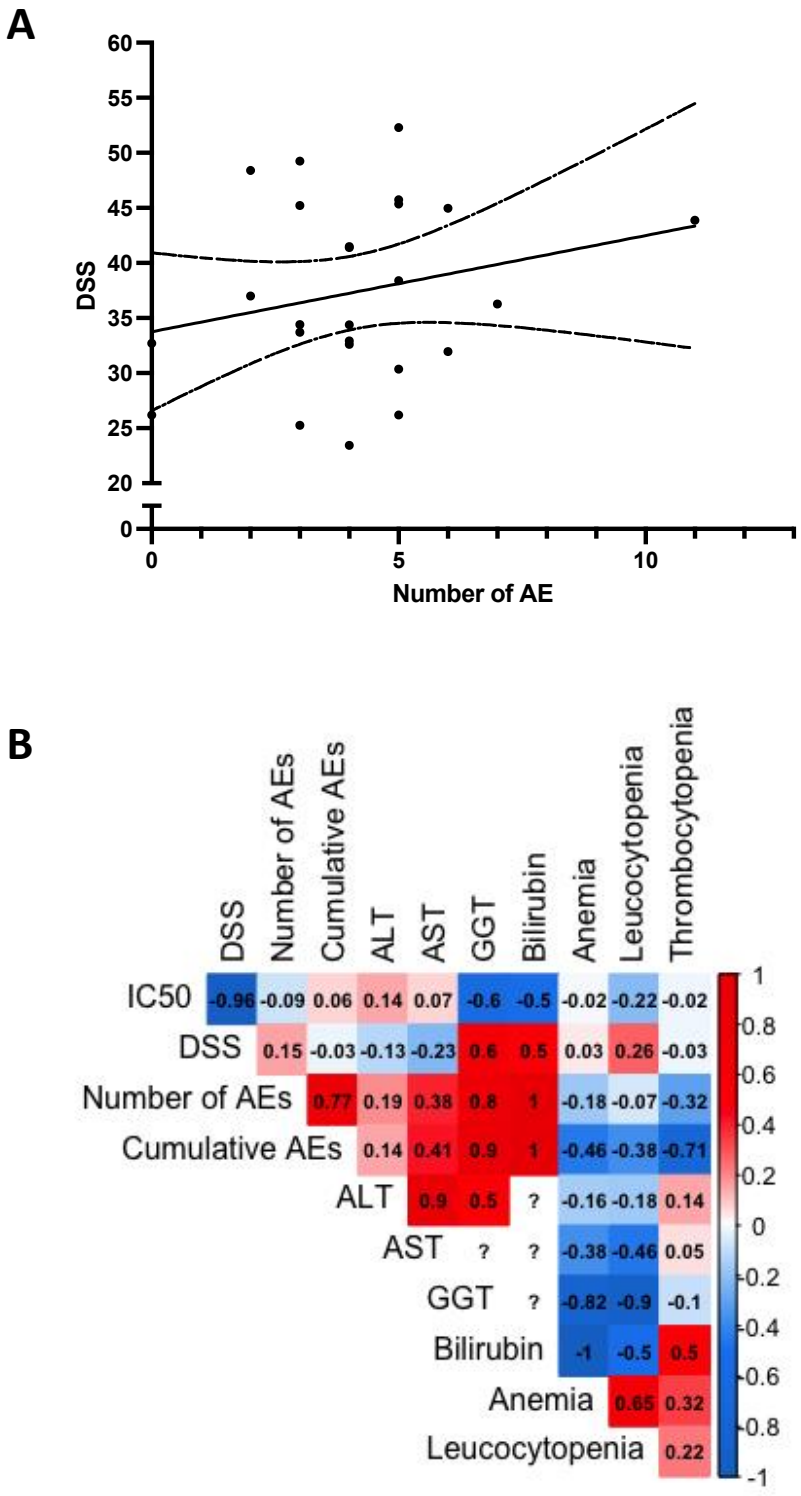

Figure 14 (A) A correlation graph of the number of adverse events and the DSS value of all drugs combined on the protocol-based plates. The equation was calculated as Y = 0.8733*X + 33.76 with a 95% confidence interval of -0.6689 to 2.416 for the slope (dotted lines) and an R^2=0.05. (B) A correlation matrix of drug screening data (DSS and IC50) of the protocol-based plates and the clinical data (number of adverse events (AEs), cumulative AEs (all occurrences of adverse events added up), and the lowest or highest parameters respectively, for the hepatotoxicity and myelosuppression markers).

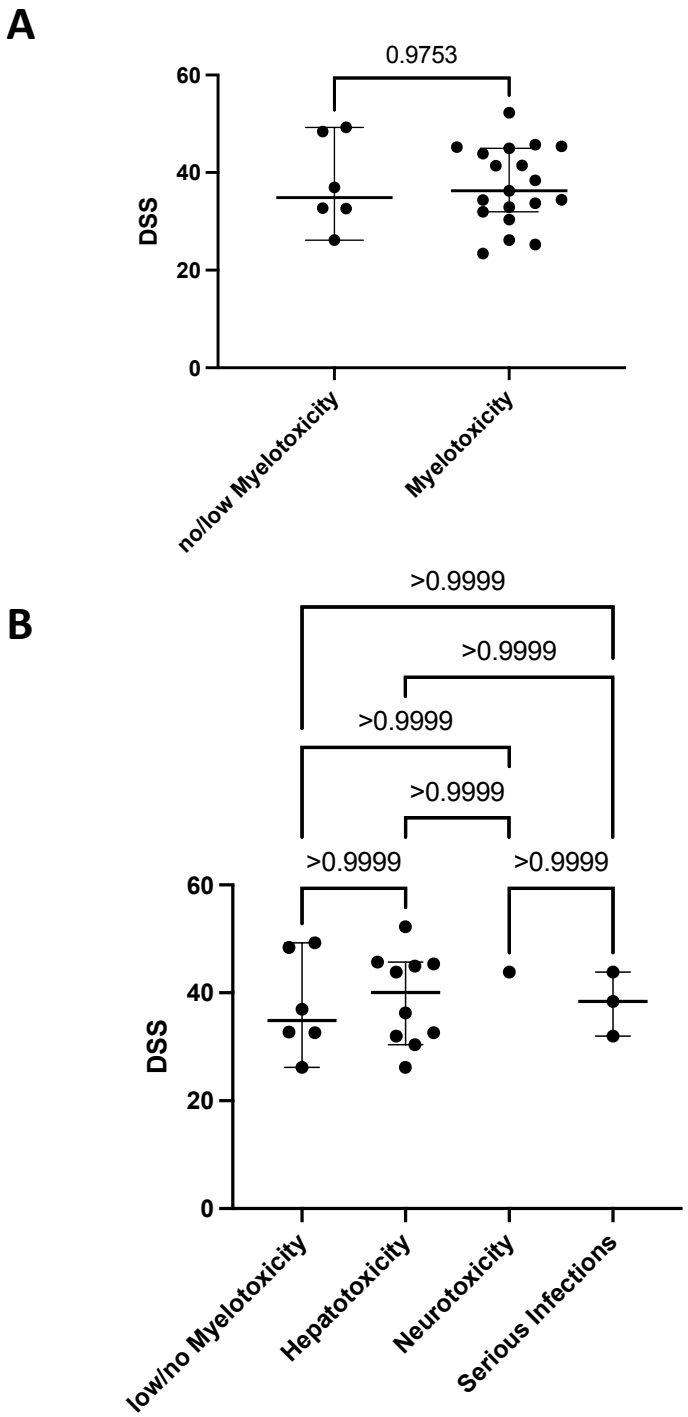

Figure 15 (A) Scatter plot of the DSS values of patients suffering from low/no or high myelosuppression. High myelosuppression was defined as all three lineages decreased. A Mann-Whitney-U-test was performed between the groups (p-value shown in the graph). (B) A scatter plot of the DSS values of patients suffering from low/no Myelotoxicity (less than three lineages decreased), Hepatotoxicity (at least two markers elevated), Neurotoxicity (at least one neurological adverse event), or a serious infection. A Kruskal-Wallis test was performed with a p=0.98 and a follow-up test with Dunn´s multiple comparisons (p-values shown in the graph).

3.3.3.3 Drug Screening Based on Therapy Protocol Falls Short in Predicting Therapy Response

At last, the MRD data for the 25 patients were analyzed. Three patients showed an MRD of 10^{-3} or higher, seven of around 10^{-4}, and eleven of 10^{-5} or lower, which was classified as negative. A Kruskal-Wallis test was conducted between these groups, but no difference could be detected with a p=0.7472 (see Figure 16). Thus, no connection between drug screening and treatment response was observable.

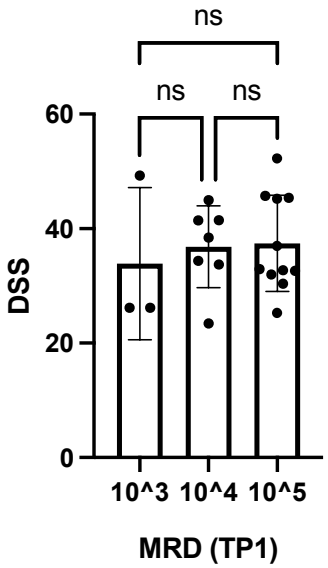

Figure 16 Bar graph of DSS values in the context of the clinical MRD at timepoint one. A Kruskal-Wallis test was performed (p=0.75) with Dunn´s multiple comparisons as a follow-up. (p>0.05=ns)

3.4 Healthy Cells and Leukemia Blasts Can be Distinguished by Drug Response Profiles

A total of 131 samples were implemented into the HTDS pipeline. The fibroblasts of the germline study represent the biggest group and were described above in depth. They are followed by 14 samples of T-ALL and ten samples of KMT2Ar leukemias. Other high- and medium-risk subgroups considered large enough for further analysis included the Ph-like (six samples) and TCF3-PBX1 (six samples) groups. The BCR-ABL1 subgroup, with its three samples, was only included as a reference and proof-of-concept. Although the TCF3-HLF1 group only contains four samples, it was included. Therefore, the data must be seen as preliminary. Six different B-cell samples were screened as healthy controls, together with three different samples of PBMCs, T-cells, and CD34-positive hematopoietic stem cells. The leukemia samples included 35 commercially available cell lines, 28 patient-derived xenografts (PDX), and three originated as primary samples directly from the patient.

Unhierarchical clustering of all samples revealed a sorting according to the overall sensitivity of each sample, as visible in Figure 17. Divided into four groups, the most resistant cluster only consists of fibroblasts. In the second cluster, most samples are fibroblasts, and other healthy samples are included. In detail, the PBMCs, T-cells, and B-cells are all included in this cluster. Only one B-cell sample, which showed hyperdiploidy in tests performed by cooperation partners, clustered with other leukemia samples. Interestingly, four leukemia samples were also paired with the healthy samples. Two of these samples were BCR-ABL1 positive chronic myeloid leukemia (CML) cell lines, one was a TCF3-HLF1 positive PDX, and one was a primary sample of an unknown subtype. Furthermore, the CMLs and the PDX sample were very sensitive to Dasatinib, Bafetinib, Bosutinib, Rebastinib, Ponatinib, Randotinib, and Nilotinib, unlike the healthy controls. In contrast, the primary patient sample displayed a very resistant phenotype, which could explain the pairing with the healthy samples. The third and fourth clusters include all remaining leukemia samples. Nevertheless, the CD34-positive hematopoietic stem and progenitor cells (HSPCs) were also assigned to the most sensitive fourth cluster. PDX, cell lines, and primary samples clustered – aside from the fibroblasts – independent from their type. This is important, as it reduces the potential bias caused by different origins of the samples. Especially as each ALL subgroup consists of different ratios of cell lines, PDX, and primary samples.

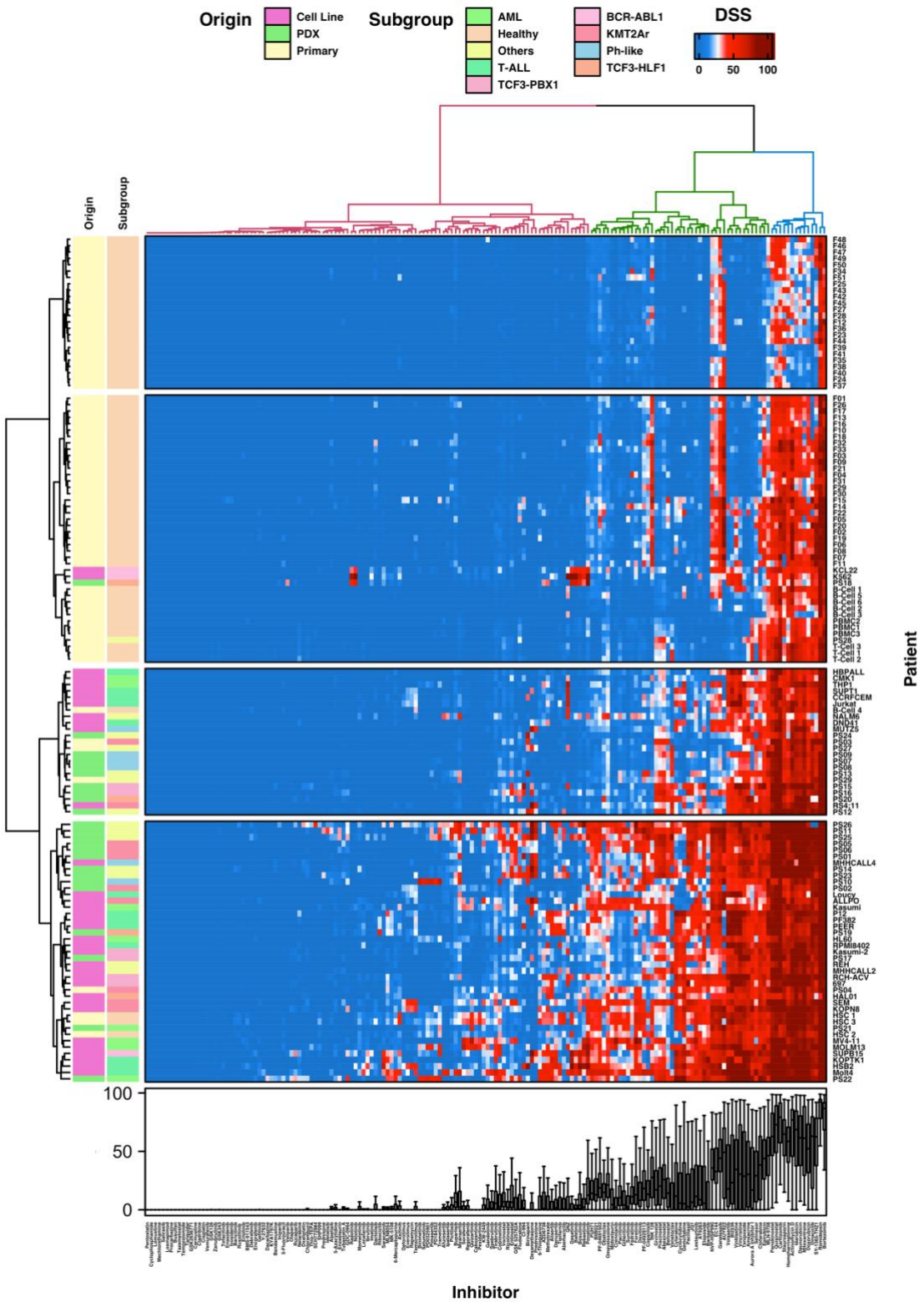

Figure 17 Heatmap visualization of DSS values from the drug screenings performed on the high throughput pipeline. The side marked with "Patient" displays the different samples that were unsupervised clustered in the four most prominent groups, while on the "Inhibitor" side, the drugs are represented. A boxplot was added with the distribution of DSS values for each drug. Whiskers display the highest and lowest values. The origin and subtypes are annotated on the left side in a color code.

3.4.1 Established Genetic Subgroups of ALL Fail to Predict Overall Drug Responses

Although the subgroups are based on similar genetic sequencing data and thus transcriptome, it was yet to show, that these translate into similar drug response profiles. Therefore, the relevance of the subgroup for the drug response was analyzed.

The HTDS data were analyzed with an unhierarchical clustering and principal component analysis. In both analyses, the fibroblasts clustered differently from all the other samples, proofing the concept of this analysis. Surprisingly, both analyses demonstrated no apparent connection between the subgroup and overall drug response. The principal component analysis in Figure 18 shows no evident relationship between ALL subgroups and clusters. Although some subgroups tended to cluster differently, single samples of these subgroups were always projected far from their groups. Moreover, the cell origin – cell line, PDX, or primary sample – and the library version also clustered seemingly randomly, as seen in Figure 19. In the unhierarchical clustering used in the heatmap in Figure 17, no subgroups were clustering together, while healthy samples showed a different drug response profile. Thus, creating the impression that the subgroups do not predict the drug response overall very well. Therefore, better biomarkers for the drug response are needed.

In conclusion, the known genetic subgroups did not show similar drug response patterns, implying the need for new biomarkers for drug response.

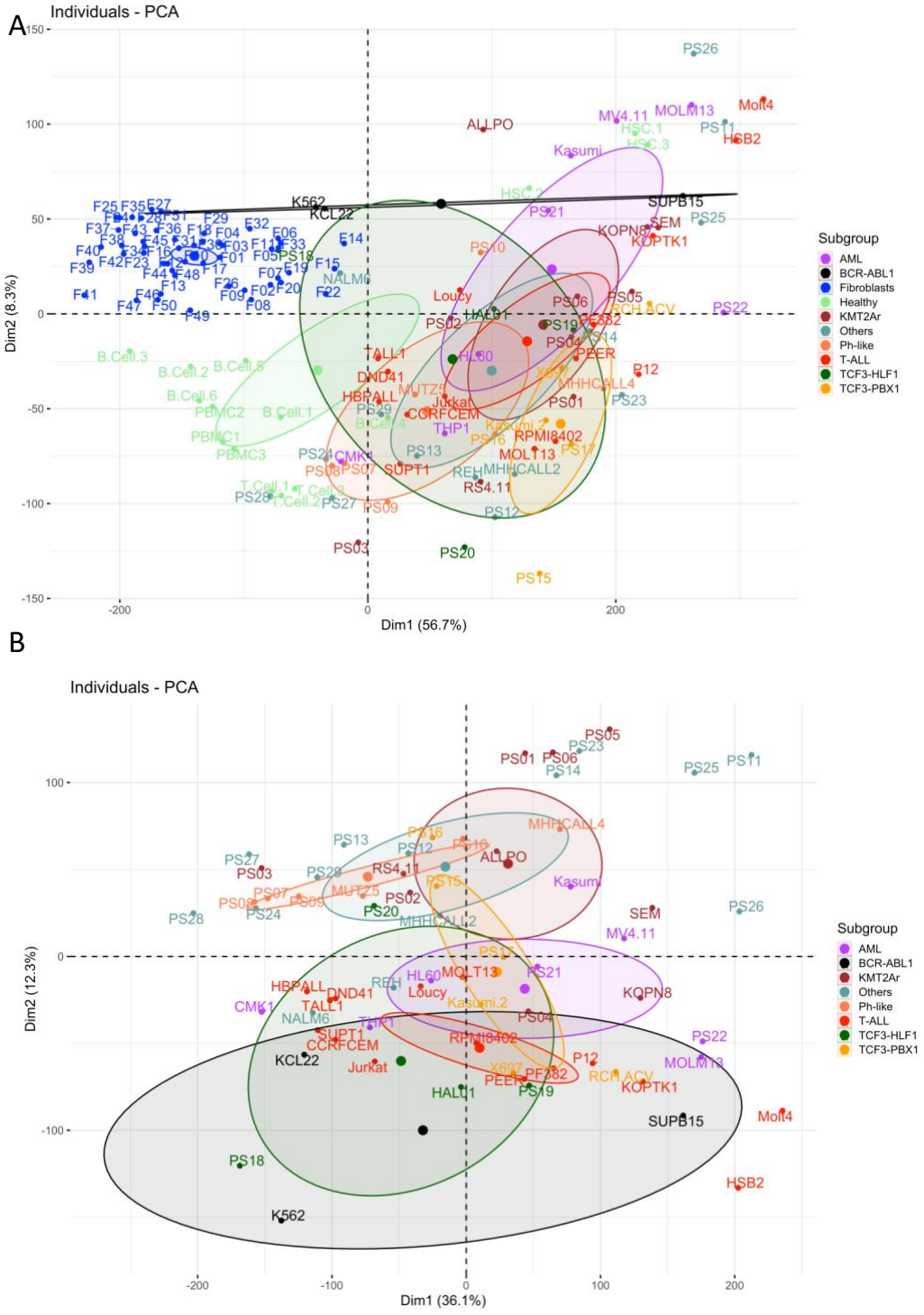

Figure 18 Visualization of a principal component analysis (PCA) of the DSS values from the high-throughput drug screening. DSS values for each drug were not scaled to one variance when the PCA was computed. (A) PCA of all 121 samples screened. The color of the names was assigned according to the subgroup of each sample. Ellipses display the confidence region of the median for each group. (B) PCA of all AML and ALL samples screened. Again colors were assigned to each subgroup individually, and the ellipse form displays the confidence region of the median for each group.

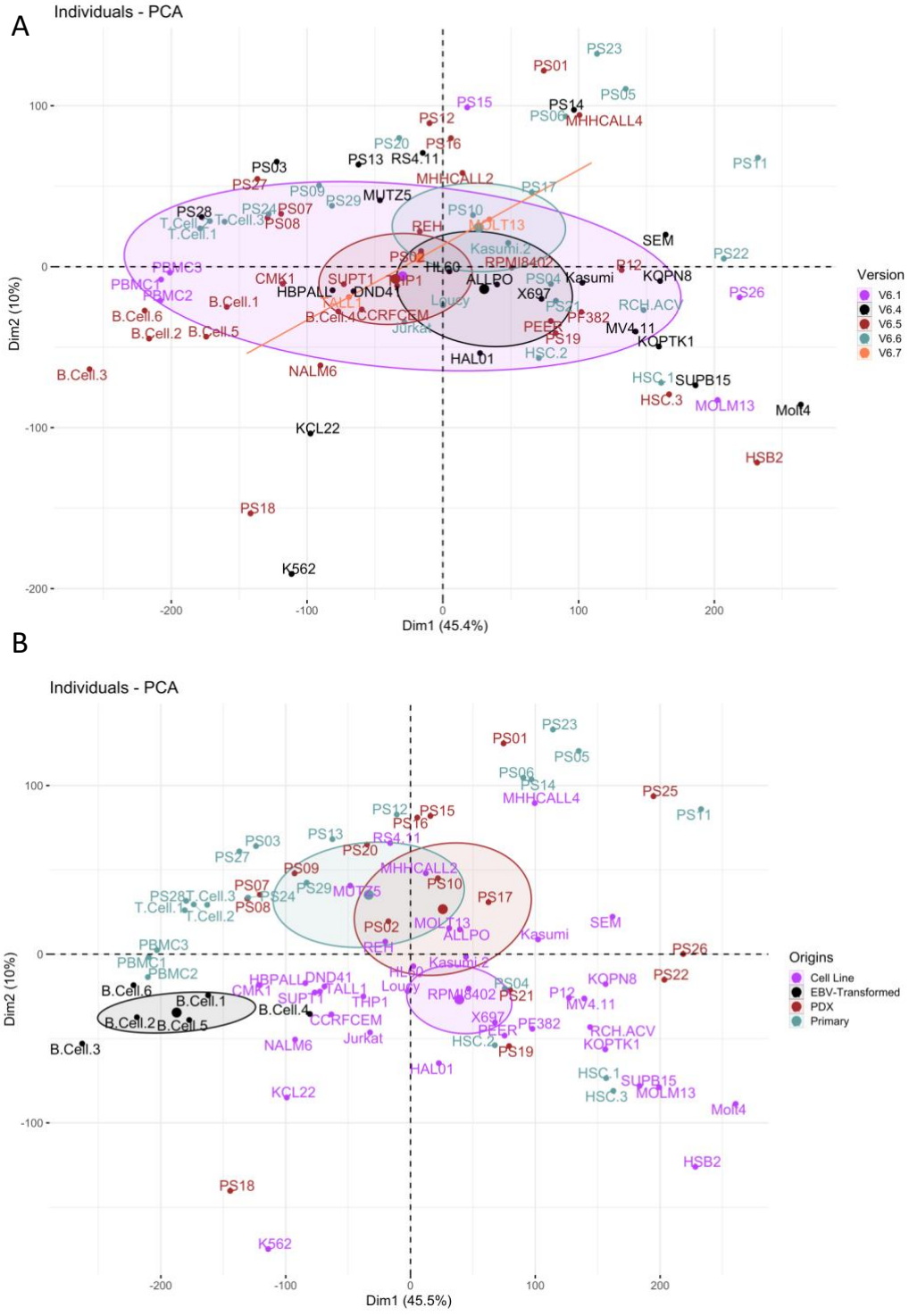

Figure 19 Visualization of a principal component analysis (PCA) of the DSS values from the high-throughput drug screening. DSS values for each drug were not scaled to one variance when the PCA was computed. (A) Display of the PCA of all ALL, AML, and healthy samples excluding fibroblasts. Colors were assigned according to the sample origin (cell line, primary, PDX, or EBV-transformed). Again, ellipses form the confidence region of the median for each version. (B) Display of all ALL, AML, and healthy samples excluding fibroblasts with colors according to the plate version on which the sample was screened. Again, ellipses form the confidence region of the median for each origin.

3.5 Distinct Drug Response Profiles of B-ALL Based on Their Differentiation Status

In the search for biomarkers to more accurately predict the drug response, a lineage-specific profile could be noticed by looking at the HTDS profiles of the healthy cells in Figure 17 and more clearly in Figure 24. Moreover, CD34-positive HSPCs showed a very different profile. Thus, suggesting an influence of both lineage and differentiation status on the drug response. To test whether this hypothesis could be transferred to B-ALL samples and could therefore represent a biomarker for drug response, the FACS profiles of leukemic cell lines screened on the library were researched in the DMSZ database. Groups large enough for statistical analysis could be generated for two markers. These two markers were CD13 and cytoplasmatic IgM. CD13 is generally considered a myeloid marker and symbolizes an earlier differentiation state of lymphoblastic blasts. In comparison, cytoplasmatic IgM expression is a marker of immature B-cells. Both markers were searched for on B-ALL samples and cell lines using FACS. Accordingly, the HTDS data was analyzed.

3.5.1 CD13-positive B-ALLs are Sensitive to FLT3 Inhibitors

The CD13 expression was measured with flow cytometry, and signals of $10^{3.1}$ were considered positive. Of the 26 B-ALL cell lines and PDX samples tested, five were positive, 17 were negative for CD13, and three showed ambiguous results and were excluded from further analysis. To search for potential differences in drug response, a non-parametric Mann-Whitney-U test was conducted. A correction for multiple testing was not performed, as new hypotheses were meant to be generated. As there were findings where only one drug of a class showed a difference in response, it was considered more susceptible to a type I error. In contrast, results with multiple drugs of one target or pathway were seen as more promising. Furthermore, all FLT3 targeting drugs included in the analysis showed increased activity in the CD13-expressing samples. Thus, suggesting a specific target for these drugs in CD13-positive B-ALLs. Furthermore, downstream targets of FLT3 also seemed upregulated. MTOR inhibitors Everolismus, Rapamycin, Temsirolimus, and JAK inhibitors like Momelotinib or Gandotinib, and the drugs targeting the RAS/RAF/MEK/ERK pathway Tipifarnib, Sorafenib, Regorafenib, all showed an increased response. Lastly, other kinase inhibitors described to inhibit FLT3, like Ponatinib or Fedratinib displayed a higher DSS value.

In conclusion, these data suggest an increased vulnerability either towards FLT3 directly or downstream targeting drugs for ALL of earlier precursor origin, expressing CD13.

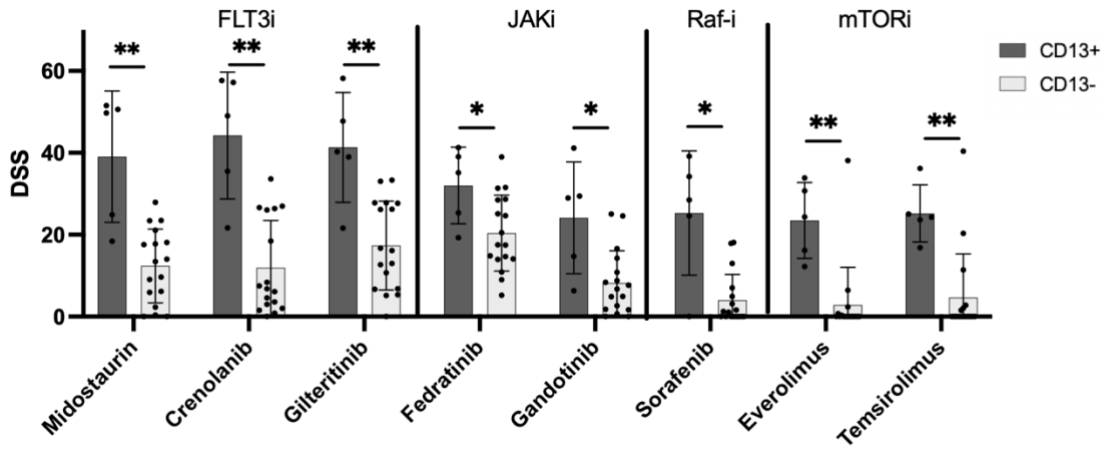

Figure 20 Bar graphs of the representative drugs that showed higher DSS values for samples expressing CD13. P-values were calculated with a Mann-Whitney U test. ($p<0.05$=*, $p<0.005$=**)

3.5.2 Cytoplasmatic-IgM-positive B-ALLs are Sensitive towards Classical Chemotherapy

The cytoplasmatic IgM (cyIgM) expression was also measured with FACS analysis. Moreover, intracellular staining was performed on B-ALL samples with five positive; 14 were determined negative, and seven showed ambiguous data. A Mann-Whitney-U-test without Bonferroni-Dunn correction manifested 5-Azacytidine as a potential candidate. Furthermore, other classical chemotherapeutics like antimetabolites, antimitotics, and topoisomerase inhibitors showed an increased response. CD13-positive cells showed decreased vulnerability to Idarubicin. The more differentiated cyIgM-expressing cells displayed higher DSS values for all topoisomerase inhibitors. Some TKIs were also calculated as possible treatment options. These included the PI3Ki Dactolisib, the JAKi AT9283, and the TKis Bosutinib, Dasatinib, and Saracatinib. Moreover, four drugs targeting the RAS/RAF/MEK/ERK pathway presented increased DSS value, suggesting a potential therapeutic option for this kind of leukemia. Lastly, Paclitaxel, Bexarotene (retinoid inhibitor), Homoharringtonine (ribosome inhibitor), and two PARP inhibitors (Olaparib, Rucaparib) were all revealed as potential hits.

Therefore, a more differentiated status of the leukemic blasts could be targeted by applying classical chemotherapeutics and different kinase inhibitors.

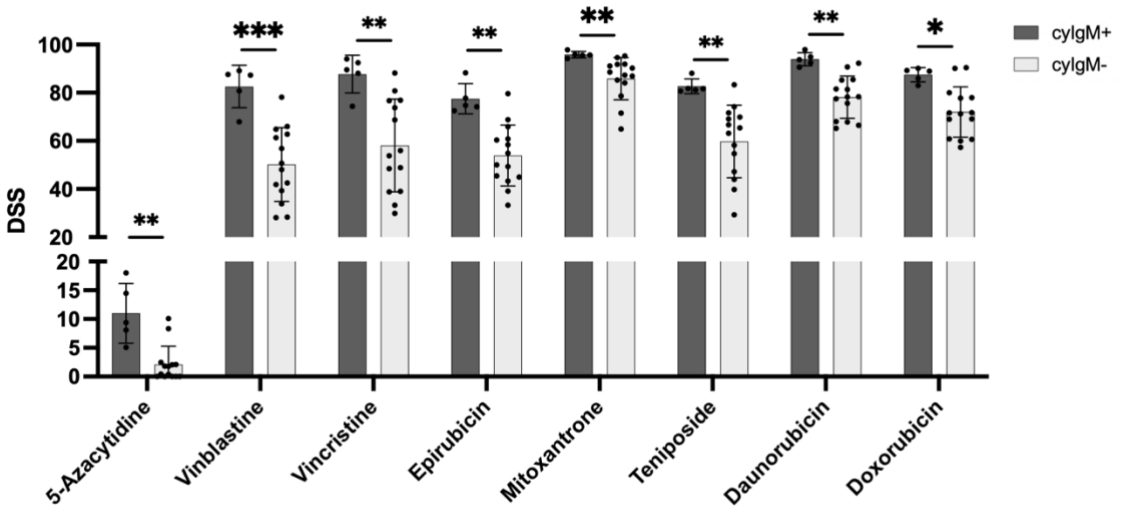

Figure 21 Bar graphs of the representative drugs that showed higher DSS values for samples expressing cytoplasmatic IgM. P-values were calculated with a Mann-Whitney U test. ($p<0.05$=*, $p<0.005$=**, $p<0.0005$=***)

3.6 Possible Combinations

As modern chemotherapy consists of multidrug regimes, potential drug combinations are searched for. Thus, a Spearman correlation for all ALL samples together was performed. Only a high correlation (>0.5) was accepted as a potential combination. Therefore, here are only hits with high correlations with multiple drugs of one target reported. The mentioned combinations are not synergistic but more likely to be active in the same samples. A simplified overview of the correlations between drug classes can be found in Figure 22, but Spearman correlation coefficients are displayed lower as the average for each drug class was computed.

3.6.1 Classical Chemotherapeutics

One might expect classical chemotherapeutics to present with a high correlation to each other. However, this could only be partially observed. In particular, antimetabolites correlated strongly with antimitotics and topoisomerase inhibitors. Regarding targeted inhibitors, antimitotics and Polo-like kinase displayed the best correlation. For all topoisomerase inhibitors, Homoharringtonine was found to be the best correlative drug.

3.6.2 Targeted Inhibitors

Interestingly, no strong negative correlation could be found. This could be a surprise, as one could expect an upregulation of one pathway if the other is downregulated. Thus, the drugs

against the first would show increased activity, while the second would be more resistant, resulting in a negative correlation. Anyhow, Aurora A inhibitors strongly correlated to drugs targeting Polo-like kinase and ATM/ATR. FLT3 inhibitors displayed a high Spearman coefficient to the multikinase inhibitor Staurosporin. Lastly, kinase inhibitors targeting different pathways show a low correlation to other drugs, as they often showed very different activity even within one sample.

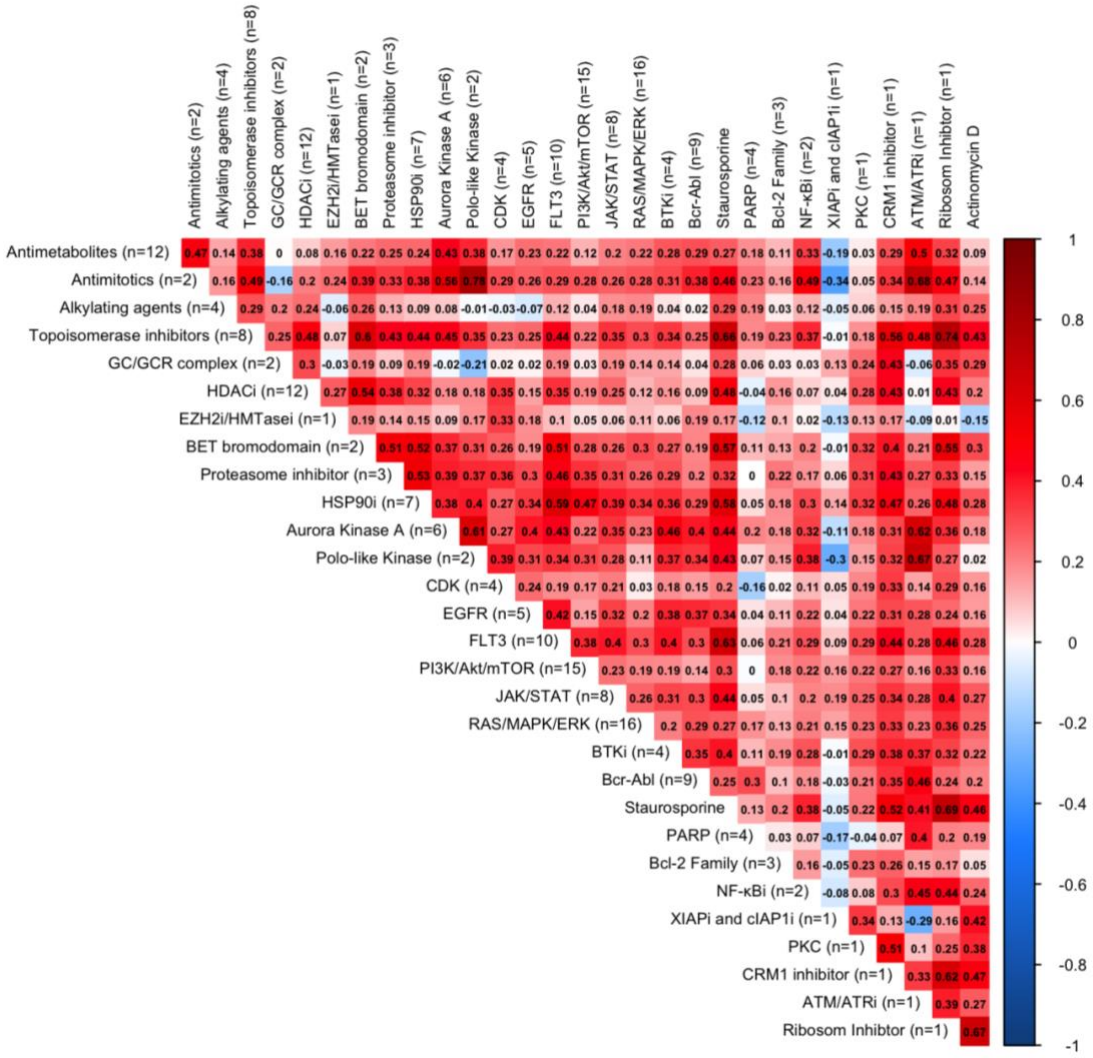

Figure 22 Correlation matrix of the Spearman correlation of all drugs and ALL samples. The Spearman correlation coefficient was averaged for each compound class. Only high correlations with a Spearman R over 0.5 were accepted as a potential combination. The number of compounds in each class is labeled behind the name of the compound class.

3.7 Subgroup Analysis

This analysis intended to find new possible drugs to repurpose for certain high- and medium-risk ALL subgroups. Although this thesis could demonstrate a low correlation between the established subgroups and their drug response, the analyses only considered the broad-spectrum drug response. Therefore, single drugs or drug classes only represented by a few drugs in the used library could still be a possible candidate to treat these high- and medium-risk subgroups more effectively. To increase the certainty of the results a three-step approach was taken, as can be seen in Figure 23. First, subgroups are compared to healthy samples to find drugs with a therapeutic window. Secondly, samples are compared to each other. As a result, drugs that show specific effects for one subgroup are detected. At last, the results of the first two steps are compared to find the best drugs for each subgroup.

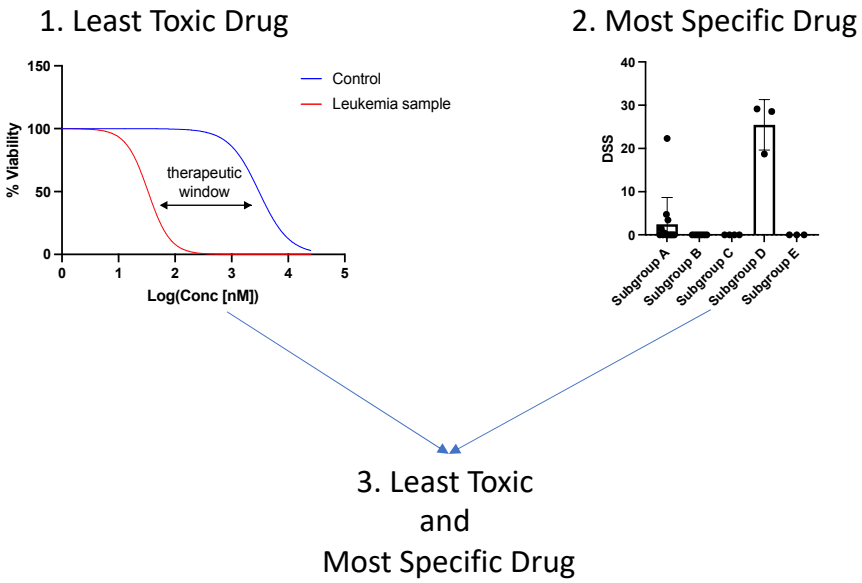

Figure 23 Overview of the analysis of the high- and medium-risk subgroups of acute lymphoblastic leukemia. First, the least toxic drug is searched for by comparing each sample to healthy controls. The most specific drug is defined by comparing each subgroup to the others and searching for drugs that show increased activity in one subgroup compared to the others. At last, both analyses are compared to find the potentially least toxic and most specific drugs for each subgroup.

3.7.1 Determining Drug Response Profiles of Healthy Controls

3.7.1.1 HTDS Profiles of Different Healthy Cells Reveal a Cell-Type-Specific Response

As described above, various healthy samples were drug screened to indicate potential toxic effects for each drug. However, since severe and life-threatening adverse events are often in

connection to myelosuppression, and not all tissues are available or could be managed to be screened, the focus was set on blood cells. As acute leukemias are dysregulated blood progenitor cells, these tissues are the most interesting for a direct comparison. Thus, healthy PBMCs, T-cells, EBV-immortalized B-cells, and CD34-positive HSPCs from healthy donors were screened. In addition, the healthy fibroblast tissues that had already been screened were included in this analysis. As the number of fibroblast samples would have overshadowed the other samples, Figure 24 only displays the mean values for each drug. Interestingly, it can be immediately noticed that HSPCs showed the most sensitive phenotype. This was unexpected, as HSPCs typically offer a very resistant phenotype, allowing chemotherapy to kill tumor cells while sparing healthy stem cells. However, as these HSPCs differentiate and proliferate, they become susceptible to chemotherapy. Nevertheless, despite being the most sensitive entity overall, there were a few drugs, for example, Venetoclax – a BCL-2 inhibitor – and QNZ– an NF-kappaB inhibitor, for which the CD34-positive HSPCs were resistant. Then again, PBMCs and T-cells displayed a similar drug profile, while B-cells and fibroblasts were clustered together. B-cells showed the most heterogeneous profile of the different cell entities. The methodical EBV immortalization cannot be ruled out as an interference factor. Moreover, the B-cell sample “3” was the most resistant, while the B-cell sample “1” was the most sensitive B-cell line. Although B-cell sample “4” was displayed in the heatmap for completeness, it was excluded from further analysis since our collaborators found a hyperdiploid chromosomal set in other experiments. It is uncertain whether PBMCs grew during the HTDS, but T-cells, B-cells, and CD34-positive HSPCs proliferated *in vitro*.

Concluding, healthy cells of different cell types show a unique drug response profile in the HTDS. Surprisingly, the CD34-positive HSPCs showed the most sensitive profile.

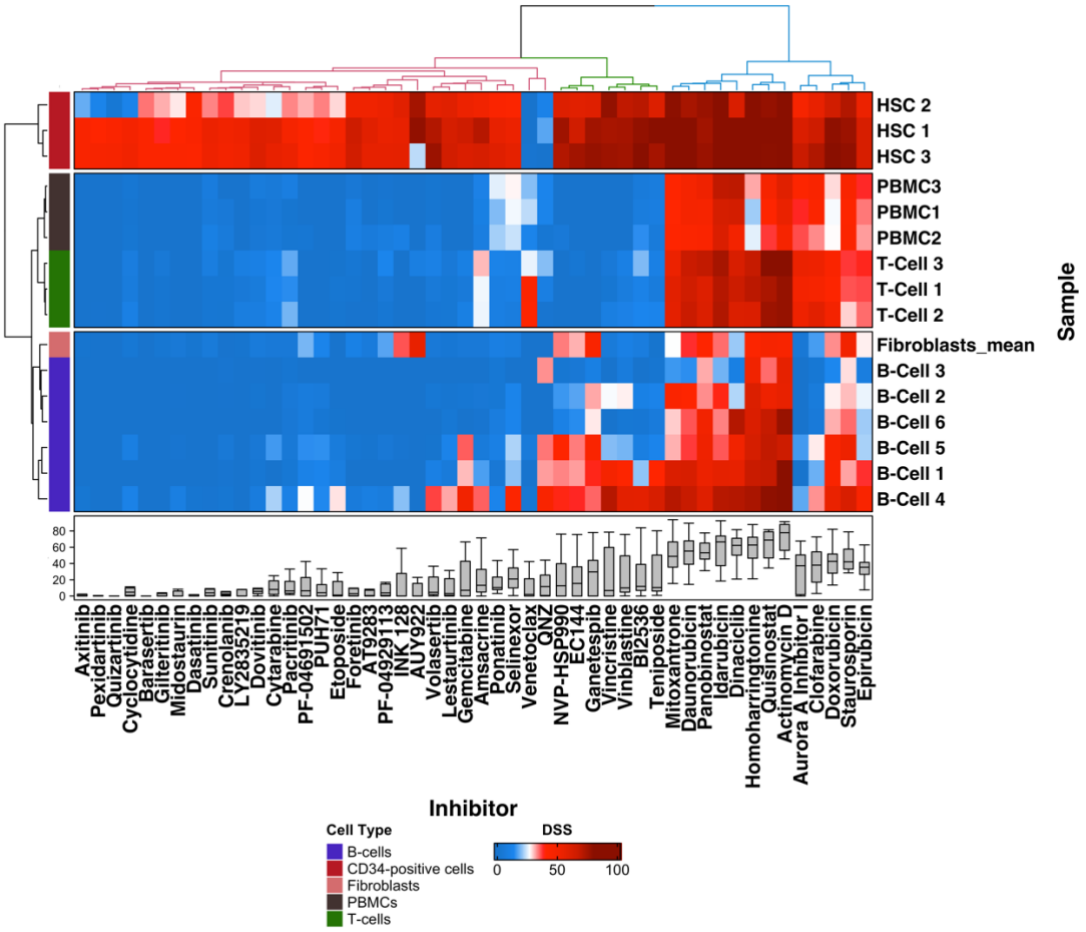

Figure 24 Heatmap visualization of the DSS values from the drug screenings of healthy samples. Only the 50 drugs with the highest variance were plotted. The Data for the PBMCs are mean values of three replicates, while the fibroblast equals the mean value of 51 samples. The boxplot again shows the distribution of DSS values with the highest and lowest scores marked by the whiskers. A color code for the cell type was added to the left.

3.7.1.2 Comparison of High- and Medium-Risk Subgroups against Healthy Samples Reveal Drugs with a Possible Therapeutic Window

A value for each drug was calculated as a reference from the screenings of healthy samples. This was done using the highest value for each drug of the screenings of PBMCs, T-cells, B-cells, and CD34-positive cells. This approach is very conservative. However, taking the mean or median would not have made sense, as these samples responded differently for each drug. The resulting reference DSS values are then subtracted from each sample individually, thereby calculating the differential DSS (dDSS). A separate one-sample Wilcoxon test with zero as the hypothetical value was conducted for each subgroup and drug. A relevant effect was assumed if the dDSS was above 10 points. The results can be seen in Figure 25.

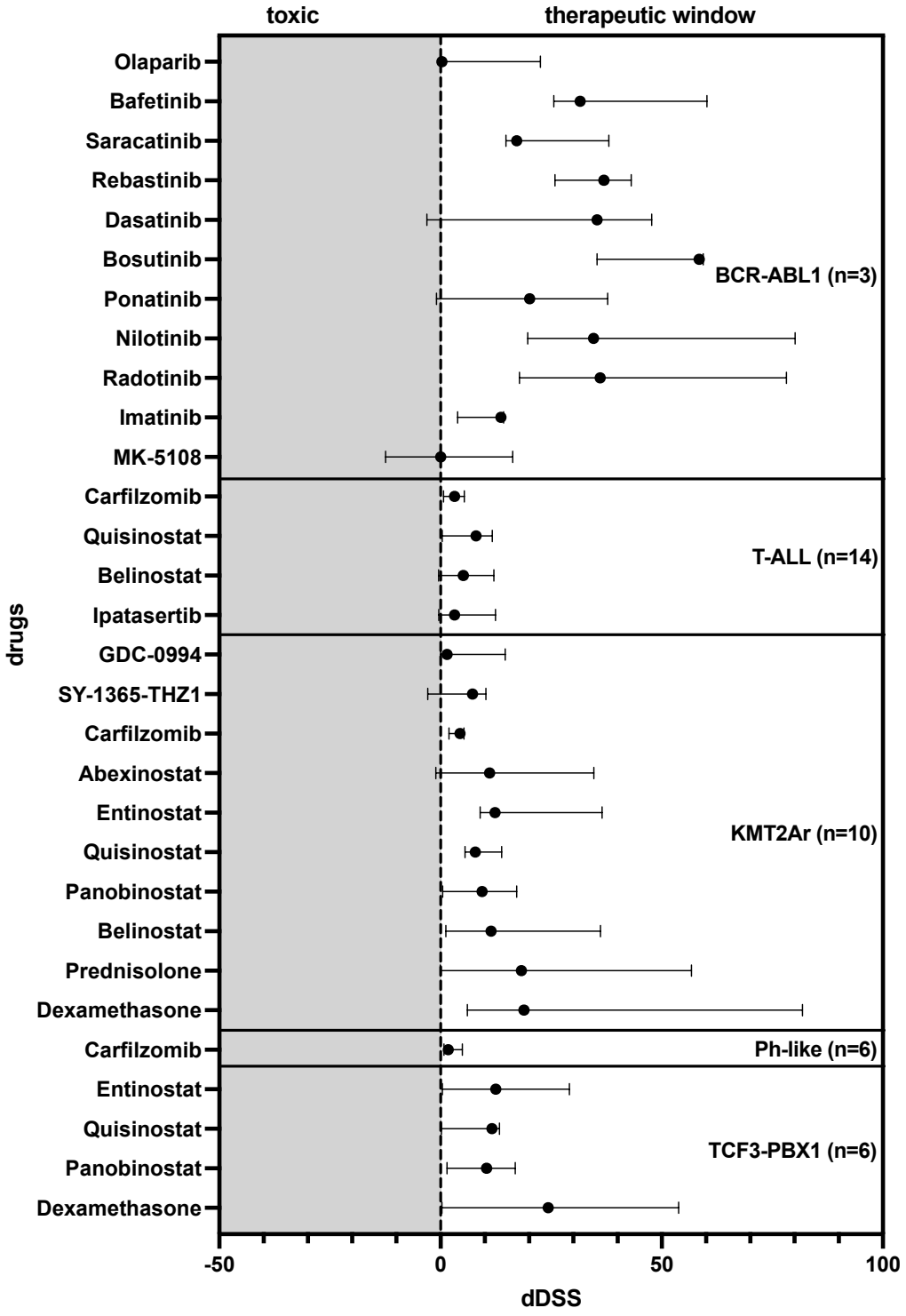

Figure 25 Graph displaying the results of the One-Sample Wilcoxon test. All compounds with a p-value <0.05 are shown, except for the BCR-ABL1 subgroup where all compounds with a median over zero are shown. The error bars show the 95%-confidence interval of the median. The x-axis displays the differential drug sensitivity score (dDSS) between the samples of each subgroup subtracted with the highest value of the healthy controls for each compound. A negative dDSS would mean a higher toxicity towards healthy than leukemia cells and therefore, the drug would be classified as toxic. A dDSS over zero would predict a potential therapeutic window for this drug, as the anti-leukemic effect is higher than the toxic effect against healthy cells.

In the BCR-ABL1 subgroup, 19 drugs presented no response in all samples. Therefore, no test was computed for them. The remaining 151 drugs were not significantly different from zero. However, due to the low number of samples, drugs with an actual median of over zero were also looked at. All nine TKi showed an increased response compared to the healthy samples as a proof-of-concept. Moreover, the 95% confidence interval for only two of the nine drugs included zero. At the same time, six of them proposed a relevant effect with the confidence interval exceeding the threshold of ten DSS points. Aside from the TKis, one Aurora Kinase inhibitor and one PARP inhibitor had a median over zero.

Eighteen drugs showed no response in T-ALL samples, so no test was calculated. Fifty-three drugs did not significantly differ from zero, while 99 did. However, of these 99 drugs, only four showed higher sensitivity in the T-ALL samples. Included in these are two HDAC inhibitors (Belinostat, Quisinostat), one Proteasome inhibitor (Carfilzomib), and at last, an AKT inhibitor (Ipatasertib). All drugs except for Carfilzomib showed a possible relevant effect of ten DSS points. Two drugs (Belinostat and Ipatasertib) included negative values in their 95% confidence interval, suggesting a potential toxic effect.

While all KMT2Ar samples did not respond to 21 drugs, 101 significantly deviated from zero in at least one sample. However, only ten drugs were superior in the activity in the KMT2Ar samples compared to the healthy control samples. Again a total of five HDAC inhibitors were found in that list. The effect compared to healthy probes was also considered possibly relevant, as all included the threshold of ten DSS points in the 95% confidence interval. Interestingly, this subgroup also seems vulnerable to glucocorticoids. Carfilzomib was already detected in the T-ALL subgroup as a potential treatment option and presented activity in the KMT2Ar group as well. The remaining two drugs included one CDK7 inhibitor and one ERK inhibitor.

In the TCF3-PBX1 subgroup, no test could be computed for 21 samples, as no response was seen. Moreover, of the 83 significant drugs, only four presented with a positive actual median. Interestingly, the two subgroups these four drugs belong to are the glucocorticoids on one side and the HDAC inhibitors on the other.

In the Ph-like group, only one of these drugs demonstrated a higher response in Ph-like ALL than in the controls. This drug was again Carfilzomib. Nevertheless, the effect measured with the 95% confidence interval did not suggest a relevant effect of ten DSS points.

The TCF3-HLF1 subgroup showed a positive actual median for 13 drugs, but the 95% confidence interval could not exclude the null hypothesis. A reason for this could be the low overall number of samples in this group.

3.7.2 Comparing Subgroups to each other Reveals the most Specific Drugs

In the search for more specific targets or treatment options, a score was calculated for each drug and subtype by awarding one point for every significant Mann-Whitney-U test between the subgroups. Therefore, higher scores suggest a more specific target for the investigated subgroup. The highest possible score is 5. The best hits for each subtype can be seen in Figure 26.

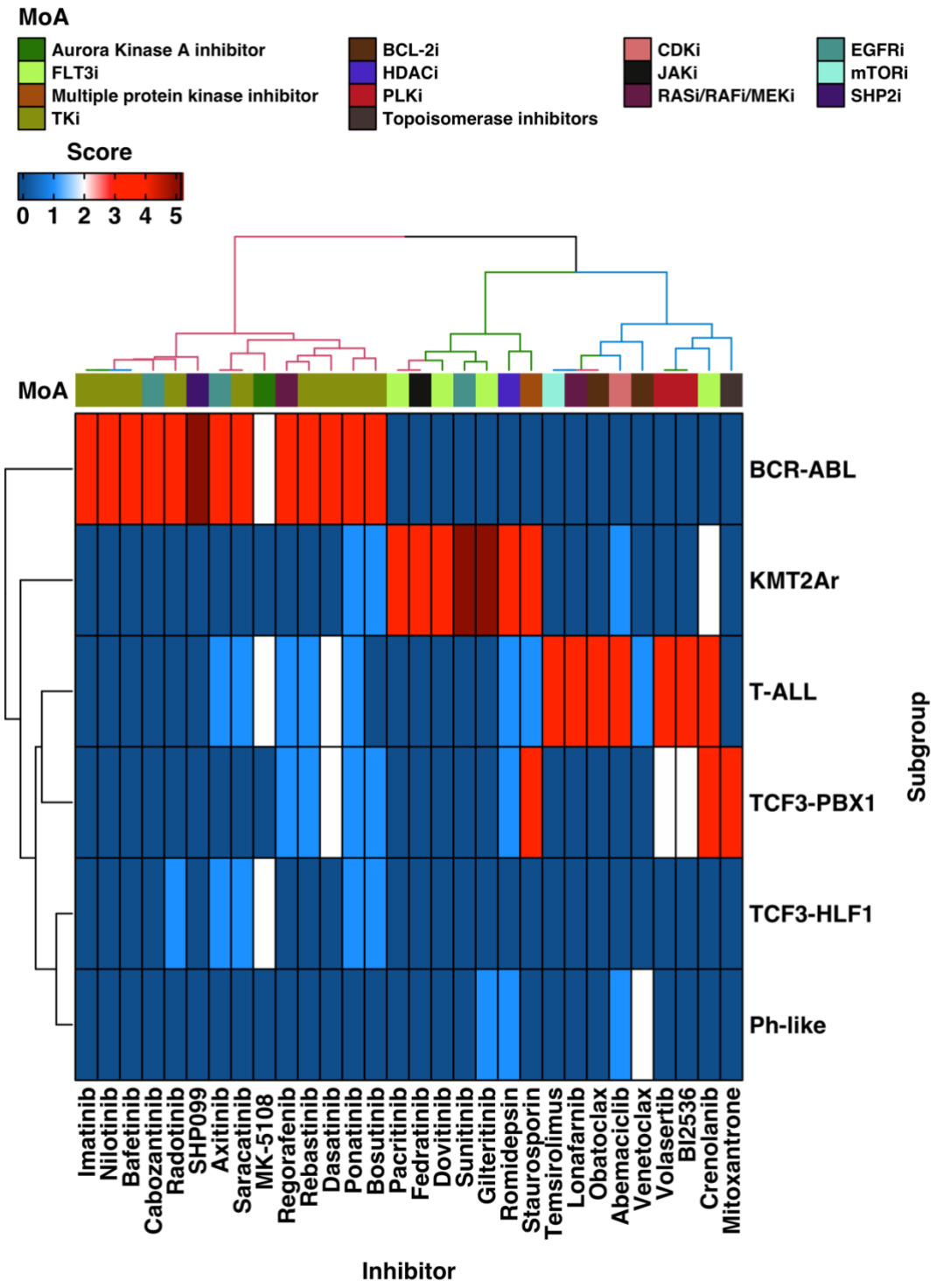

Figure 26 Heatmap displaying the score calculated by Mann-Whitney-U-tests. For each significantly higher DSS value between the subgroups was assigned one point for the specific drug and subgroup. Therefore, a higher score or a darker red in the heatmap resembles a higher specificity for that subgroup. Only drugs with a score of 3 or higher for at least one subgroup are displayed here. The color annotation shows the mechanisms of action for each drug.

As a proof-of-concept, all TKis presented with high scores, as seven of nine compounds achieved a score of four and the other two a score of three. However, the best hit for this subgroup was an experimental SHP2 inhibitor (SHP099). Other drugs targeting the same proteins or pathways scored three points (Regorafenib) or one point (Dabrafenib, Sorafenib, Binimetinib, Pimasertib), respectively. Nevertheless, the small sample size of this group could have biased these scores and reduced their validity.

For the T-ALL group, the most specific target was the Polo-like kinase, as both inhibitors included in the analysis had the highest score for this subgroup with three points. Both BCL-2 inhibitors and drugs targeting the PI3K/AKT/mTOR or RAS/RAF/MEK/ERK pathway showed high specificity for one drug (three points), while others of the group only scored one point. Interestingly, drugs currently used in treatment, such as Methotrexate or Vincristine, as well as other drugs from their groups, scored two points and, therefore, medium specificity.

The most specific hits for KMT2Ar ALL included FLT3 and growth hormone receptor inhibitors, as Sunitinib and Gilteritinib scored the highest possible value. Other drugs with the same target also presented high specificity. Other potential candidates included HDAC and kinase inhibitors targeting the JAK/STAT and PI3K/AKT/mTOR pathway.

The best results for the TCF3-PBX1 samples were achieved by the topoisomerase inhibitors, as well as other classical chemotherapeutics like antimetabolites and antimitotics. Moreover, the samples demonstrated a vulnerability against kinase inhibitors, as Staurosporine had one of the highest scores, and other TKis also presented with lower scores. Lastly, HDAC and BET bromodomain inhibitors scored low to medium-high values.

Both the Ph-like and TCF3-HLF1 samples showed a very resistant drug response. Therefore, the highest score achieved by both subgroups was two. The best result of the Ph-like group was the BCL-2 inhibitor Venetoclax. Several Aurora kinase inhibitors scored two points for the TCF3-HLF1 subgroup.

3.7.3 Least Toxic and Most Specific Drugs for each Subgroup

In this step, both prior analyses are combined. Thus, the most specific and possibly least toxic drug is identified.

3.7.3.1 BCR-ABL1

As expected, the combined strategy once again demonstrated that TKIs exhibit excellent specificity against the BCR-ABL1 subgroup, with minimal toxicity against the healthy control group. (see Figure 27A). Furthermore, MK-5108, an Aurora A inhibitor, presented with a score of two compared to other cell lines while predicting a possible treatment window, although toxicity could not be ruled out (see Figure 27B). On the contrary, the SHP2 inhibitor (SHP099), identified as the most specific hit in the BCR-ABL1 subgroup from the previous strategy, exhibited significant toxicity when tested against healthy samples. Nevertheless, directing efforts towards targeting SHP2 could hold promise as an approach for combating BCR-ABL1 B-ALL cells, although there may be a requirement for enhancing its toxicity profile.

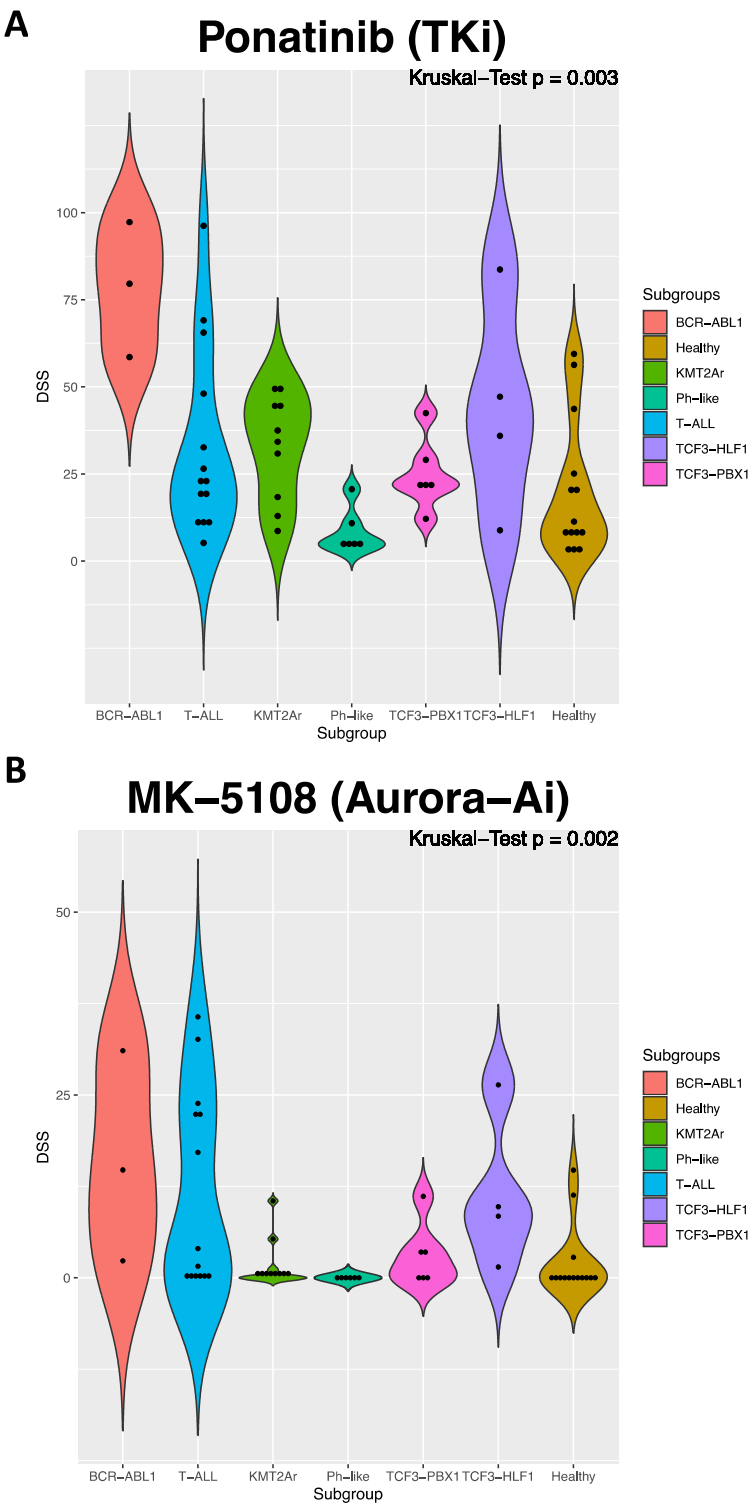

Figure 27 Violin plot of the three best drugs for both analyses for the BCR-ABL1 subgroup. The y-axis represents the drug response using the drug sensitivity score. A higher value means higher sensitivity. On the x-axis, each subgroup is represented and each subgroup has an individual color. The global p-value using a Kruskal-Test is given in the top right corner of the graph. Pairwise comparison was performed with a Wilcoxon test and corrected with the Bonferroni method. Only p-values < 0.05 are displayed on the graph. (A) Violin plot of the tyrosine kinase inhibitor (TKi) Ponatinib. (B) Violin plot of the Aurora A inhibitor MK-5108.

3.7.3.2 T-ALL

The Polo-like kinase inhibitors presented the most prominent treatment option for this group, as they scored the highest points compared to other subtypes and – although not significantly – even demonstrated a possible therapeutic window (see Figure 28A-B). However, further research must investigate whether the toxicity is manageable and whether the effect is worth it. Moreover, the BCL-2 inhibitor Obatoclax could also display an option, as the score was high, and a positive effect compared to healthy samples could not be ruled out. The currently used antimitotic Vincristine was also found as a target. Less specific but still suitable options included HDAC and Proteasome inhibitors.

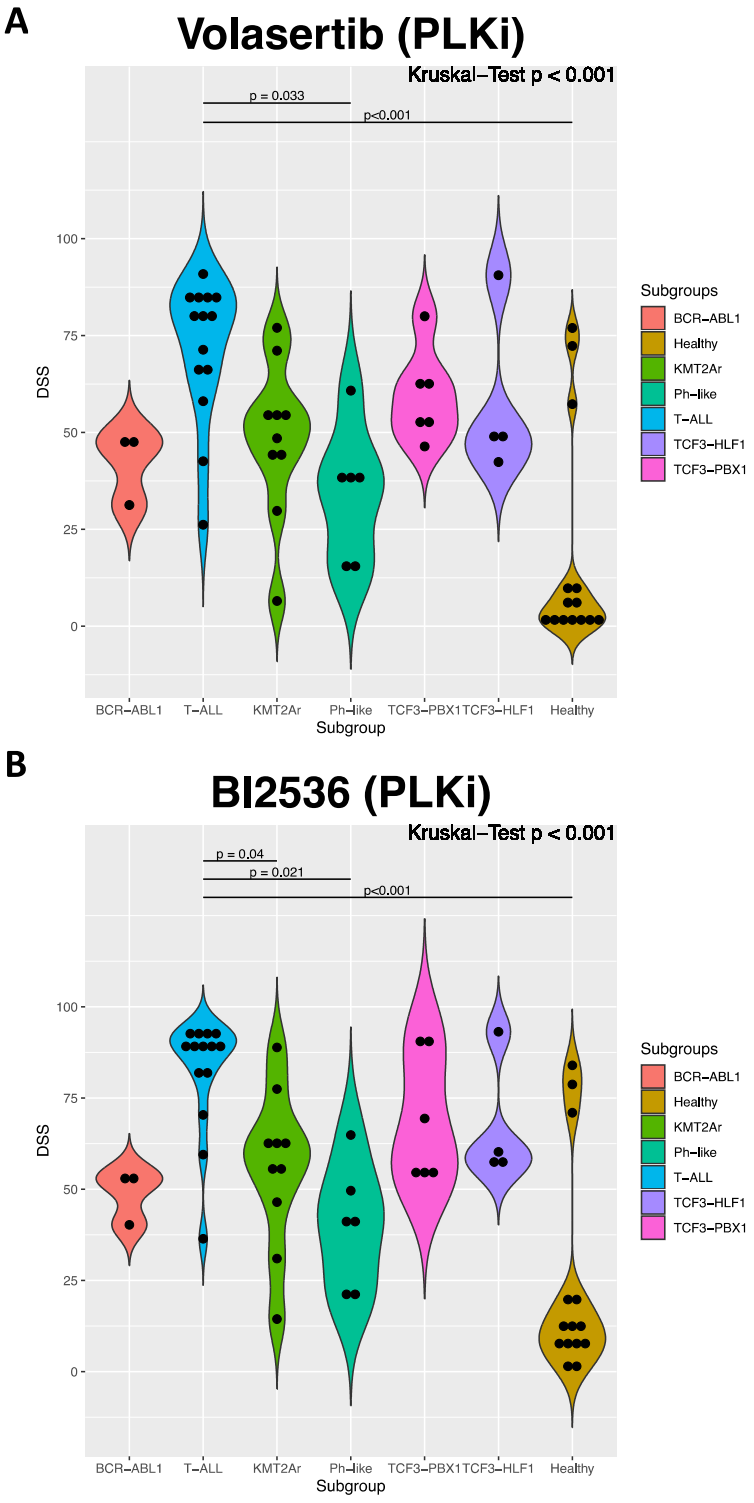

Figure 28 Violin plot of the three best drugs for both analyses for the T-ALL subgroup. The y-axis represents the drug response using the drug sensitivity score. A higher value means higher sensitivity. On the x-axis, each subgroup is represented and each subgroup has an individual color. The global p-value using a Kruskal-Test is given in the top right corner of the graph. Pairwise comparison was performed with a Wilcoxon test and corrected with the Bonferroni method. Only p-values < 0.05 are displayed on the graph. (A) Violin plot of the PLK inhibitor Volasertib. (B) Violin plot of the PLK inhibitor BI2536.

3.7.3.3 KMT2Ar

Although KMT2Ar leukemias seemed to have specific vulnerabilities to growth factor and FLT3 targeting drugs, both groups of drugs could not achieve higher DSS values in the blasts than the healthy samples (see Figure 29A). Either the drugs need to be more specific, or these proteins could not be as crucial for blast survival in this group. In contrast, HDAC inhibitors showed medium to high specificity and positive median values for the dDSS. Hence, this specific subgroup, with a notable mention of the drug Entinostat, emerged as a promising potential target (see Figure 29B). Notably, Proteasome inhibitors and glucocorticoids displayed lower scores but exhibited increased effectiveness against KMT2Ar leukemia cells compared to healthy controls.

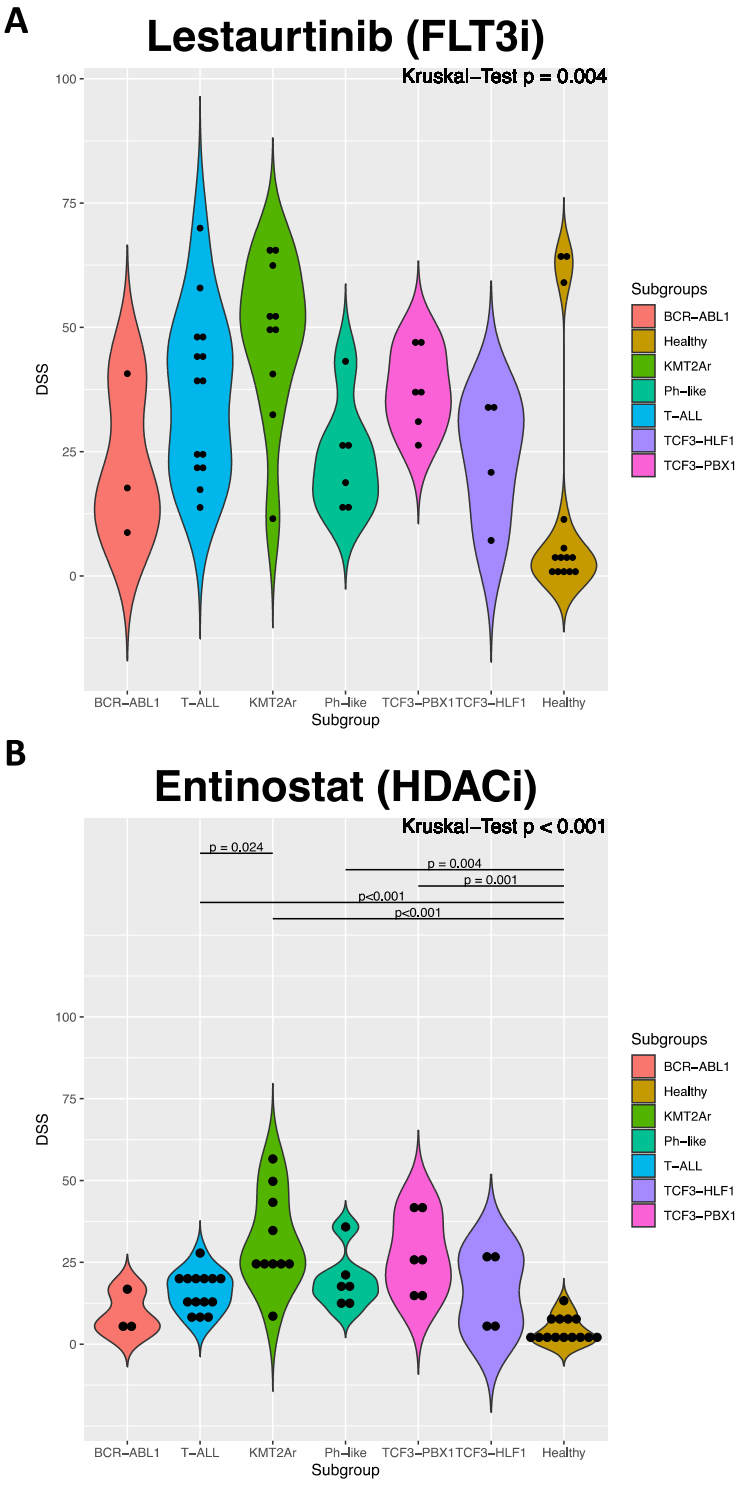

Figure 29 Violin plot of the three best drugs for both analyses for the KMT2Ar subgroup. The y-axis represents the drug response using the drug sensitivity score. A higher value means higher sensitivity. On the x-axis, each subgroup is represented and each subgroup has an individual color. The global p-value using a Kruskal-Test is given in the top right corner of the graph. Pairwise comparison was performed with a Wilcoxon test and corrected with the Bonferroni method. Only p-values < 0.05 are displayed on the graph. (A) Violin plot of the FLT3 inhibitor Lestaurtinib. (B) Violin plot of the HDAC inhibitor Entinostat.

3.7.3.4 TCF3-PBX1

Interestingly, the HTDS identified classical chemotherapeutics like antimitotics, antimetabolites, and anthracyclines as the best hits for both analyses (see Figure 30A-B). However, targeted approaches with HDAC inhibitors, BET bromodomain inhibitors, PARP inhibitors, and Bosutinib seemed promising.

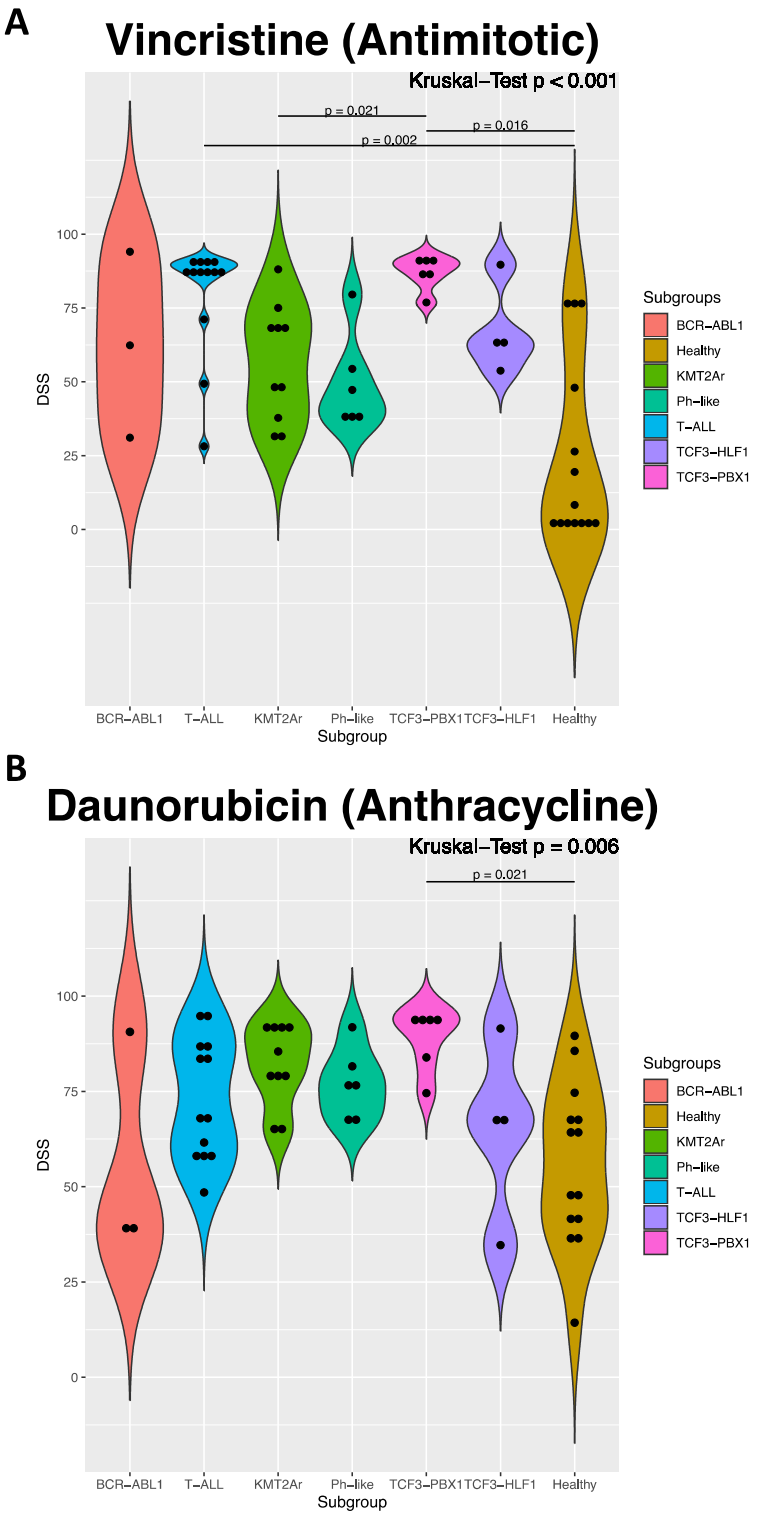

Figure 30 Violin plot of the three best drugs for both analyses for the TCF3-PBX1 subgroup. The y-axis represents the drug response using the drug sensitivity score. A higher value means higher sensitivity. On the x-axis, each subgroup is represented and each subgroup has an individual color. The global p-value using a Kruskal-Test is given in the top right corner of the graph. Pairwise comparison was performed with a Wilcoxon test and corrected with the Bonferroni method. Only p-values < 0.05 are displayed on the graph. (A) Violin plot of the antimitotic Vincristine. (B) Violin plot of the anthracycline Daunorubicin.

3.7.3.5 Ph-like

The comparison to healthy samples as well as to other subtypes, the Ph-like group displayed a heterogenous phenotype with an overall resistant drug response. Therefore, only two drug classes with low specificity and possibly fewer toxic effects could be identified. These are the HDAC and Proteasome inhibitors. Furthermore, MLN-9708 (Proteasome inhibitor) and CI-994 (HDAC inhibitor) promised the best compromise of toxicity and specificity.

3.7.3.6 TCF3-HLF1

The only overlap for this subtype was for three TKis, Bosutinib, Bafetinib, and Rebastinib. However, once again, the low sample size demonstrated an issue in finding more and better targets for this subtype.

4 Discussion

Within this thesis, new treatment options for high-risk ALL using HTDS were presented. The screening was done with commercially available leukemia cell lines and patient-derived Fibroblast and leukemia samples.

4.1 Acute Lymphoblastic Leukemia Model

Commercially available cell lines are easy to culture and robust to external factors, predisposing them for the use of drug target finding. Even more, multiomics data is widely available for these samples, allowing the connection of multiple layers of phenotypical screenings. However, a study comparing gene expression data of the NCI-60 cell lines and patient-derived glioblastoma samples could detect differences between both groups. Thus, questioning the sole use of commercially available cell lines for disease modeling [140]. Furthermore, the necessity of long *in vitro* cultivation could have an impact on its own, as new genetic mutations occur over time [141, 142]. Patient-derived leukemia samples, in contrast, recapitulate different aspects of the original disease. These include the preservation of clonal heterogeneity, genetic profiles, and other characteristics such as growth, disease outcome, and even metastasis in solid tumors [143-146]. Even during the *in vitro* culture of patient-derived samples, the self-renewal and leukemia-initiating potential is preserved [147]. However, these methods are time-consuming, and the culture is often unsuccessful. Since only successful *in vitro* cultured samples were implemented on this pipeline, a survivorship bias must be considered. However, implementing freshly available PDX and primary samples counteracted this to a certain degree. Although both models have advantages and disadvantages, integrating both can complement each other. At best, this results in a more diverse and hopefully more clinically relevant model [144].

4.2 High-Throughput Drug Screening

HTDS also has its limitations. The integration of routine *in vitro* drug sensitivity screenings in treatment protocols was done with varying success in different studies. The German CoALL 07-03 study displayed a low correlation between the *in vitro* and *in vivo* drug response [148]. The long-term outcome and response in the predecessor study CoALL 06-97 came to a similar result. With the short-term response looking promising, the long-term response correlated low with the *in vitro* response [149]. Thus, *in vitro* drug testing was abolished for future trials. In both studies, only chemotherapeutics currently used in treatment protocols were tested. In contrast,

a trial implementing drug testing and other molecular profiling to tailor individualized and targeted treatments for relapsed and refractory acute myeloid leukemias could induce clinical response [150]. Even though long-term remission was not achieved, this data encourages applying *in vitro* drug sensitivity scoring to finding new targets, at least in relapsed and refractory leukemia. Other studies tried to implement Drug Sensitivity Scoring into clinical decision-making with more success. SpheroNeo – a study about breast cancer –and others investigating hematologic malignancies could translate their *in vitro* results into treatment approaches [125, 150-152]. A recent study analyzing retrospectively over 800 samples of children with ALL could demonstrate correlations between *in vitro* drug response and clinical outcome [153]. Nevertheless, the evidence for implementing this technique as a diagnostic test for single patients is insufficient, while potential could be in introducing targeted inhibitors into regular clinical use. However, this method has not only been used for treatment stratification of individual patients but was also successful in finding new possible targets for subgroups or diseases.

Looking at the hallmarks of cancer proposed by Hanahan and Weinberg, Tognon et al. describe the limitations of different methods comprehensively [119, 154]. With the methods implemented in this thesis, the categories proliferation, replicative immortality, and evading cell death could be investigated. However, invasion into other tissues – such as the CNS –, genetic instability, immune evasion, and deregulated metabolism could not be addressed. Furthermore, toxicity, tolerance, and pharmacological properties *in vivo*, such as admission, distribution, metabolism, and excretion, could not be modeled. Moreover, drug effects caused by immune modulation cannot be modeled with the method used in this thesis. The tumor-microenvironment also impacts drug response and is not studied in this thesis [155]. Thus, here described targets need further validation by biomolecular assays, higher sample sizes for each group, and, most importantly, *in vivo* xenograft models.

4.3 Protocols for Culturing Healthy Samples for HTDS

This study implemented a modified protocol from Yost et al. They described the expansion of T-cells *in vitro* [132]. The HTDS of PBMCs and T-cells presented a similar drug response profile in this thesis. As the amount of PBMCs declines over time, the time point for the HTDS executed in this paper could have been chosen too early, and the number of T-cells could have been higher than initially measured. Moreover, by modifying the protocol published by Kraus et al. CD34-positive HSPCs could be isolated and expanded [156]. Existing protocols for the study of hematotoxicity show a high correlation with clinical response [157, 158]. Nevertheless, the

HSPCs had the most sensitive drug response profile of all healthy cells in this thesis. This was counterintuitive, as they usually are very resistant, thus allowing chemotherapy to eradicate the malignant cells while sparing the HSPCs. An essential mechanism for chemotherapy resistance of HSPCs is quiescence. This G0 cell cycle state is carefully regulated, impacting several cell functions [159]. Important for this state, as well as regeneration of HSPCs after stress, were found to be megakaryocytes [160]. As these are not present in the *in vitro* culture and the HSPCs were activated, proliferated, and partially differentiated *in vitro*, these protective functions could have gotten lost. Another theory could be that the origin of the HSPCs impacted the drug response. No difference between cord blood-derived HSPCs – as used here – and adult mobilized HSPCs concerning the FasL-mediated cell death and downstream targets were reported [161]. But other distinctions cannot be ruled out and must be tested in the future. In summary, these cells could represent the fast-proliferating common progenitor into which HSPCs differentiate more accurately. These cells are mainly affected by chemotherapy and cause severe side effects if depleted. In addition, implementing healthy controls into the HTDS of tumor samples is an effective way of evaluating the toxicity of anticancer drugs [162]. It is a strength of this work. However, the focus of the healthy samples remained on blood cells. Other organ systems as the liver, myocardia, neural system, kidney, and epithelia, needed to be evaluated for a more holistic view.

4.4 Fibroblast HTDS

This work proposed an analysis to convert the HTDS data of fibroblasts into a quinary code (resistant outlier, resistant, normal response, sensitive, sensitive outlier). In future steps, these results were meant to be combined with Whole Exome Sequencing data for the fibroblasts and clinical data of the patients. Exploring the influence of mutations in fibroblasts seems tempting since the mutational burden is lower than in malignant cells carrying complex karyotypes and aberrations. Furthermore, fibroblasts are easy to obtain and culture *in vitro*.

In a proof-of-concept experiment, the results of the HTDS performed on the fibroblasts could not be replicated on the HEK293T cell line. This cell line, however, has a near triploid karyotype which could have affected the drug response as well. In addition, RAD21 overexpression has been shown to have an impact on itself. Thus, the model has strong weaknesses. This highlights the importance of investigating mutational effects on drug response in different cell models and tissue types.

4.5 Fibroblast Drug Screening and Clinical Data

This thesis includes a study on the connection between *in vitro* and clinical drug toxicity. There was no correlation between the *in vitro* drug response of healthy tissue and the frequency or severity of adverse events in the respective patient.

Only three of the five drugs examined showed a cytotoxic influence on the fibroblasts. Prednisone and Methotrexate did not induce apoptosis in fibroblast in this thesis. In general, it is unlikely that Prednisone could have a cytotoxic effect on fibroblasts, but Methotrexate should have. A possible explanation could be the enrichment of folic acid in the culture media. Folic acid acts as an antidote to Methotrexate, rescuing cells. By reducing the concentration of folic acid in the media, *in vitro* models to study Methotrexate toxicity have been described [163]. These technical limitations create a bias, which could have affected the correlation.

Regarding the clinical data, difficulties were faced when defining and measuring toxicity. While different drugs can lead to a range of adverse effects, the challenge arises when these compounds are combined in a treatment regimen, making it difficult to attribute a specific toxicity to the particular drug responsible. Thus, several toxicities of different organ systems had to be compared and quantified. Moreover, as the clinical data were analyzed retrospectively, the number of records varied heavily between patients. Thus, a bias cannot be ruled out by patients or parents who consult the ambulance for different degrees of toxicities. Accordingly, some patients will visit the hospital when experiencing slight adverse effects, while others will wait longer or seek advice from a resident pediatrician.

With the above-described challenges, no correlation could be found between the clinical and experimental data. A similar approach to modeling donor-specific, broad-spectrum toxicities in an oncological cohort has not been published yet. Nevertheless, two studies could recapitulate cardiac response to drugs *in vitro* on healthy donors [164, 165]. One study was published following a similar approach but investigating the cardiac side effects of Doxorubicin in a breast cancer cohort [166]. All these studies could identify a connection between *in vitro* and clinical data but were questioned by Blinova et al. Blinova et al. failed to recreate the first two papers with a randomly selected healthy cohort [167]. Compared to the presented experiments, these authors used induced pluripotent stem cells, which were then differentiated into cardiomyocytes. Therefore, the cells affected by the adverse reactions were also tested in the experiments, as opposed to simulating toxicities of various organ systems and tissues with one cell type, like fibroblasts. Although it still stands to question whether clinical toxicity can be reproduced or predicted by personalized *in vitro* drug screening, further experiments should

focus more on one organ system or tissue at a time. This could be a promising approach as myelotoxicity is often observed during chemotherapy and is relatively simple to measure.

4.6 Drug Response Profiles of ALL Subgroups

Contrary to the assumption that the samples would group according to their subtype, in the unsupervised clustering of all HTDSs, the samples didn´t. A recently published multiomics approach also described this finding. They could detect a high concordance in drug screening and mass spectrometry clustering, but the correlation towards the RNA sequencing was low. [168]. In addition, a study published by the St. Jude Children's Hospital investigated the drug response of over 800 patients to 18 drugs. They also described a low correlation between genetic subtypes and their drug response profile [153]. This thesis complements these findings by demonstrating similar results with fewer samples but a more extensive library of drugs. Further, this underlines the need for new predictive biomarkers for drug response. HTDS can play a crucial method in this search.

4.7 Differentiation and Drug Response

Earlier studies demonstrated a connection between drug response and the differentiation stage in the myeloid and the lymphoid lineage [169-171]. As flow cytometry is a widely available method and plays a central role in diagnosing leukemia, it seems reasonable to investigate these markers with respect to drug response.

4.7.1 CD13 Expression in B-ALL

This work evaluated the connection between the myeloid marker CD13 and drug response. Earlier studies in T-ALL showed reduced cytotoxic effect of Daunorubicin and Azacytidine if CD13 is expressed on blasts [172]. The impact of expressing myeloid antigens such as CD13 on the clinical outcome of patients is debated in the literature. On the one hand, many studies suggest no significant or relevant association between the co-expression of myeloid markers on B-ALL and the outcome of the patient [173-176]. On the other hand, a few trials identified CD13 expression as an independent risk factor for poorer outcomes [177-180]. These studies have focused mainly on pediatric cohorts. CD13 was accepted more mutually in adult patients as an indicator for a worse outcome [181, 182]. Although the clinical significance of CD13 expression remains unclear, Saxena et al. detected CD13 also in healthy B-cells. This marker was shortly expressed by B-cells maturing from the pre-B to the immature B-cell stage [183]. Likewise, they found CD13 expression negatively correlated with cytoplasmatic IgM expression, with no sample

co-expressing both markers. Taking together, this data suggests that leukemogenesis takes part at an earlier differentiation stage as CD13 is expressed.

The data of this thesis proposes FLT3 as a possible target for this subset. Moreover, pathways that are downstream targets of FLT3 displayed a vulnerability in CD13 expressing B-ALLs in this work, underlining the possibility of targeting this subset effectively. Early T-cell-precursor ALLs expressing CD13 have been shown to harbor FLT3 mutations often [184]. In summary, CD13 expression in B-ALL could correlate with a more immature B-cell status and implies the use of kinase inhibitors, which should be investigated in further studies.

4.7.2 cyIgM Expression in B-ALL

Besides CD13, cytoplasmatic IgM expression and its correlation to drug response were investigated. As described above, Saxena et al. proposed cyIgM expression as a more mature marker of B-cell development [183]. Moreover, pre-B-cell leukemia was first characterized in 1978 with the unique immunophenotype of cytoplasmatic IgM expression [185]. Other authors also suggest cyIgM as a marker for pe-B-ALLs [186]. As the presented data suggest a higher sensitivity towards classical chemotherapeutics, a better outcome would be expected. While the first describer claimed these patients responded well to chemotherapy, other authors could not prove this hypothesis [185, 187]. Nevertheless, this biomarker could mark a subset of ALLs that responded well to current treatment and should be further investigated. If this theory cannot be upheld, the investigation of kinase inhibitors targeting especially the RAS pathway as an alternative could be explored.

Concluding, here presented are two immunophenotype markers that demonstrated a possible relationship between differentiation and drug response. Flow cytometry is robust and relatively cost-efficient compared to sequencing and other methods. Therefore, the correlation between immunophenotype and drug response should be investigated further.

4.8 New Agents for High- and Medium-Risk ALLs

This thesis presented new potential therapeutic options for high- and medium-risk subtypes of ALL.

4.8.1 BCR-ABL1

The BCR-ABL1 subgroup was used as a proof-of-concept group. Nevertheless, the statistical value is limited by their sample size, which is very small (n=3). This can be seen as a weakness of

the displayed data. The small sample size was also reflected in the statistical analysis, where only a few drugs showed a consistent response. These inhibitors have been approved by both the FDA and EMA for treating a variety of BCR-ABL1 positive hematologic malignancies and are regularly used for that cause. This was seen as a proof-of-concept for the method. The experimental SHP2 inhibitor SHP099 has also been effective in this work. The role of SHP2 in the leukemogenesis of BCR-ABL1 positive ALL has been well described [188]. Nevertheless, Aurora A inhibitors have also been proposed in this thesis with the sample size restriction as a possible target. Especially the inhibitor MK-0457 was seen as potent in this subgroup [189]. In a phase I/II clinical trial, this compound also demonstrated encouraging results regarding response rates [190]. A subsequent phase II trial could not validate these findings but was limited by many drop-out patients [191]. Cheetham et al. proposed an inhibitory effect of MK-0457 on the ABL kinase [192]. However, additional assessment and optimization are required for a more comprehensive understanding of its potential.

4.8.2 T-ALL

Polo-like kinases (PLK) emerged as a promising target for T-ALL in this study. Previous research has indicated a proapoptotic effect when the PLK pathway is inhibited, as demonstrated in several studies [193, 194]. The only pediatric phase I trial conducted using the PLK inhibitor Volasertib failed to demonstrate convincing responses but did not show severe side effects [195]. However, this trial only included a small number of ALL patients, while the subset of T-ALLs was not published. Other trials in adult cohorts with AML came to similar conclusions [51]. In addition, Oliveira et al. could not find an association between prognosis and PLK mRNA expression. Even more, the expression was not elevated compared to healthy bone marrow samples [196]. Anyhow, the here demonstrated data suggest a possible therapeutic window and selective inhibition of T-ALL samples. Therefore, further investigations should be conducted.

BCL-2 has been suggested before as a potent target for T-ALL and other ALL subgroups [123]. However, clinical experience in utilizing Venetoclax for T-ALL is limited to case reports or series but provides encouraging evidence with good tolerability and response [197, 198].

This particular subgroup included the largest number of samples included in the screenings. However, with only one PDX sample available, it is crucial to validate the observations described here with a more extensive set of patient-derived samples. Consequently, additional research is warranted to investigate the potential utility of PLK and BCL-2 inhibitors in the context of T-ALL.

4.8.3 KMT2Ar

This subgroup underwent screening with the second-largest sample size, with nearly half of these samples originating either directly from patients or as PDX models. Nevertheless, KMT2A rearrangements can involve various gene partners, this subgroup exhibits heterogeneity in its biological characteristics and drug response.

FLT3 has been proposed as a target for this high-risk leukemia, as high levels show a dismal prognosis [199]. Furthermore, KMT2Ar leukemias display higher levels of FLT3 overall compared to other subgroups and were already described as sensitive towards kinase inhibitors [200]. However, a recent clinical study could not support the addition of Lestaurtinib to standard chemotherapy in general. But sub-analysis revealed a benefit for patients with a sensitivity towards Lestaurtinib *in vitro* [201]. Thus, biomarkers are needed to predict response to these drugs.

The data presented here implied using HDAC inhibitors for several ALL subgroups. It was also suggested that KMT2Ar ALL was most specifically inhibited by the compounds. The same results were published before and even replicated in mouse models [202-204]. Considering the *in vitro* data indicating the potential for histone deacetylase inhibitors (HDACi) to enhance the sensitivity of currently employed drugs, combining these agents appears to be a logical course of action. [205]. However, in a recent study, the enthusiasm for combining it with currently used agents was reduced by the emergence of severe toxicities. [206]. Thus, new protocols have to be created that improve toxicity while still providing a promising improvement of outcome.

Like the HDAC inhibitors, the Proteasome inhibitors provided evidence for therapeutic use *in vitro* [207]. But toxicities also seemed to restrict the direct clinical implication (NCT02419755, NCT02553460) [208].

Interestingly, most KMT2Ar samples screened for this thesis were sensitive to Glucocorticoids. This stands in contrast to publications defining this subgroup as resistant to these drugs. Moreover, other authors' proposed sensitivity towards Cytarabine was also not observed in this work [94, 95].

4.8.4 TCF3-PBX1

In line with recent clinical findings supporting TCF3-PBX1 as an intermediate risk group, the samples were more sensitive to classical chemotherapeutics, such as topoisomerase inhibitors,

antimetabolites, and antimitotics, compared to their counterparts with a dismal prognosis which were investigated here [92].

Several kinase inhibitors were proposed in this work. FLT3 inhibitors could have an effect through an interaction between HOXA9 and TCF3-PBX1, described in a murine model before [209].

PARP inhibitors showed a good response in this subgroup. These drugs are typically used for BRCA1/2 mutated cancers. Smith et al. described an apoptosis pathway activated by the TCF3-PBX1 oncogene in hematopoietic cells, which resulted in PARP inactivation and was suppressed by BCL-2 [210]. Whether this pathway is affected by PARP inhibitors can only be speculated, mainly as BCL-2 inhibitors worked well in this group. Another hypothesis is that genomic instability mediates PARP sensitivity in acute leukemias [211]. Since compounds targeting PARP seem active *in vitro*, the mechanism should be further explored.

BET bromodomain and multi-kinase inhibitors, such as Bosutinib, have not been described yet with a focus on this subtype. Therefore, these could be noteworthy drugs.

4.8.5 Ph-like

With many possible activating kinase alterations, this group is very heterogeneous and responds poorly to current therapy regimes [212, 213]. In this thesis, similar results were presented. Only a few drugs could be found consistently active against this group. These drugs were HDAC and Proteasome inhibitors and therefore did not target any signaling pathways directly. Both classes have been described as active against ALL several times but have yet to be further investigated with a focus on this subtype [214, 215]. As Bortezomib was newly added to the current AEIOP BFM 2017 protocol, clinical data could be available in the future on the efficiency of proteasome inhibitors for Ph-like ALLs. Establishing biomarkers for active signaling pathways is essential to guide targeted therapies for effectively addressing the heterogeneity within this subgroup.

4.8.6 TCF3-HLF1

Although the number of samples screened for this subtype was deficient, a recent study supports the here described finding of Aurora kinase inhibitors as potent drugs for TCF3-HLF1 ALLs [216]. In addition, multi-kinase inhibitors such as Bosutinib and Ponatinib have yet to be researched further and could be agents for this very rare subtype.

4.9 Combinations

Combinational partners could be suggested by correlating the response of different drugs to each other. While this method does not state anything about synergism, additive effect, or antagonism, current therapy protocols implement drugs with different targets. This reduces the occurrence of resistance by attacking different targets at once. Therefore, to find drugs that statistically could work together well, the correlation was computed.

The most prominent result was that no high negative correlation was found. This opposes results indicating divergent pathways in B-cell leukemia [217]. Aside from that, many here illustrated correlations were defined as synergistic by other authors, especially for targeted therapies in hematological or solid malignancies [218-224]. Larger sample sizes are needed for the not-yet-described combinations to uncover potential combinations, and antagonistic effects must be ruled out.

4.10 Closing Remarks and Outlook

Throughout this thesis, different targeted inhibitors were suggested for high- and medium-risk ALL. While PLK inhibition specifically targeted T-ALL, FLT3 inhibition showed a good response against KMT2Ar ALL. By comparing these responses to a set of healthy controls these results are more likely to be sustained in further experiments. Nevertheless, further *in vitro* and *in vivo* experiments are needed to validate these findings. Moreover, the established subgroups did not predict the overall drug response well, highlighting the need for reliable biomarkers for drug response. A first experiment suggested surface antigens as possible biomarkers, as CD13 expression in this B-ALL cohort predicted a FLT3 vulnerability, while cytoplasmatic IgM expressing B-ALL were sensitive to classical chemotherapeutics. These results also need further validation in different cohorts, while larger studies are needed to suggest further biomarkers. Lastly, different combinations of targeted inhibitors and classical chemotherapeutics were suggested through the correlation of their response. Further studies are needed to unveil if these combinations are beneficial for patients through synergistic effects.

Concluding, this work investigated different ways of utilizing *in vitro* HTDS in personalized precision oncology. While this method could help implement new targeted therapies into clinical practice and reduce side effects in the future, it failed to recreate toxicities *in vitro*. Moreover, this study underlines the need for new and practical biomarkers for drug response to pave the way for precision oncology in the daily clinical routine. However, with continued advances in the

field of drug screening, future efforts in both approaches could lead to a more effective and safer treatment of childhood ALL.

5 Literature

1. *Krebs in Deutschland für 2017/2018*. 2021, Robert Koch-Institut (Hrsg) und die Gesellschaft der epidemiologischen Krebsregister in Deutschland e.V. (Hrsg).
2. Hunger, S.P. and C.G. Mullighan, *Acute Lymphoblastic Leukemia in Children.* New England Journal of Medicine, 2015. **373**(16): p. 1541-1552.
3. Shuster, J.J., et al., *Prognostic significance of sex in childhood B-precursor acute lymphoblastic leukemia: a Pediatric Oncology Group Study.* J Clin Oncol, 1998. **16**(8): p. 2854-63.
4. Pui, C.H., et al., *Sex differences in prognosis for children with acute lymphoblastic leukemia.* J Clin Oncol, 1999. **17**(3): p. 818-24.
5. Lim, J.Y.-S., et al., *Genomics of racial and ethnic disparities in childhood acute lymphoblastic leukemia.* Cancer, 2014. **120**(7): p. 955-962.
6. Buitenkamp, T.D., et al., *Acute lymphoblastic leukemia in children with Down syndrome: a retrospective analysis from the Ponte di Legno study group.* Blood, 2014. **123**(1): p. 70-7.
7. Maloney, K.W., et al., *Down syndrome childhood acute lymphoblastic leukemia has a unique spectrum of sentinel cytogenetic lesions that influences treatment outcome: a report from the Children's Oncology Group.* Blood, 2010. **116**(7): p. 1045-50.
8. Sirvent, N., et al., *Overt testicular disease (OTD) at diagnosis is not associated with a poor prognosis in childhood acute lymphoblastic leukemia: results of the EORTC CLG Study 58881.* Pediatr Blood Cancer, 2007. **49**(3): p. 344-8.
9. Sirvent, N., et al., *Prognostic significance of the initial cerebro-spinal fluid (CSF) involvement of children with acute lymphoblastic leukaemia (ALL) treated without cranial irradiation: results of European Organization for Research and Treatment of Cancer (EORTC) Children Leukemia Group study 58881.* Eur J Cancer, 2011. **47**(2): p. 239-47.
10. Bürger, B., et al., *Diagnostic cerebrospinal fluid examination in children with acute lymphoblastic leukemia: significance of low leukocyte counts with blasts or traumatic lumbar puncture.* J Clin Oncol, 2003. **21**(2): p. 184-8.
11. Muriel, F.S., et al., *Comparison of central nervous system prophylaxis with cranial radiation and intrathecal methotrexate versus intrathecal methotrexate alone in acute lymphoblastic leukemia.* Blood, 1983. **62**(2): p. 241-50.
12. Teachey, D.T. and C.H. Pui, *Comparative features and outcomes between paediatric T-cell and B-cell acute lymphoblastic leukaemia.* Lancet Oncol, 2019. **20**(3): p. e142-e154.
13. Smith, M., et al., *Uniform approach to risk classification and treatment assignment for children with acute lymphoblastic leukemia.* J Clin Oncol, 1996. **14**(1): p. 18-24.
14. Hastings, C., et al., *Increased post-induction intensification improves outcome in children and adolescents with a markedly elevated white blood cell count (≥200 × 10(9) /l) with T cell acute lymphoblastic leukaemia but not B cell disease: a report from the Children's Oncology Group.* Br J Haematol, 2015. **168**(4): p. 533-46.
15. Iacobucci, I. and C.G. Mullighan, *Genetic Basis of Acute Lymphoblastic Leukemia.* J Clin Oncol, 2017. **35**(9): p. 975-983.
16. Davis, A.S., A.J. Viera, and M.D. Mead, *Leukemia: an overview for primary care.* Am Fam Physician, 2014. **89**(9): p. 731-8.
17. Chen, K.Z., et al., *Germline mutations: many roles in leukemogenesis.* Curr Opin Hematol, 2020. **27**(4): p. 288-293.
18. Hein, D., et al., *The preleukemic TCF3-PBX1 gene fusion can be generated in utero and is present in ≈0.6% of healthy newborns.* Blood, 2019. **134**(16): p. 1355-1358.

19. Marcotte, E.L., et al., *The Prenatal Origin of Childhood Leukemia: Potential Applications for Epidemiology and Newborn Screening.* Front Pediatr, 2021. **9**: p. 639479.
20. Latino-Martel, P., et al., *Maternal alcohol consumption during pregnancy and risk of childhood leukemia: systematic review and meta-analysis.* Cancer Epidemiol Biomarkers Prev, 2010. **19**(5): p. 1238-60.
21. Krille, L., et al., *Risk of cancer incidence before the age of 15 years after exposure to ionising radiation from computed tomography: results from a German cohort study.* Radiat Environ Biophys, 2015. **54**(1): p. 1-12.
22. Axelson, O., et al., *Leukemia in childhood and adolescence and exposure to ionizing radiation in homes built from uranium-containing alum shale concrete.* Epidemiology, 2002. **13**(2): p. 146-50.
23. Arber, D.A., et al., *The 2016 revision to the World Health Organization classification of myeloid neoplasms and acute leukemia.* Blood, 2016. **127**(20): p. 2391-2405.
24. Gu, Z., et al., *PAX5-driven subtypes of B-progenitor acute lymphoblastic leukemia.* Nature Genetics, 2019. **51**(2): p. 296-307.
25. Cordo', V., et al., *T-cell Acute Lymphoblastic Leukemia: A Roadmap to Targeted Therapies.* Blood Cancer Discovery, 2021. **2**(1): p. 19-31.
26. Coccaro, N., et al., *Next-Generation Sequencing in Acute Lymphoblastic Leukemia.* Int J Mol Sci, 2019. **20**(12).
27. Bernbeck, B., et al., *Symptoms of childhood acute lymphoblastic leukemia: red flags to recognize leukemia in daily practice.* Klin Padiatr, 2009. **221**(6): p. 369-73.
28. Sinigaglia, R., et al., *Musculoskeletal manifestations in pediatric acute leukemia.* J Pediatr Orthop, 2008. **28**(1): p. 20-8.
29. Bodzas, A., P. Kodytek, and J. Zidek, *Automated Detection of Acute Lymphoblastic Leukemia From Microscopic Images Based on Human Visual Perception.* Front Bioeng Biotechnol, 2020. **8**: p. 1005.
30. Cheng, J., M.M. Klairmont, and J.K. Choi, *Peripheral blood flow cytometry for the diagnosis of pediatric acute leukemia: Highly reliable with rare exceptions.* Pediatr Blood Cancer, 2019. **66**(1): p. e27453.
31. Gabriele Escherich, M.S. *Akute lymphoblastische Leukämie – ALL - im Kindesalter*. AWMF Register-Nr. 025/014 2021 [cited 2023 01.20.2023]; Version 05_2021:[Available from: https://register.awmf.org/assets/guidelines/025-014l_S1_Akute-lymphoblastische-Leukaemie-ALL-im-Kindesalter_2021-07.pdf.
32. Inaba, H., M. Greaves, and C.G. Mullighan, *Acute lymphoblastic leukaemia.* Lancet, 2013. **381**(9881): p. 1943-55.
33. Gaudichon, J., et al., *Mechanisms of extramedullary relapse in acute lymphoblastic leukemia Reconciling biological concepts and clinical issues.* Blood Reviews, 2019. **36**: p. 40-56.
34. *AIEOP-BFM ALL 2017: A randomized phase III study conducted by the AIEOP-BFM study group*. 2020, AIEOP-BFM study group.
35. Reiter, A., et al., *Chemotherapy in 998 unselected childhood acute lymphoblastic leukemia patients. Results and conclusions of the multicenter trial ALL-BFM 86.* Blood, 1994. **84**(9): p. 3122-33.
36. Riehm, H., et al., *[Corticosteroid-dependent reduction of leukocyte count in blood as a prognostic factor in acute lymphoblastic leukemia in childhood (therapy study ALL-BFM 83)].* Klin Padiatr, 1987. **199**(3): p. 151-60.
37. Dworzak, M.N., et al., *Prognostic significance and modalities of flow cytometric minimal residual disease detection in childhood acute lymphoblastic leukemia.* Blood, 2002. **99**(6): p. 1952-1958.
38. Panzer-Grümayer, E.R., et al., *Rapid molecular response during early induction chemotherapy predicts a good outcome in childhood acute lymphoblastic leukemia.* Blood, 2000. **95**(3): p. 790-794.

39. Zhou, J., et al., *Quantitative analysis of minimal residual disease predicts relapse in children with B-lineage acute lymphoblastic leukemia in DFCI ALL Consortium Protocol 95-01.* Blood, 2007. **110**(5): p. 1607-1611.
40. Parker, W.B., *Enzymology of purine and pyrimidine antimetabolites used in the treatment of cancer.* Chem Rev, 2009. **109**(7): p. 2880-93.
41. van Vuuren, R.J., et al., *Antimitotic drugs in the treatment of cancer.* Cancer Chemother Pharmacol, 2015. **76**(6): p. 1101-12.
42. Fu, D., J.A. Calvo, and L.D. Samson, *Balancing repair and tolerance of DNA damage caused by alkylating agents.* Nat Rev Cancer, 2012. **12**(2): p. 104-20.
43. Delgado, J.L., et al., *Topoisomerases as anticancer targets.* Biochem J, 2018. **475**(2): p. 373-398.
44. Schmidt, S., et al., *Glucocorticoid-induced apoptosis and glucocorticoid resistance: molecular mechanisms and clinical relevance.* Cell Death Differ, 2004. **11 Suppl 1**: p. S45-55.
45. Ho, T.C.S., A.H.Y. Chan, and A. Ganesan, *Thirty Years of HDAC Inhibitors: 2020 Insight and Hindsight.* J Med Chem, 2020. **63**(21): p. 12460-12484.
46. Duan, R., W. Du, and W. Guo, *EZH2: a novel target for cancer treatment.* J Hematol Oncol, 2020. **13**(1): p. 104.
47. Basheer, F. and B.J. Huntly, *BET bromodomain inhibitors in leukemia.* Exp Hematol, 2015. **43**(8): p. 718-31.
48. Fricker, L.D., *Proteasome Inhibitor Drugs.* Annu Rev Pharmacol Toxicol, 2020. **60**: p. 457-476.
49. Birbo, B., et al., *Role of HSP90 in Cancer.* Int J Mol Sci, 2021. **22**(19).
50. Du, R., et al., *Targeting AURKA in Cancer: molecular mechanisms and opportunities for Cancer therapy.* Mol Cancer, 2021. **20**(1): p. 15.
51. Goroshchuk, O., et al., *Polo-like kinases and acute leukemia.* Oncogene, 2019. **38**(1): p. 1-16.
52. Reinius, M.A.V. and E. Smyth, *Anti-cancer therapy with cyclin-dependent kinase inhibitors: impact and challenges.* Expert Rev Mol Med, 2021. **23**: p. e6.
53. Sabbah, D.A., R. Hajjo, and K. Sweidan, *Review on Epidermal Growth Factor Receptor (EGFR) Structure, Signaling Pathways, Interactions, and Recent Updates of EGFR Inhibitors.* Curr Top Med Chem, 2020. **20**(10): p. 815-834.
54. Gilliland, D.G. and J.D. Griffin, *The roles of FLT3 in hematopoiesis and leukemia.* Blood, 2002. **100**(5): p. 1532-1542.
55. Matthews, W., et al., *A receptor tyrosine kinase specific to hematopoietic stem and progenitor cell-enriched populations.* Cell, 1991. **65**(7): p. 1143-1152.
56. Rosnet, O., et al., *Isolation and chromosomal localization of a novel FMS-like tyrosine kinase gene.* Genomics, 1991. **9**(2): p. 380-385.
57. Holmes, M.L., et al., *Repression of Flt3 by Pax5 is crucial for B-cell lineage commitment.* Genes Dev, 2006. **20**(8): p. 933-8.
58. Li, L.X., et al., *A Flt3- and Ras-dependent pathway primes B cell development by inducing a state of IL-7 responsiveness.* J Immunol, 2010. **184**(4): p. 1728-36.
59. Cook, A.M., et al., *Role of altered growth factor receptor-mediated JAK2 signaling in growth and maintenance of human acute myeloid leukemia stem cells.* Blood, 2014. **123**(18): p. 2826-37.
60. Zhang, S. and H.E. Broxmeyer, *p85 subunit of PI3 kinase does not bind to human Flt3 receptor, but associates with SHP2, SHIP, and a tyrosine-phosphorylated 100-kDa protein in Flt3 ligand-stimulated hematopoietic cells.* Biochem Biophys Res Commun, 1999. **254**(2): p. 440-5.
61. Bertacchini, J., et al., *Targeting PI3K/AKT/mTOR network for treatment of leukemia.* Cellular and Molecular Life Sciences, 2015. **72**(12): p. 2337-2347.

62. Simioni, C., et al., *Targeting the phosphatidylinositol 3-kinase/Akt/mechanistic target of rapamycin signaling pathway in B-lineage acute lymphoblastic leukemia: An update.* J Cell Physiol, 2018. **233**(10): p. 6440-6454.
63. Fasouli, E.S. and E. Katsantoni, *JAK-STAT in Early Hematopoiesis and Leukemia.* Front Cell Dev Biol, 2021. **9**: p. 669363.
64. Prior, I.A., F.E. Hood, and J.L. Hartley, *The Frequency of Ras Mutations in Cancer.* Cancer Res, 2020. **80**(14): p. 2969-2974.
65. Dillon, M., et al., *Progress on Ras/MAPK Signaling Research and Targeting in Blood and Solid Cancers.* Cancers (Basel), 2021. **13**(20).
66. Wen, T., et al., *Inhibitors targeting Bruton's tyrosine kinase in cancers: drug development advances.* Leukemia, 2021. **35**(2): p. 312-332.
67. Cilloni, D. and G. Saglio, *Molecular pathways: BCR-ABL.* Clin Cancer Res, 2012. **18**(4): p. 930-7.
68. Druker, B.J., et al., *Effects of a selective inhibitor of the Abl tyrosine kinase on the growth of Bcr-Abl positive cells.* Nat Med, 1996. **2**(5): p. 561-6.
69. Abou Dalle, I., et al., *Treatment of Philadelphia Chromosome-Positive Acute Lymphoblastic Leukemia.* Current Treatment Options in Oncology, 2019. **20**(1): p. 4.
70. Padella, A., et al., *Targeting PARP proteins in acute leukemia: DNA damage response inhibition and therapeutic strategies.* J Hematol Oncol, 2022. **15**(1): p. 10.
71. Yalniz, F.F. and W.G. Wierda, *Targeting BCL2 in Chronic Lymphocytic Leukemia and Other Hematologic Malignancies.* Drugs, 2019. **79**(12): p. 1287-1304.
72. Imbert, V. and J.F. Peyron, *NF-κB in Hematological Malignancies.* Biomedicines, 2017. **5**(2).
73. Kordes, U., et al., *Transcription factor NF-kappaB is constitutively activated in acute lymphoblastic leukemia cells.* Leukemia, 2000. **14**(3): p. 399-402.
74. Martelli, M.P., et al., *Enasidenib and ivosidenib in AML.* Minerva Med, 2020. **111**(5): p. 411-426.
75. Christensen, M.S., et al., *Treatment-related death in childhood acute lymphoblastic leukaemia in the Nordic countries: 1992-2001.* Br J Haematol, 2005. **131**(1): p. 50-8.
76. O'Connor, D., et al., *Infection-related mortality in children with acute lymphoblastic leukemia: an analysis of infectious deaths on UKALL2003.* Blood, 2014. **124**(7): p. 1056-1061.
77. Valer, J.B., et al., *Oral mucositis in childhood cancer patients receiving high-dose methotrexate: Prevalence, relationship with other toxicities and methotrexate elimination.* Int J Paediatr Dent, 2021. **31**(2): p. 238-246.
78. Stone, J.B. and L.M. DeAngelis, *Cancer-treatment-induced neurotoxicity--focus on newer treatments.* Nat Rev Clin Oncol, 2016. **13**(2): p. 92-105.
79. Chen, C.B., et al., *Acute pancreatitis in children with acute lymphoblastic leukemia correlates with L-asparaginase dose intensity.* Pediatr Res, 2021.
80. Zawitkowska, J., et al., *Grade 3 and 4 Toxicity Profiles During Therapy of Childhood Acute Lymphoblastic Leukemia.* In Vivo, 2019. **33**(4): p. 1333-1339.
81. Bhakta, N., et al., *The cumulative burden of surviving childhood cancer: an initial report from the St Jude Lifetime Cohort Study (SJLIFE).* Lancet, 2017. **390**(10112): p. 2569-2582.
82. Haddy, T.B., R.B. Mosher, and G.H. Reaman, *Late effects in long-term survivors after treatment for childhood acute leukemia.* Clin Pediatr (Phila), 2009. **48**(6): p. 601-8.
83. Chen, P., et al., *Health utilities in pediatric cancer patients and survivors: a systematic review and meta-analysis for clinical implementation.* Qual Life Res, 2022. **31**(2): p. 343-374.
84. Relling, M.V., et al., *Clinical Pharmacogenetics Implementation Consortium Guideline for Thiopurine Dosing Based on TPMT and NUDT15 Genotypes: 2018 Update.* Clin Pharmacol Ther, 2019. **105**(5): p. 1095-1105.

85. Maamari, D., et al., *Implementation of Pharmacogenetics to Individualize Treatment Regimens for Children with Acute Lymphoblastic Leukemia.* Pharmgenomics Pers Med, 2020. **13**: p. 295-317.
86. Umerez, M., et al., *Role of miRNAs in treatment response and toxicity of childhood acute lymphoblastic leukemia.* Pharmacogenomics, 2018. **19**(4): p. 361-373.
87. Tkachuk, D.C., S. Kohler, and M.L. Cleary, *Involvement of a homolog of Drosophila trithorax by 11q23 chromosomal translocations in acute leukemias.* Cell, 1992. **71**(4): p. 691-700.
88. Meyer, C., et al., *The MLL recombinome of acute leukemias in 2017.* Leukemia, 2018. **32**(2): p. 273-284.
89. Khalidi, H.S., et al., *Acute lymphoblastic leukemia. Survey of immunophenotype, French-American-British classification, frequency of myeloid antigen expression, and karyotypic abnormalities in 210 pediatric and adult cases.* Am J Clin Pathol, 1999. **111**(4): p. 467-76.
90. Pui, C.H., et al., *Reappraisal of the clinical and biologic significance of myeloid-associated antigen expression in childhood acute lymphoblastic leukemia.* J Clin Oncol, 1998. **16**(12): p. 3768-73.
91. Pui, C.H., et al., *Outcome of treatment in childhood acute lymphoblastic leukaemia with rearrangements of the 11q23 chromosomal region.* Lancet, 2002. **359**(9321): p. 1909-15.
92. Jeha, S., et al., *Clinical significance of novel subtypes of acute lymphoblastic leukemia in the context of minimal residual disease-directed therapy.* Blood Cancer Discov, 2021. **2**(4): p. 326-337.
93. Pieters, R., et al., *Outcome of Infants Younger Than 1 Year With Acute Lymphoblastic Leukemia Treated With the Interfant-06 Protocol: Results From an International Phase III Randomized Study.* J Clin Oncol, 2019. **37**(25): p. 2246-2256.
94. Ramakers-van Woerden, N.L., et al., *In vitro drug-resistance profile in infant acute lymphoblastic leukemia in relation to age, MLL rearrangements and immunophenotype.* Leukemia, 2004. **18**(3): p. 521-9.
95. Pieters, R., et al., *Relation between age, immunophenotype and in vitro drug resistance in 395 children with acute lymphoblastic leukemia--implications for treatment of infants.* Leukemia, 1998. **12**(9): p. 1344-8.
96. Mullighan, C.G., et al., *BCR-ABL1 lymphoblastic leukaemia is characterized by the deletion of Ikaros.* Nature, 2008. **453**(7191): p. 110-4.
97. Churchman, M.L., et al., *Efficacy of Retinoids in IKZF1-Mutated BCR-ABL1 Acute Lymphoblastic Leukemia.* Cancer Cell, 2015. **28**(3): p. 343-56.
98. Martinelli, G., et al., *IKZF1 (Ikaros) deletions in BCR-ABL1-positive acute lymphoblastic leukemia are associated with short disease-free survival and high rate of cumulative incidence of relapse: a GIMEMA AL WP report.* J Clin Oncol, 2009. **27**(31): p. 5202-7.
99. Burmeister, T., et al., *Patients' age and BCR-ABL frequency in adult B-precursor ALL: a retrospective analysis from the GMALL study group.* Blood, 2008. **112**(3): p. 918-9.
100. Ribeiro, R.C., et al., *Clinical and biologic hallmarks of the Philadelphia chromosome in childhood acute lymphoblastic leukemia.* Blood, 1987. **70**(4): p. 948-53.
101. Den Boer, M.L., et al., *A subtype of childhood acute lymphoblastic leukaemia with poor treatment outcome: a genome-wide classification study.* Lancet Oncol, 2009. **10**(2): p. 125-34.
102. Mullighan, C.G., et al., *Deletion of IKZF1 and prognosis in acute lymphoblastic leukemia.* N Engl J Med, 2009. **360**(5): p. 470-80.
103. Jain, S. and A. Abraham, *BCR-ABL1-like B-Acute Lymphoblastic Leukemia/Lymphoma: A Comprehensive Review.* Arch Pathol Lab Med, 2020. **144**(2): p. 150-155.
104. Raimondi, S.C., et al., *New recurring chromosomal translocations in childhood acute lymphoblastic leukemia.* Blood, 1991. **77**(9): p. 2016-22.

105. Inukai, T., et al., *Hypercalcemia in childhood acute lymphoblastic leukemia: frequent implication of parathyroid hormone-related peptide and E2A-HLF from translocation 17;19.* Leukemia, 2007. **21**(2): p. 288-96.
106. Fischer, U., et al., *Genomics and drug profiling of fatal TCF3-HLF-positive acute lymphoblastic leukemia identifies recurrent mutation patterns and therapeutic options.* Nat Genet, 2015. **47**(9): p. 1020-1029.
107. Watanabe, A., et al., *Resistance of t(17;19)-acute lymphoblastic leukemia cell lines to multiagents in induction therapy.* Cancer Med, 2019. **8**(11): p. 5274-5288.
108. van Grotel, M., et al., *Prognostic significance of molecular-cytogenetic abnormalities in pediatric T-ALL is not explained by immunophenotypic differences.* Leukemia, 2008. **22**(1): p. 124-131.
109. Liu, Y., et al., *The genomic landscape of pediatric and young adult T-lineage acute lymphoblastic leukemia.* Nat Genet, 2017. **49**(8): p. 1211-1218.
110. Bardelli, V., et al., *T-Cell Acute Lymphoblastic Leukemia: Biomarkers and Their Clinical Usefulness.* Genes (Basel), 2021. **12**(8).
111. Schrappe, M., et al., *Late MRD response determines relapse risk overall and in subsets of childhood T-cell ALL: results of the AIEOP-BFM-ALL 2000 study.* Blood, 2011. **118**(8): p. 2077-84.
112. Winter, S.S., et al., *Improved Survival for Children and Young Adults With T-Lineage Acute Lymphoblastic Leukemia: Results From the Children's Oncology Group AALL0434 Methotrexate Randomization.* J Clin Oncol, 2018. **36**(29): p. 2926-2934.
113. Teachey, D.T. and C.-H. Pui, *Comparative features and outcomes between paediatric T-cell and B-cell acute lymphoblastic leukaemia.* The Lancet Oncology, 2019. **20**(3): p. e142-e154.
114. McMahon, C.M. and S.M. Luger, *Relapsed T Cell ALL: Current Approaches and New Directions.* Curr Hematol Malig Rep, 2019. **14**(2): p. 83-93.
115. Reismüller, B., et al., *Long-term outcome of initially homogenously treated and relapsed childhood acute lymphoblastic leukaemia in Austria--a population-based report of the Austrian Berlin-Frankfurt-Münster (BFM) Study Group.* Br J Haematol, 2009. **144**(4): p. 559-70.
116. Zhou, B., et al., *The clinical outcomes and genomic landscapes of acute lymphoblastic leukemia patients with E2A-PBX1: A 10-year retrospective study.* Am J Hematol, 2021. **96**(11): p. 1461-1471.
117. Diakos, C., et al., *Direct and indirect targets of the E2A-PBX1 leukemia-specific fusion protein.* PLoS One, 2014. **9**(2): p. e87602.
118. Felice, M.S., et al., *Prognostic impact of t(1;19)/ TCF3-PBX1 in childhood acute lymphoblastic leukemia in the context of Berlin-Frankfurt-Münster-based protocols.* Leuk Lymphoma, 2011. **52**(7): p. 1215-21.
119. Tognon, C.E., et al., *Ex Vivo Analysis of Primary Tumor Specimens for Evaluation of Cancer Therapeutics.* Annu Rev Cancer Biol, 2021. **5**: p. 39-57.
120. Dietrich, S., et al., *Drug-perturbation-based stratification of blood cancer.* The Journal of Clinical Investigation, 2018. **128**(1): p. 427-445.
121. Huang, A., et al., *Synthetic lethality as an engine for cancer drug target discovery.* Nature Reviews Drug Discovery, 2020. **19**(1): p. 23-38.
122. Basu, A., et al., *An interactive resource to identify cancer genetic and lineage dependencies targeted by small molecules.* Cell, 2013. **154**(5): p. 1151-1161.
123. Frismantas, V., et al., *Ex vivo drug response profiling detects recurrent sensitivity patterns in drug-resistant acute lymphoblastic leukemia.* Blood, 2017. **129**(11): p. e26-e37.
124. He, L., et al., *Patient-Customized Drug Combination Prediction and Testing for T-cell Prolymphocytic Leukemia Patients.* Cancer Res, 2018. **78**(9): p. 2407-2418.

125. Kurtz, S.E., et al., *Dual inhibition of JAK1/2 kinases and BCL2: a promising therapeutic strategy for acute myeloid leukemia.* Leukemia, 2018. **32**(9): p. 2025-2028.
126. Spinner, M.A., et al., *Ex vivo drug screening defines novel drug sensitivity patterns for informing personalized therapy in myeloid neoplasms.* Blood Adv, 2020. **4**(12): p. 2768-2778.
127. Pan, R., et al., *Selective BCL-2 inhibition by ABT-199 causes on-target cell death in acute myeloid leukemia.* Cancer Discov, 2014. **4**(3): p. 362-75.
128. DiNardo, C.D., et al., *10-day decitabine with venetoclax for newly diagnosed intensive chemotherapy ineligible, and relapsed or refractory acute myeloid leukaemia: a single-centre, phase 2 trial.* Lancet Haematol, 2020. **7**(10): p. e724-e736.
129. DiNardo, C.D., et al., *Safety and preliminary efficacy of venetoclax with decitabine or azacitidine in elderly patients with previously untreated acute myeloid leukaemia: a non-randomised, open-label, phase 1b study.* Lancet Oncol, 2018. **19**(2): p. 216-228.
130. Konopleva, M., et al., *Efficacy and Biological Correlates of Response in a Phase II Study of Venetoclax Monotherapy in Patients with Acute Myelogenous Leukemia.* Cancer Discov, 2016. **6**(10): p. 1106-1117.
131. Kucukyurt, S. and A.E. Eskazan, *New drugs approved for acute myeloid leukaemia in 2018.* Br J Clin Pharmacol, 2019. **85**(12): p. 2689-2693.
132. Yost, A.J., et al., *Defined, serum-free conditions for in vitro culture of primary human T-ALL blasts.* Leukemia, 2013. **27**(6): p. 1437-40.
133. Saitta, C., et al., *Potential role of STAG1 mutations in genetic predisposition to childhood hematological malignancies.* Blood Cancer J, 2022. **12**(6): p. 88.
134. Yadav, B., et al., *Quantitative scoring of differential drug sensitivity for individually optimized anticancer therapies.* Sci Rep, 2014. **4**: p. 5193.
135. Gu, Z., R. Eils, and M. Schlesner, *Complex heatmaps reveal patterns and correlations in multidimensional genomic data.* Bioinformatics, 2016. **32**(18): p. 2847-9.
136. Services, U.S.D.o.H.a.H. *Common Terminology Criteria for Adverse Events (CTCAE) Version 5.0*. 2017; Available from: https://ctep.cancer.gov/protocoldevelopment/electronic_applications/docs/ctcae_v5_quick_reference_5x7.pdf.
137. Wickham, H., *ggplot2: Elegant Graphics for Data Analysis*. 2016: Springer-Verlag New York.
138. Simko, T.W.a.V. *R package 'corrplot': Visualization of a Correlation Matrix*. 2021; Version 0.92:[Available from: https://github.com/taiyun/corrplot.
139. Kassambara, A. *factoextra: Extract and Visualize the Results of Multivariate Data Analyses*. 2016; R package version 1.0.7:[Available from: https://cran.r-project.org/web/packages/factoextra.
140. Zeeberg, B.R., et al., *Concordance of gene expression and functional correlation patterns across the NCI-60 cell lines and the Cancer Genome Atlas glioblastoma samples.* PLoS One, 2012. **7**(7): p. e40062.
141. Gazdar, A.F., B. Gao, and J.D. Minna, *Lung cancer cell lines: Useless artifacts or invaluable tools for medical science?* Lung Cancer, 2010. **68**(3): p. 309-18.
142. Gillet, J.P., S. Varma, and M.M. Gottesman, *The clinical relevance of cancer cell lines.* J Natl Cancer Inst, 2013. **105**(7): p. 452-8.
143. DeRose, Y.S., et al., *Tumor grafts derived from women with breast cancer authentically reflect tumor pathology, growth, metastasis and disease outcomes.* Nat Med, 2011. **17**(11): p. 1514-20.
144. Di Renzo, M.F. and S. Corso, *Patient-Derived Cancer Models.* Cancers (Basel), 2020. **12**(12).
145. Dobson, S.M., et al., *Relapse-Fated Latent Diagnosis Subclones in Acute B Lineage Leukemia Are Drug Tolerant and Possess Distinct Metabolic Programs.* Cancer Discov, 2020. **10**(4): p. 568-587.

146. Wang, K., et al., *Patient-derived xenotransplants can recapitulate the genetic driver landscape of acute leukemias.* Leukemia, 2017. **31**(1): p. 151-158.
147. Pal, D., et al., *Long-term in vitro maintenance of clonal abundance and leukaemia-initiating potential in acute lymphoblastic leukaemia.* Leukemia, 2016. **30**(8): p. 1691-700.
148. Schramm, F., et al., *Results of CoALL 07-03 study childhood ALL based on combined risk assessment by in vivo and in vitro pharmacosensitivity.* Blood Adv, 2019. **3**(22): p. 3688-3699.
149. Escherich, G., et al., *The long-term impact of in vitro drug sensitivity on risk stratification and treatment outcome in acute lymphoblastic leukemia of childhood (CoALL 06-97).* Haematologica, 2011. **96**(6): p. 854-62.
150. Pemovska, T., et al., *Individualized systems medicine strategy to tailor treatments for patients with chemorefractory acute myeloid leukemia.* Cancer Discov, 2013. **3**(12): p. 1416-29.
151. Boidol, B., et al., *First-in-human response of BCL-2 inhibitor venetoclax in T-cell prolymphocytic leukemia.* Blood, 2017. **130**(23): p. 2499-2503.
152. Halfter, K., et al., *Prospective cohort study using the breast cancer spheroid model as a predictor for response to neoadjuvant therapy--the SpheroNEO study.* BMC Cancer, 2015. **15**: p. 519.
153. Lee, S.H.R., et al., *Pharmacotypes across the genomic landscape of pediatric acute lymphoblastic leukemia and impact on treatment response.* Nat Med, 2023. **29**(1): p. 170-179.
154. Hanahan, D. and Robert A. Weinberg, *Hallmarks of Cancer: The Next Generation.* Cell, 2011. **144**(5): p. 646-674.
155. Bakker, E., et al., *The role of microenvironment and immunity in drug response in leukemia.* Biochim Biophys Acta, 2016. **1863**(3): p. 414-426.
156. Kraus, H., et al., *A feeder-free differentiation system identifies autonomously proliferating B cell precursors in human bone marrow.* J Immunol, 2014. **192**(3): p. 1044-54.
157. Guo, L., et al., *Human CD34+ progenitor hematopoiesis in liquid culture for in vitro assessment of drug-induced myelotoxicity.* Toxicology in Vitro, 2016. **31**: p. 103-113.
158. Haglund, C., et al., *The FMCA-GM assays, high throughput non-clonogenic alternatives to CFU-GM in preclinical hematotoxicity testing.* Toxicology Letters, 2010. **194**(3): p. 102-107.
159. O'Reilly, E., H.A. Zeinabad, and E. Szegezdi, *Hematopoietic versus leukemic stem cell quiescence: Challenges and therapeutic opportunities.* Blood Rev, 2021: p. 100850.
160. Zhao, M., et al., *Megakaryocytes maintain homeostatic quiescence and promote post-injury regeneration of hematopoietic stem cells.* Nat Med, 2014. **20**(11): p. 1321-6.
161. Kim, H., et al., *Human CD34+ hematopoietic stem/progenitor cells express high levels of FLIP and are resistant to Fas-mediated apoptosis.* Stem Cells, 2002. **20**(2): p. 174-82.
162. Haglund, C., et al., *In vitro evaluation of clinical activity and toxicity of anticancer drugs using tumor cells from patients and cells representing normal tissues.* Cancer Chemother Pharmacol, 2012. **69**(3): p. 697-707.
163. Driehuis, E., et al., *Patient-derived oral mucosa organoids as an in vitro model for methotrexate induced toxicity in pediatric acute lymphoblastic leukemia.* PLoS One, 2020. **15**(5): p. e0231588.
164. Shinozawa, T., et al., *Recapitulation of Clinical Individual Susceptibility to Drug-Induced QT Prolongation in Healthy Subjects Using iPSC-Derived Cardiomyocytes.* Stem Cell Reports, 2017. **8**(2): p. 226-234.
165. Stillitano, F., et al., *Modeling susceptibility to drug-induced long QT with a panel of subject-specific induced pluripotent stem cells.* Elife, 2017. **6**.

166. Burridge, P.W., et al., *Human induced pluripotent stem cell-derived cardiomyocytes recapitulate the predilection of breast cancer patients to doxorubicin-induced cardiotoxicity.* Nat Med, 2016. **22**(5): p. 547-56.
167. Blinova, K., et al., *Clinical Trial in a Dish: Personalized Stem Cell-Derived Cardiomyocyte Assay Compared With Clinical Trial Results for Two QT-Prolonging Drugs.* Clin Transl Sci, 2019. **12**(6): p. 687-697.
168. Leo, I.R., et al., *Integrative multi-omics and drug response profiling of childhood acute lymphoblastic leukemia cell lines.* Nature Communications, 2022. **13**(1): p. 1691.
169. Kuusanmäki, H., et al., *Phenotype-based drug screening reveals association between venetoclax response and differentiation stage in acute myeloid leukemia.* Haematologica, 2020. **105**(3): p. 708-720.
170. Pietarinen, P.O., et al., *Differentiation status of primary chronic myeloid leukemia cells affects sensitivity to BCR-ABL1 inhibitors.* Oncotarget, 2017. **8**(14): p. 22606-22615.
171. Pieters, R., et al., *Cellular drug resistance profiles that might explain the prognostic value of immunophenotype and age in childhood acute lymphoblastic leukemia.* Leukemia, 1993. **7**(3): p. 392-7.
172. Savaşan, S., et al., *Evaluation of cytotoxicity by flow cytometric drug sensitivity assay in childhood T-cell acute lymphoblastic leukemia.* Leuk Lymphoma, 2005. **46**(6): p. 833-40.
173. Guglielmi, C., et al., *Immunophenotype of adult and childhood acute lymphoblastic leukemia: changes at first relapse and clinico-prognostic implications.* Leukemia, 1997. **11**(9): p. 1501-7.
174. Ng, S.M., et al., *Clinical features and treatment outcome of children with myeloid antigen coexpression in B-lineage acute lymphoblastic leukemia: a study of 151 Malaysian children.* J Trop Pediatr, 2000. **46**(2): p. 73-8.
175. Supriyadi, E., et al., *Myeloid Antigen Expression in Childhood Acute Lymphoblastic Leukemia and Its Relevance for Clinical Outcome in Indonesian ALL-2006 Protocol.* J Oncol, 2012. **2012**: p. 135186.
176. Uckun, F.M., et al., *Clinical features and treatment outcome of children with myeloid antigen positive acute lymphoblastic leukemia: a report from the Children's Cancer Group.* Blood, 1997. **90**(1): p. 28-35.
177. Amirghofran, Z., et al., *The influence of Bcl-2 and myeloid antigen expression on response to therapy in childhood acute lymphoblastic leukemia.* Arch Iran Med, 2011. **14**(3): p. 170-4.
178. Cantù-Rajnoldi, A., et al., *Co-expression of myeloid antigens in childhood acute lymphoblastic leukaemia: relationship with the stage of differentiation and clinical significance.* Br J Haematol, 1991. **79**(1): p. 40-3.
179. Fink, F.M., et al., *Prognostic significance of myeloid-associated antigen expression on blast cells in children with acute lymphoblastic leukemia. The Austrian Pediatric Oncology Group.* Med Pediatr Oncol, 1993. **21**(5): p. 340-6.
180. Sobol-Milejska, G., A. Mizia-Malarz, and H. Wos, *Expression of myeloid antigens on lymphoblast surface in childhood acute lymphoblastic leukemia at diagnosis and its effect on early response to treatment: a preliminary report.* Int J Hematol, 2013. **98**(3): p. 331-6.
181. Craddock, K.J., et al., *CD13 expression is an independent adverse prognostic factor in adults with Philadelphia chromosome negative B cell acute lymphoblastic leukemia.* Leukemia Research, 2013. **37**(7): p. 759-764.
182. Dalal, B.I., et al., *Aberrant expression of CD13 identifies a subgroup of standard-risk adult acute lymphoblastic leukemia with inferior survival.* Clin Lymphoma Myeloma Leuk, 2014. **14**(3): p. 239-44.
183. Saxena, A., et al., *Expression of CD13/aminopeptidase N in precursor B-cell leukemia: role in growth regulation of B cells.* Cancer Immunology, Immunotherapy, 2009. **59**(1): p. 125.

184. Neumann, M., et al., *FLT3 mutations in early T-cell precursor ALL characterize a stem cell like leukemia and imply the clinical use of tyrosine kinase inhibitors.* PLoS One, 2013. **8**(1): p. e53190.
185. Vogler, L.B., et al., *Pre-B-cell leukemia. A new phenotype of childhood lymphoblastic leukemia.* N Engl J Med, 1978. **298**(16): p. 872-8.
186. Koníková, E., et al., *Some early differentiation markers detected in cytoplasm of pre-B cells by flow cytometry.* Neoplasma, 1996. **43**(6): p. 373-9.
187. Crist, W., et al., *Prognostic importance of the pre-B-cell immunophenotype and other presenting features in B-lineage childhood acute lymphoblastic leukemia: a Pediatric Oncology Group study.* Blood, 1989. **74**(4): p. 1252-9.
188. Gu, S., et al., *SHP2 is required for BCR-ABL1-induced hematologic neoplasia.* Leukemia, 2018. **32**(1): p. 203-213.
189. Dai, Y., et al., *Vorinostat synergistically potentiates MK-0457 lethality in chronic myelogenous leukemia cells sensitive and resistant to imatinib mesylate.* Blood, 2008. **112**(3): p. 793-804.
190. Giles, F.J., et al., *MK-0457, an Aurora kinase and BCR–ABL inhibitor, is active in patients with BCR–ABL T315I leukemia.* Leukemia, 2013. **27**(1): p. 113-117.
191. Seymour, J.F., et al., *A phase 2 study of MK-0457 in patients with BCR-ABL T315I mutant chronic myelogenous leukemia and philadelphia chromosome-positive acute lymphoblastic leukemia.* Blood Cancer Journal, 2014. **4**(8): p. e238-e238.
192. Cheetham, G.M.T., et al., *Structural basis for potent inhibition of the Aurora kinases and a T315I multi-drug resistant mutant form of Abl kinase by VX-680.* Cancer Letters, 2007. **251**(2): p. 323-329.
193. Kolosenko, I., et al., *RNAi prodrugs targeting Plk1 induce specific gene silencing in primary cells from pediatric T-acute lymphoblastic leukemia patients.* J Control Release, 2017. **261**: p. 199-206.
194. Spartà, A.M., et al., *Therapeutic targeting of Polo-like kinase-1 and Aurora kinases in T-cell acute lymphoblastic leukemia.* Cell Cycle, 2014. **13**(14): p. 2237-47.
195. Doz, F., et al., *Phase I dose-escalation study of volasertib in pediatric patients with acute leukemia or advanced solid tumors.* Pediatric Blood & Cancer, 2019. **66**(10): p. e27900.
196. Oliveira, J.C., et al., *PLK1 expression and BI 2536 effects in childhood acute lymphoblastic leukemia.* Pediatric Blood & Cancer, 2014. **61**(7): p. 1227-1231.
197. Farhadfar, N., et al., *Venetoclax and decitabine for treatment of relapsed T-cell acute lymphoblastic leukemia: A case report and review of literature.* Hematol Oncol Stem Cell Ther, 2021. **14**(3): p. 246-251.
198. Richard-Carpentier, G., et al., *Clinical Experience With Venetoclax Combined With Chemotherapy for Relapsed or Refractory T-Cell Acute Lymphoblastic Leukemia.* Clin Lymphoma Myeloma Leuk, 2020. **20**(4): p. 212-218.
199. Chillón, M.C., et al., *Prognostic significance of FLT3 mutational status and expression levels in MLL-AF4+ and MLL-germline acute lymphoblastic leukemia.* Leukemia, 2012. **26**(11): p. 2360-6.
200. Stam, R.W., et al., *Targeting FLT3 in primary MLL-gene-rearranged infant acute lymphoblastic leukemia.* Blood, 2005. **106**(7): p. 2484-90.
201. Brown, P.A., et al., *FLT3 inhibitor lestaurtinib plus chemotherapy for newly diagnosed KMT2A-rearranged infant acute lymphoblastic leukemia: Children's Oncology Group trial AALL0631.* Leukemia, 2021. **35**(5): p. 1279-1290.
202. Garrido Castro, P., et al., *The HDAC inhibitor panobinostat (LBH589) exerts in vivo anti-leukaemic activity against MLL-rearranged acute lymphoblastic leukaemia and involves the RNF20/RNF40/WAC-H2B ubiquitination axis.* Leukemia, 2018. **32**(2): p. 323-331.
203. Stumpel, D.J., et al., *Connectivity mapping identifies HDAC inhibitors for the treatment of t(4;11)-positive infant acute lymphoblastic leukemia.* Leukemia, 2012. **26**(4): p. 682-92.

204. Tonelli, R., et al., *G1 cell-cycle arrest and apoptosis by histone deacetylase inhibition in MLL-AF9 acute myeloid leukemia cells is p21 dependent and MLL-AF9 independent.* Leukemia, 2006. **20**(7): p. 1307-1310.
205. Bhatla, T., et al., *Epigenetic reprogramming reverses the relapse-specific gene expression signature and restores chemosensitivity in childhood B-lymphoblastic leukemia.* Blood, 2012. **119**(22): p. 5201-10.
206. Burke, M.J., et al., *Decitabine and Vorinostat with Chemotherapy in Relapsed Pediatric Acute Lymphoblastic Leukemia: A TACL Pilot Study.* Clin Cancer Res, 2020. **26**(10): p. 2297-2307.
207. Liu, H., et al., *Proteasome inhibitors evoke latent tumor suppression programs in pro-B MLL leukemias through MLL-AF4.* Cancer Cell, 2014. **25**(4): p. 530-42.
208. El Chaer, F., M. Keng, and K.K. Ballen, *MLL-Rearranged Acute Lymphoblastic Leukemia.* Curr Hematol Malig Rep, 2020. **15**(2): p. 83-89.
209. Hassawi, M., et al., *Hoxa9 collaborates with E2A-PBX1 in mouse B cell leukemia in association with Flt3 activation and decrease of B cell gene expression.* Dev Dyn, 2014. **243**(1): p. 145-58.
210. Smith, K.S., et al., *Chimeric oncoprotein E2a-Pbx1 induces apoptosis of hematopoietic cells by a p53-independent mechanism that is suppressed by Bcl-2.* Oncogene, 1997. **14**(24): p. 2917-2926.
211. Faraoni, I., et al., *Targeting ADP-ribosylation by PARP inhibitors in acute myeloid leukaemia and related disorders.* Biochem Pharmacol, 2019. **167**: p. 133-148.
212. Chiaretti, S., et al., *Philadelphia-like acute lymphoblastic leukemia is associated with minimal residual disease persistence and poor outcome. First report of the minimal residual disease-oriented GIMEMA LAL1913.* Haematologica, 2021. **106**(6): p. 1559-1568.
213. Tasian, S.K., M.L. Loh, and S.P. Hunger, *Philadelphia chromosome-like acute lymphoblastic leukemia.* Blood, 2017. **130**(19): p. 2064-2072.
214. Man, L.M., A.L. Morris, and M. Keng, *New Therapeutic Strategies in Acute Lymphocytic Leukemia.* Curr Hematol Malig Rep, 2017. **12**(3): p. 197-206.
215. Sin, C.F. and P.M. Man, *The Role of Proteasome Inhibitors in Treating Acute Lymphoblastic Leukaemia.* Front Oncol, 2021. **11**: p. 802832.
216. Leonard, J., et al., *Aurora A kinase as a target for therapy in TCF3-HLF rearranged acute lymphoblastic leukemia.* Haematologica, 2021. **106**(11): p. 2990-2994.
217. Chan, L.N., et al., *Signalling input from divergent pathways subverts B cell transformation.* Nature, 2020. **583**(7818): p. 845-851.
218. Jayanthan, A., et al., *Targeted Polo-like Kinase Inhibition Combined With Aurora Kinase Inhibition in Pediatric Acute Leukemia Cells.* J Pediatr Hematol Oncol, 2019. **41**(6): p. e359-e370.
219. Jemaà, M., et al., *Preferential Killing of Tetraploid Colon Cancer Cells by Targeting the Mitotic Kinase PLK1.* Cell Physiol Biochem, 2020. **54**(2): p. 303-320.
220. Ma, J., et al., *Mechanisms responsible for the synergistic antileukemic interactions between ATR inhibition and cytarabine in acute myeloid leukemia cells.* Sci Rep, 2017. **7**: p. 41950.
221. Schäker-Hübner, L., et al., *4-Acyl Pyrrole Capped HDAC Inhibitors: A New Scaffold for Hybrid Inhibitors of BET Proteins and Histone Deacetylases as Antileukemia Drug Leads.* J Med Chem, 2021. **64**(19): p. 14620-14646.
222. Weisberg, E., et al., *Using combination therapy to override stromal-mediated chemoresistance in mutant FLT3-positive AML: synergism between FLT3 inhibitors, dasatinib/multi-targeted inhibitors and JAK inhibitors.* Leukemia, 2012. **26**(10): p. 2233-44.
223. Yamauchi, T., et al., *Aurora B inhibitor barasertib and cytarabine exert a greater-than-additive cytotoxicity in acute myeloid leukemia cells.* Cancer Sci, 2013. **104**(7): p. 926-33.

224. Yao, Q., et al., *Human leukemias with mutated FLT3 kinase are synergistically sensitive to FLT3 and Hsp90 inhibitors: the key role of the STAT5 signal transduction pathway.* Leukemia, 2005. **19**(9): p. 1605-12.

6 Appendix

Supplementary Table 1: Drugs used in the High Throughput Drug Screening consistent over the different versions of the library and therefore used for all analyses. Data on whether these drugs are EMA and FDA-approved were gathered on the 15th of August 2023 using the website of the BfAM (https://portal.dimdi.de/amguifree/am/search.xhtml) or the orange book (https://www.accessdata.fda.gov/scripts/cder/ob/index.cfm) respectively.

#	Drug	MoA	EMA approved?	FDA approved?	#	Drug	MoA	EMA approve	FDA approve
1	5-Azacytidine	Antimetabolites	Yes	Yes	86	Foretinib	FLT3i	No	No
2	5-Fluorouracil	Antimetabolites	Yes	Yes	87	Dovitinib	FLT3i	No	No
3	6-Mercaptopurine (Mo	Antimetabolites	Yes	Yes	88	Crenolanib	FLT3i	No	No
4	6-Thioguanine	Antimetabolites	Yes	Yes	89	Pexidartinib	FLT3i	No	Yes
5	Clofarabine	Antimetabolites	Yes	Yes	90	Lestaurtinib	FLT3i	No	No
6	Cytarabine (Hydrochlo	Antimetabolites	Yes	Yes	91	Quizartinib	FLT3i	No	Yes
7	Cyclocytidine HCL	Antimetabolites	No	No	92	KW-2449	FLT3i	No	No
8	Fludarabine (phosphat	Antimetabolites	Yes	Yes	93	Pacritinib	FLT3i	No	Yes
9	Nelarabine	Antimetabolites	Yes	Yes	94	Gilteritinib	FLT3i	Yes	Yes
10	Gemcitabine	Antimetabolites	Yes	Yes	95	Buparlisib	PI3K/AKT/mTORi	No	No
11	Methotrexate	Antimetabolites	Yes	Yes	96	Idelalisib	PI3K/AKT/mTORi	Yes	Yes
12	Pentostatin	Antimetabolites	Yes	Yes	97	Pictilisib GDC-0941	PI3K/AKT/mTORi	No	No
13	Cladribine	Antimetabolites	Yes	Yes	98	GSK2636771	PI3K/AKT/mTORi	No	No
14	Dacarbazine	Antimetabolites	Yes	Yes	99	Alpelisib	PI3K/AKT/mTORi	Yes	Yes
15	Vinblastine (sulfate)	Antimitotics	Yes	Yes	100	Dactolisib (BEZ235)	PI3K/AKT/mTORi	No	No
16	Vincristine (sulfate)	Antimitotics	Yes	Yes	101	GSK2110183 (Afuresertib)	PI3K/AKT/mTORi	No	No
17	Busulfan	Alkylating agents	Yes	Yes	102	ARQ-092 (Miransertib)	PI3K/AKT/mTORi	No	No
18	Carmustine	Alkylating agents	Yes	Yes	103	Ipatasertib (GDC-0068)	PI3K/AKT/mTORi	No	No
19	Cyclophosphamide (C	Alkylating agents	Yes	Yes	104	Deforolimus	PI3K/AKT/mTORi	No	No
20	Lomustine	Alkylating agents	Yes	Yes	105	Everolimus	PI3K/AKT/mTORi	Yes	Yes
21	Cisplatin	Alkylating agents	Yes	Yes	106	Rapamycin	PI3K/AKT/mTORi	Yes	Yes
22	Oxaliplatin	Alkylating agents	Yes	Yes	107	Temsirolimus	PI3K/AKT/mTORi	Yes	Yes
23	Procarbazine (Hydrocl	Alkylating agents	Yes	Yes	108	PF-04691502	PI3K/AKT/mTORi	No	No
24	Thio-TEPA	Alkylating agents	Yes	Yes	109	INK 128 (Sapanisertib)	PI3K/AKT/mTORi	No	No
25	Temozolomide	Alkylating agents	Yes	Yes	110	BMS-911543	JAKi	No	No
26	Chlorambucil	Alkylating agents	Yes	Yes	111	AT9283	JAKi	No	No
27	Bendamustine (hydroc	Alkylating agents	Yes	Yes	112	Baricitinib (phosphate)	JAKi	Yes	Yes
28	Mechlorethamine hyd	Alkylating agents	Yes	Yes	113	CYT387 (Momelotinib)	JAKi	No	No
29	Epirubicin (hydrochlo	Topoisomerase inhibitors	Yes	Yes	114	Ruxolitinib	JAKi	Yes	Yes
30	Etoposide	Topoisomerase inhibitors	Yes	Yes	115	Tofacitinib (citrate)	JAKi	Yes	Yes
31	Idarubicin (hydrochlo	Topoisomerase inhibitors	Yes	Yes	116	Fedratinib	JAKi	Yes	Yes
32	Mitoxantrone	Topoisomerase inhibitors	Yes	Yes	117	Gandotinib	JAKi	No	No
33	Teniposide	Topoisomerase inhibitors	No	Yes	118	Tipifarnib	Ras/Raf/MEK/ERKi	No	No
34	Daunorubicin (Hydroc	Topoisomerase inhibitors	Yes	Yes	119	Lonafarnib	Ras/Raf/MEK/ERKi	Yes	Yes
35	Doxorubicin (hydroch	Topoisomerase inhibitors	Yes	Yes	120	Salirasib	Ras/Raf/MEK/ERKi	No	No
36	Amsacrine (Hydochlor	Topoisomerase inhibitors	Yes	No	121	Dabrafenib (Mesylate)	Ras/Raf/MEK/ERKi	Yes	Yes
37	Dexamethasone	GC/GCR complex	Yes	Yes	122	Sorafenib (Tosylate)	Ras/Raf/MEK/ERKi	Yes	Yes
38	Prednisone	GC/GCR complex	Yes	Yes	123	Regorafenib	Ras/Raf/MEK/ERKi	Yes	Yes
39	Prednisolone (Acetate	GC/GCR complex	Yes	Yes	124	Vemurafenib	Ras/Raf/MEK/ERKi	Yes	Yes
40	Belinostat	HDACi	No	Yes	125	LGX818 (Encorafenib)	Ras/Raf/MEK/ERKi	Yes	Yes
41	CI-994 (Tacedinaline)	HDACi	No	No	126	Cobimetinib	Ras/Raf/MEK/ERKi	Yes	Yes
42	Panobinostat	HDACi	Yes	Yes	127	MEK162 (Binimetinib)	Ras/Raf/MEK/ERKi	Yes	Yes
43	Romidepsin	HDACi	No	Yes	128	Selumetinib	Ras/Raf/MEK/ERKi	Yes	Yes
44	Quisinostat	HDACi	No	No	129	Trametinib	Ras/Raf/MEK/ERKi	Yes	Yes
45	Tubastatin A (Hydroch	HDACi	No	No	130	PD0325901	Ras/Raf/MEK/ERKi	No	No
46	Givinostat (ITF2357)	HDACi	No	No	131	PD184352	Ras/Raf/MEK/ERKi	No	No
47	Vorinostat	HDACi	No	Yes	132	Pimasertib	Ras/Raf/MEK/ERKi	No	No
48	Entinostat	HDACi	No	No	133	SHP099	Ras/Raf/MEK/ERKi	No	No
49	Ricolinostat	HDACi	No	No	134	SCH772984	Ras/Raf/MEK/ERKi	No	No
50	Pracinostat	HDACi	No	No	135	GDC-0994 (Ravoxertinib)	Ras/Raf/MEK/ERKi	No	No
51	Abexinostat	HDACi	No	No	136	Losmapimod	Ras/Raf/MEK/ERKi	No	No
52	EPZ-6438 (Tazemetost	EZH2i/HMTasei	No	Yes	137	Zanubrutinib	BTKi	Yes	Yes
53	GSK126	EZH2i/HMTasei	No	No	138	Tirabrutinib	BTKi	No	No
54	GSK343	EZH2i/HMTasei	No	No	139	Spebrutinib	BTKi	No	No
55	GSK 525762A	BET bromodomain;	No	No	140	Ibrutinib	BTKi	Yes	Yes
56	Paclitaxel	BET bromodomain;	Yes	Yes	141	Imatinib	Bcr-Abl/Tki	Yes	Yes
57	JQ1	BET bromodomain	No	No	142	Radotinib	Bcr-Abl/Tki	No	No
58	Bortezomib	Proteasome inhibitor	Yes	Yes	143	Nilotinib	Bcr-Abl/Tki	Yes	Yes
59	MLN-9708 (Ixazomib)	Proteasome inhibitor	Yes	Yes	144	Ponatinib	Bcr-Abl/Tki	Yes	Yes
60	Carfilzomib	Proteasome inhibitor	Yes	Yes	145	Bosutinib	Bcr-Abl/Tki	Yes	Yes
61	Ganetespib	HSP90i	No	No	146	Dasatinib	Bcr-Abl/Tki	Yes	Yes
62	PUH71	HSP90i	No	No	147	Rebastinib	Bcr-Abl/Tki	No	No
63	AUY922 (LUMINESPIB)	HSP90i	No	No	148	Saracatinib	Bcr-Abl/Tki	No	No
64	NVP-HSP990	HSP90i	No	No	149	Bafetinib	Bcr-Abl/Tki	No	No
65	EC144	HSP90i	No	No	150	Staurosporin	Multiple protein kinase inhibitor	No	No
66	PF-04929113	HSP90i	No	No	151	BSI-201 (Iniparib)	PARPi	No	No
67	BIIB021	HSP90i	No	No	152	Olaparib	PARPi	Yes	Yes
68	Alisertib	Aurora Kinase A inhibitor	No	No	153	Rucaparib (phosphate)	PARPi	Yes	Yes
69	Aurora A Inhibitor I	Aurora Kinase A inhibitor	No	No	154	Veliparib (dihydrochloride)	PARPi	No	No
70	MLN8054	Aurora Kinase A inhibitor	No	No	155	Venetoclax	Bcl-2i	Yes	Yes
71	MK-5108	Aurora Kinase A inhibitor	No	No	156	Obatoclax	Bcl-2i	No	No
72	Danusertib	Aurora Kinase A inhibitor	No	No	157	Y-27632 (Dihydrochloride)	ROCK	No	No
73	Barasertib	Aurora Kinase A inhibitor	No	No	158	QNZ (EVP4593)	NF-κBi	No	No
74	Volasertib	PLKi	No	No	159	Omaveloxolone	NF-κBi	No	Yes
75	BI2536	PLKi	No	No	160	Enasidenib	IDH2i	No	Yes
76	LEE011 (Ribociclib)	CDKi	Yes	Yes	161	Ivosidenib	IDH1i	No	Yes
77	Abemaciclib	CDKi	Yes	Yes	162	Birinapant	XIAPi and cIAP1i	No	No
78	Dinaciclib	CDKi	No	No	163	Tariquidar	P-glycoprotein;	No	No
79	SY-1365-THZ1	CDKi	No	No	164	Enzastaurin	PKC;	No	No
80	Cabozantinib	VEGFRi	Yes	Yes	165	KYA1797K	wnt/catenin	No	No
81	Erlotinib	EGFRi	Yes	Yes	166	Selinexor	CRM1 inhibitor	Yes	Yes
82	Gefitinib (Hydrochlori	EGFRi	Yes	Yes	167	AZD6738 (Ceralasertib)	ATM/ATRi	No	No
83	Sunitinib	PDGFRi	Yes	Yes	168	Omacetaxine Mepesuccinate (Homoharringtonine)	Ribosom Inhibtor	No	Yes
84	Axitinib	VEGFRi	Yes	Yes	169	Actinomycin D	Antibacterial	Yes	Yes
85	Midostaurin	FLT3i	Yes	Yes	170	BAY 80-6946 (Copanlisib)	PI3K/AKT/mTORi	No	Yes

Acknowledgments

I would like to express my sincere thanks to:

Dr. Sanil Bhatia for his continuous support and supervision of this work, not only during my active time in the laboratory but also beyond that. He was always available for questions and continuously improved this work through suggestions and critical questioning. I would like to especially thank him for teaching me scientific methods and thinking.

Prof. Dr. Arndt Borkhardt for giving me this unique chance to work on this interesting project. Moreover, his critical questions and comments help in writing this thesis. I would like to thank him also for his quick availability during the whole work progress.

Prof. Dr. Nikolas Stoecklein for taking over the co-supervision of this thesis. I would like to especially thank him for his quick and straightforward responses to any concerns.

The **GRK2158** and especially **Prof. Dr. Holger Gohlke** and **Dr. Martina Holz** for the financial and content-related assistance.

To all members of the "**Team Target**" group and "**KMT lab**" for their content-related and emotional support. I will never forget the fun times we had during our lunch breaks or regular burger eating. I want to especially thank **Katerina Scharov** and **Jia-Wey Tu** for their active help in processing patient-derived samples. Moreover, I would like to thank **Julian Schliehe-Diecks** for teaching me the rudimental handling of R and his technical support. A special thanks also goes to **Dr. Triantafyllia Brozou** and **Dr. Rabea Wagener** for their help regarding the clinical data gathering and their insights into the project of the patient-derived fibroblasts.

My big and small family for their emotional aid. My special thanks go to my parents **Dr. Anne Watrin** (to whom this work is dedicated) and **Prof. Dr. Christoph Watrin** for their sponsorship and for cheering me up during frustrating times. I also want to include my siblings, **Victoria Watrin** and **Vincent Watrin**, in the thank you for their strengthening support during the particularly hard time. A big thank you also goes to my **whole friend group** for being there for me when I needed them, even during times when we did not keep in touch for a long time.

Hanna Hoffmann for always being there for me and listening to my complaints and frustration. Thank you for being so patient and especially for your tolerance, as our shared time was often limited during the particularly hard time. Lastly, I also want to thank you for fighting through the first, very rough draft of this thesis and correcting it. I am looking forward to our joint future.